Western University
Scholarship@Western

Digitized Theses | Digitized Special Collections

1984

Spectroscopic Studies Of Metal Binding To Metallothioneins

Annie Yiu-chu Law

Follow this and additional works at: https://ir.lib.uwo.ca/digitizedtheses

Recommended Citation
Law, Annie Yiu-chu, "Spectroscopic Studies Of Metal Binding To Metallothioneins" (1984). *Digitized Theses*. 1374.
https://ir.lib.uwo.ca/digitizedtheses/1374

This Dissertation is brought to you for free and open access by the Digitized Special Collections at Scholarship@Western. It has been accepted for inclusion in Digitized Theses by an authorized administrator of Scholarship@Western. For more information, please contact tadam@uwo.ca, wlswadmin@uwo.ca.

The author of this thesis has granted The University of Western Ontario a non-exclusive license to reproduce and distribute copies of this thesis to users of Western Libraries. Copyright remains with the author.

Electronic theses and dissertations available in The University of Western Ontario's institutional repository (Scholarship@Western) are solely for the purpose of private study and research. They may not be copied or reproduced, except as permitted by copyright laws, without written authority of the copyright owner. Any commercial use or publication is strictly prohibited.

The original copyright license attesting to these terms and signed by the author of this thesis may be found in the original print version of the thesis, held by Western Libraries.

The thesis approval page signed by the examining committee may also be found in the original print version of the thesis held in Western Libraries.

Please contact Western Libraries for further information:
E-mail: libadmin@uwo.ca
Telephone: (519) 661-2111 Ext. 84796
Web site: http://www.lib.uwo.ca/

CANADIAN THESES ON MICROFICHE

I.S.B.N.

THESES CANADIENNES SUR MICROFICHE

National Library of Canada
Collections Development Branch

Canadian Theses on
Microfiche Service

Ottawa, Canada
K1A 0N4

Bibliothèque nationale du Canada
Direction du développement des collections

Service des thèses canadiennes
sur microfiche

NOTICE

The quality of this microfiche is heavily dependent upon the quality of the original thesis submitted for microfilming. Every effort has been made to ensure the highest quality of reproduction possible.

If pages are missing, contact the university which granted the degree.

Some pages may have indistinct print especially if the original pages were typed with a poor typewriter ribbon or if the university sent us a poor photocopy.

Previously copyrighted materials (journal articles, published tests, etc.) are not filmed.

Reproduction in full or in part of this film is governed by the Canadian Copyright Act, R.S.C. 1970, c. C-30. Please read the authorization forms which accompany this thesis.

THIS DISSERTATION
HAS BEEN MICROFILMED
EXACTLY AS RECEIVED

AVIS

La qualité de cette microfiche dépend grandement de la qualité de la thèse soumise au microfilmage. Nous avons tout fait pour assurer une qualité supérieure de reproduction.

S'il manque des pages, veuillez communiquer avec l'université qui a conféré le grade.

La qualité d'impression de certaines pages peut laisser à désirer, surtout si les pages originales ont été dactylographiées à l'aide d'un ruban usé ou si l'université nous a fait parvenir une photocopie de mauvaise qualité.

Les documents qui font déjà l'objet d'un droit d'auteur (articles de revue, examens publiés, etc.) ne sont pas microfilmés.

La reproduction, même partielle, de ce microfilm est soumise à la Loi canadienne sur le droit d'auteur, SRC 1970, c. C-30. Veuillez prendre connaissance des formules d'autorisation qui accompagnent cette thèse.

LA THÈSE A ÉTÉ
MICROFILMÉE TELLE QUE
NOUS L'AVONS REÇUE

NL-339 (r. 82/08)

Canada

SPECTROSCOPIC STUDIES OF METAL BINDING TO METALLOTHIONEINS

by

Annie Yiu-Chu Law

Department of Chemistry

Submitted in partial fulfillment
of the requirements for the degree of
Doctor of Philosophy

Faculty of Graduate Studies
The University of Western Ontario
London, Ontario
July, 1984

© Annie Yiu-Chu Law 1984

ABSTRACT

Metallothioneins (MT) are a class of cysteine-rich proteins that bind a wide variety of metal ions. Although it has been suggested that the structure of the metal binding sites in Cd,Zn-MT involves two metal clusters (alpha and beta) which coordinate the metals through a tetrahedral arrangement of cysteine residues, considerably less information is available concerning the metal binding sites in MT containing Hg^{2+} and Cu^{+}. In this work, absorption, circular dichroism (CD) and magnetic circular dichroism (MCD) spectroscopies have been used to characterize metal binding to metallothioneins. The CD spectrum provides information on stereochemistry while the MCD spectrum gives symmetry information on the metal binding sites in MT.

Three species of MT's (rat liver, guinea pig liver and crab hepatopancreas) have been studied. In addition to the metal binding properties of MT itself, changes in the spectroscopic properties when the Cd^{2+} and Zn^{2+} of the native protein are replaced by Hg^{2+} and Cu^{+} in vitro have also been investigated.

A comparison of the MCD spectrum of Cd,Zn-MT with that obtained for a tetrahedrally-coordinated Cd-BAL (BAL= 2,3-dimercaptopropanol) complex shows that the metal binding sites in Cd,Zn-MT involve a tetrahedral symmetry and that the Cd-BAL complex represents a good model for the geometry of the metal binding sites in Cd,Zn-MT.

Although the MCD spectra of the native Cd,Zn-MT from all three species resemble each other closely, the CD spectra indicate a difference in the protein conformation in the crab protein. However, all three species behave in a similar manner to protonation and metal loading with Cd^{2+}.

Spectral changes in the absorption, CD and MCD spectra during metal replacement studies with Hg^{2+} and Cu^{+} clearly demonstrate that first Zn^{2+} and then Cd^{2+} ions are displaced in a sequential fashion from the MT. In addition, the metal binding in the alpha and beta clusters are specific and the following order of binding can be concluded from this study (in vitro):

Alpha cluster: Hg > Cd > Cu > Zn

Beta cluster : Hg, Cu > Cd > Zn

Titration studies of native Cd,Zn-MT with Hg^{2+} show the isomorphous replacement of Cd^{2+} and Zn^{2+}. The MCD spectrum obtained for the Hg-substituted MT differs quite significantly from that observed for a Hg-BAL model complex, which suggests that the Hg^{2+} ions bound to the protein are not in a tetrahedral environment.

Titration studies with Cu^{+} results in an intermediate species which exhibits a well-defined CD spectrum. Four Cu^{+} ions can be bound to the alpha fragment, while a total of six Cu^{+} ions are associated with the beta domain. The MCD spectrum obtained for the MT reconstituted with Cu^{+} is not consistent with a tetrahedral symmetry around the Cu^{+} ions.

ACKNOWLEDGEMENTS

I would like to express my sincere gratitude to my supervisor, Dr. Martin Stillman for all his helpful suggestions and encouragement during the course of this work.

Special thanks to Dr. Jadwiga Szymanska for providing some of the protein samples used in this work as well as her help and stimulating discussions. I would also like to thank Drs. Bill Browett and Zbigniew Gasyna for their helpful suggestions.

Finally, I would like to thank my mother and my husband, Philip, for their support and encouragement.

TABLE OF CONTENTS

LIST OF TABLES

LIST OF FIGURES

ABBREVIATIONS

CD	Circular Dichroism
MCD	Magnetic Circular Dichroism
nmr	Nuclear Magnetic Resonance
MT	Metallothionein
BAL	2,3-dimercaptopropanol
DTNB	5,5′-dithiobis-(2-nitrobenzoic acid)
AAS	Atomic Absorption Spectrophotometry

CHAPTER 1 - GENERAL INTRODUCTION

The outbreak of the Itai-Itai disease in Japan in the 1950's (1), a disease demonstratably associated with Cd^{2+} poisoning, has stimulated much interest over the toxicological effects of Cd^{2+} to the general population. Unlike other metals, Cd^{2+} is excreted very slowly from the body, and has a long biological half life in humans of about 9-30 years (2,3). At low level exposure from food, Cd^{2+} is mainly accumulated in the liver and kidneys. The kidneys have been found to be the organ most sensitive to the effects of Cd^{2+} after chronic exposure (2). However, little is known regarding the identity of the cadmium complex present in the body. It was not until 1957 that the first Cd^{2+}-containing protein was isolated by Margoshes and Vallee from horse kidney cortex (4). This protein was later named metallothionein (MT) by Kagi and Vallee in 1960 (5).

Following the discovery of the horse metallothionein, similar proteins have since been identified and isolated from a wide variety of mammals (including humans, rat, chicken, mouse, guinea pig, rabbit) as well as plants (6,7), fish (8-11), microorganisms (12,13) and invertebrates (14-16). In mammals, the metallothionein is found predominantly in the kidneys and livers, however, a much lower concentration of the protein can also be observed in tissues of other organs such as spleen, pancreas, testis and brain (17).

Metallothioneins may be induced by the injection of a wide range of metal ions, e.g. Cd^{2+}, Zn^{2+}, Cu^{2+}, Hg^{2+}, Au^{3+} and Bi^{3+} (18). Other metals such as Ag^{+} and Pb^{2+} have also been investigated, however, their induction properties have not been well established (19-22). Nevertheless, both of these metals have been shown to bind to

metallothionein in vitro (23,24). Amongst the wide variety of metal ions used in the induction of metallothionein synthesis, Cd^{2+} and Zn^{2+} are by far the most effective. In addition to the induction of the protein by the injection of group IIB metal ions, it is possible to induce the protein by a variety of other methods as shown in Table I. However, the concentrations of the protein produced from these other methods are often much lower compared with that obtained from the injections of metal salts.

Metallothionein has been a subject of special interest, largely due to its unique metal binding properties, its widespread occurrence and its possible involvement in the regulation and metabolism of metal ions (e.g. Zn^{2+} and Cu^{+}) in the body. The majority of the native metallothioneins isolated thus far consist of a single-chain polypeptide with 61 amino acid residues and a molecular weight range of 6500-7000. However, early studies using gel chromatography (42,43) have reported a molecular weight of 10,000-12,000 for the rat and mouse MTs. The discrepancy in the molecular weight measurements was later rationalized by the fact that MT has an elongated shape with an axial ratio of a prolate ellipsoid (a/b = 6) (44). While the gel chromatography technique provides a reasonable estimate for the molecular weight of globular proteins, the significant difference between the shape of MT and a globular protein introduces substantial error. The elongated shape of MT was later confirmed by dark-field electron microscopy (45). Most metallothioneins have been shown to contain two or more isoforms which differ only slightly in their amino acid compositions (46). Measurements by free boundary electrophoresis have shown that the MT 1 isoforms of a number of MTs possess two

TABLE I

Methods of induction of metallothionein

Methods	References
1. Metal ions injection (Cd, Zn, Cu, Hg, Au, Ag)	25-36
2. Food restriction	30
3. Stress conditions and CCl_4 intoxication	37
4. Alkylating agent	38
5. Bacterial infection	39
6. Hypersensitivity reaction	40
7. Adrenocortical steroids	41

negative charges, while the MT 2 isoforms carry three negative charges (47-49).

One of the exceptional properties of MT which distinguish it from other low molecular weight proteins is the presence of a high metal content (6-7 mole equivalents of Cd^{2+} and Zn^{2+} ions)(50,51), and a high percentage of cysteine residues (20 out of a total of 61 amino acid residues). The primary structures of several metallothioneins are now known (52). A remarkable homology of the amino acid sequence has been observed in metallothioneins from different species. The amino acid sequence shown in FIG. 1, for equine kidney MT 2B (53), shows a predominant occurrence of cys-x-cys (a total of 7), as well as 3 each of the cys-cys and cys-x-x-cys units throughout the entire sequence, where x represents amino acid residues other than cysteine. The presence of these unique cys-x-cys units has been found to be highly conserved in MT's from other species (52). The lack of both aromatic amino acids and histidine is also a characteristic feature of this protein.

A number of biological functions have been suggested for this protein but none of them has been firmly established to date (54,55). TABLE II shows a list of the proposed biological functions for MT.

Several studies have indicated that the synthesis of hepatic MT is mediated by an increase in the exposure to Cd^{2+} ions, which suggests that in binding Cd^{2+}, MT may function as a detoxification mechanism (56-58). However, it was later observed that Cd-MT is 7-8 times more toxic than Cd^{2+} ions alone. When Cd^{2+} and Cd-MT were injected into animals, a difference in the distribution of Cd^{2+} and Cd-MT was observed (60-63). Cd^{2+} predominantly accumulates in the liver while

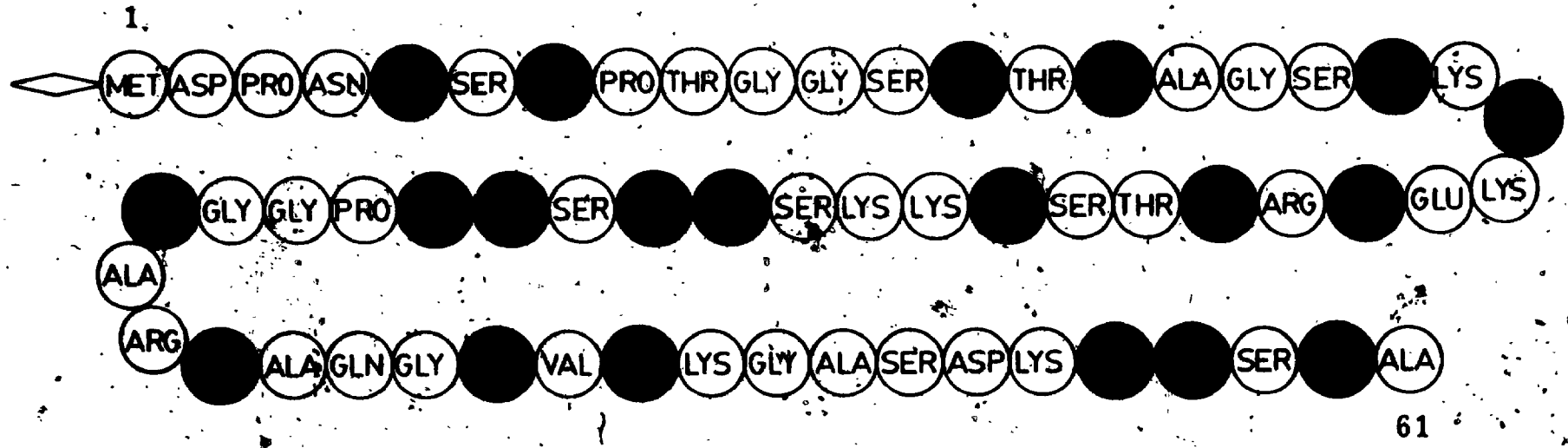

FIG. 1. Amino acid sequence of equine kidney MT, from Ref. (53)

● = Cysteine

Cd-MT was found in the kidney (64). The MT was taken up by the renal tubules where catabolism and release of Cd^{2+} was effected by the lysosomes (59). The high concentration of Cd^{2+} released thus resulted in severe renal damage.

TABLE II

Possible functions of metallothionein

1. detoxification of toxic metals
2. regulation of zinc and copper metabolism
3. storage of metal ions
4. transport of metal ions

The transport role of MT for Cd^{2+}, from liver to kidney, has been suggested in several studies (65,66), while refuted by others (67). Examinations of Cd-exposed workers have indicated that the toxic effects of Cd^{2+} in kidneys occur at a much later time than that expected if the transport of Cd^{2+} to the kidneys was to be mediated by MT.

Cherian (68) has proposed a metal storage function for MT. It was shown that Cd-pretreated rats contain a much higher concentration of the Cd-binding protein in the liver than non-pretreated rats. A decrease in biliary excretion of Cd^{2+} was also observed and there was no Cd-MT excreted in the bile. This implied that the MT functions as a storage site for Cd^{2+}. Others have also supported the temporary storage role of MT in rat livers (30), as well as in sheep fetal livers (69).

The presence of a naturally occurring Zn-MT in human livers (48) suggests that the primary role of MT in liver may be related to Zn^{2+}, in particular to the regulation of Zn^{2+} metabolism. Both the induced synthesis of Zn-MT in rats after partial starvation (30) and the accumulation of Zn^{2+} in the MT fraction in growing chicks fed high levels of dietary Zn^{2+} demonstrate the possible role of MT in Zn^{2+} homeostasis (70). Additionally, Udom & Brady demonstrated the ability of Zn-MT to transfer Zn^{2+} ions to Zn^{2+}-requiring apoproteins in vitro (71). Zn-MT was found to be superior to other Zn^{2+} salts in reactivating Zn^{2+}-metalloenzymes such as apo-bovine erythrocyte carbonic anhydrase B, apo-alcohol dehydrogenase, apo-thermolysin, and apo-aldolase. Further support for the role of Zn-MT as a physiological Zn^{2+} donor was given by Li et al. (72) in studies of the ligand substitution reactions of MT with EDTA and apo-carbonic anhydrase.

Of all the metallothioneins investigated so far, the Cd,Zn-MT isolated from rat, chicken and horse are the most actively studied. Besides Cd^{2+} and Zn^{2+}, MT's containing other metal ions have also been found in tissues, e.g. native Cu,Zn-MT from calf liver (73), Cu,Hg-MT isolated from rat kidney after Hg^{2+} injections (74). The occurrence of these MTs raises questions regarding the possible involvement of MT in the metabolic pathway of metal ions other than Zn^{2+}. Furthermore, the existence of naturally-occurring Cu-MT's in neonatal and fetal livers implies that metallothioneins may be involved in copper metabolism (75,76).

Metallothionein is thought to play a very important role in the metabolism of essential, as well as toxic heavy metals. Therefore, it

is vital to establish the chemical nature and structure of the metal binding sites in this protein in order to assess the relationship between its molecular features and the proposed metabolic functions. Of the several attempts made to obtain crystals of metallothionein todate, only recently have the preparations of crystals of suitable quality for X-ray crystals study been described (77). However, the three dimensional structure of the metal binding sites in metallothionein has not yet been determined. Hence the majority of the structural information obtained so far is based primarily on spectroscopic studies.

Shortly after its discovery, the protein was characterized using absorption spectroscopy. Owing to the lack of aromatic amino acids in this protein, no significant absorption is present in the 280 nm region. Neither Cd^{2+} nor Zn^{2+} gives rise to any absorption in the visible or UV regions because of the filled d-shells. The absorption spectrum of metallothionein at pH 7 exhibits a broad shoulder at 250 nm, which is on the low energy side of an intense background absorption that arises from the secondary amide and thiol transitions near 190 nm (78). This characteristic absorption shoulder at 250 nm is commonly used as an indicator for the presente of metallothionein. Early model compound studies with mercaptoethanol complexes of Cd^{2+} and Zn^{2+} suggested that this shoulder was due to charge transfer transitions (79), with the S->Cd and the S->Zn charge transfer bands at 254 nm and 231 nm, respectively. Line shape analysis has revealed that the broad absorption profile consists of at least three transitions (80). Based upon the semiempirical theory of Jorgensen (81) and comparison with spectra of complexes between Cd^{2+} and 2-

mercaptoethanol, the lowest energy transition of the absorption spectrum of MT has been assigned to the first Laporte-allowed electron transfer transition (81). However, the origin of the remaining transitions has not been established.

Cd,Zn-MTs from different mammalian species exhibit similar chiroptical properties (82-84). The CD spectrum is characterized by two bands of opposite signs in the 260 nm to 225 nm region. The molecular mechanism which contributes to the optical properties is not clear, but it is likely to arise from the dissymmetric coordination by the chiral cysteines. Rupp & Weser (82) have shown that the CD band intensity associated with the Cd-thiolate chromophore does not increase linearly with the increase in the Cd^{2+} content, hence this suggests that the optical properties observed are of complex origin.

Results from X-ray photoelectron spectroscopy (XPS) studies have suggested that all the thiolate sulfur atoms of the cysteine residues in metallothionein are involved in metal binding and there is no evidence of disulfide bonds in MT (44,,85,86). Although the presence of 20 cysteinyl residues together with the 7 moles of bound metal ions suggested that each metal is bound to 3 thiolate sulfurs, the coordination chemistry of both the Cd^{2+} and Zn^{2+} have indicated preference for the formation of complexes involving at least four or higher coordination number. Therefore, extensive ^1H nmr studies (87-90) were carried out in an attempt to identify the coordinating groups involved in the binding of the metal ions. These data also provide information on the tertiary structure of the protein. The ^1H nmr data indicated that the resonances associated with the cysteinyl residues were markedly perturbed on metal binding thus confirming the

suggestion that the sulfur atoms are coordinated to the metal ions. No evidence was obtained for the involvement of other amino acid residues in the metal binding sites . The ^{1}H nmr spectrum of the apo-MT also suggested a random coil structure, since the ^{1}H nmr spectrum of apo-MT exhibits a remarkably similar pattern to that obtained for a mixture of amino acids which has the same composition as apo-MT. The presence of a wide range of amide resonances indicate that the holoprotein has a well defined tertiary structure (87,89), in contrast to the previous conclusion given by Rupp et al. (88). The fact that metallothioneins from a variety of species exhibited quite similar nmr spectra serves to confirm the extensive sequence homology observed among metallothioneins from different sources (90).

Early ^{113}Cd nmr data (91) obtained at 22.06 MHz showed the presence of 7 resonances between 610 and 670 ppm, in a chemical shift region expected for CdS_4 coordination (92-94). Similar spectra were also reported for a ^{113}Cd- enriched MT obtained from rabbit and rat livers (95-97). A significant advance in the structural studies of MT was presented recently in a series of ^{113}Cd nmr studies at 44 MHz by Otvos & Armitage (97-99). By using selective ^{113}Cd decouplings, they have demonstrated the presence of discrete cluster units in the metal binding sites of metallothionein. Comparison between the proton decoupled ^{113}Cd nmr spectra of the two isoproteins of native rabbit liver MT showed that they were very similar (100). The fact that all but one of these resonances were split into multiplets suggests that they arise from ^{113}Cd - ^{113}Cd scalar coupling through adjacent Cd^{2+} ions connected by 2 bonds (97-99). Analysis of the selective homonuclear ^{113}Cd decoupling data showed the presence of two types of

clusters, one containing 4 and the other 3 metal ions (98). The clusters involve both terminal and bridging sulfur atoms. The structures of the two clusters are shown in FIG. 2. The B cluster involves 9 cysteine residues from the NH_2-terminus of the sequence (residues 1-30 in FIG. 1) and the A cluster has 11 cysteine residues (residues 31-61). The presence of two types of binding sites was also supported by data obtained from the perturbed angular correlation of gamma rays technique (101). ^{113}Cd nmr spectra of native rat liver ^{113}Cd,Zn-MT isoforms at 88 MHz were reported recently in which the overlapping resonances were significantly better resolved than previously reported (102). A comparison of the spectra of the two isoforms indicated that there was more heterogeneity in the distribution of Cd^{2+} and Zn^{2+} in isoform 2 of this protein.

Extended X-ray absorption fine structure spectroscopy (EXAFS) has also been used to study the Zn^{2+} sites in sheep MT and the results suggested that all the sites are essentially equivalent and involve four sulfur atoms (103). The Zn-S bond distance observed is comparable to that for tetrahedrally-coordinated Zn^{2+} thiolate complexes (104,105).

Spectroscopic studies of MT in which the Cd^{2+} and Zn^{2+} ions have been replaced have also concluded that the metal binding sites in these MT's involve a tetrahedral symmetry. Absorption and MCD studies of Co^{2+}- and Ni^{2+}- substituted MT (106-108) showed that the broad absorption bands in the visible and near IR regions resemble those observed for known inorganic tetrathiolate complexes and cobalt derivatives of metalloproteins containing the $[Co(cys)_4]^{2-}$ unit (109). The MCD spectra observed are consistent with a tetrahedral

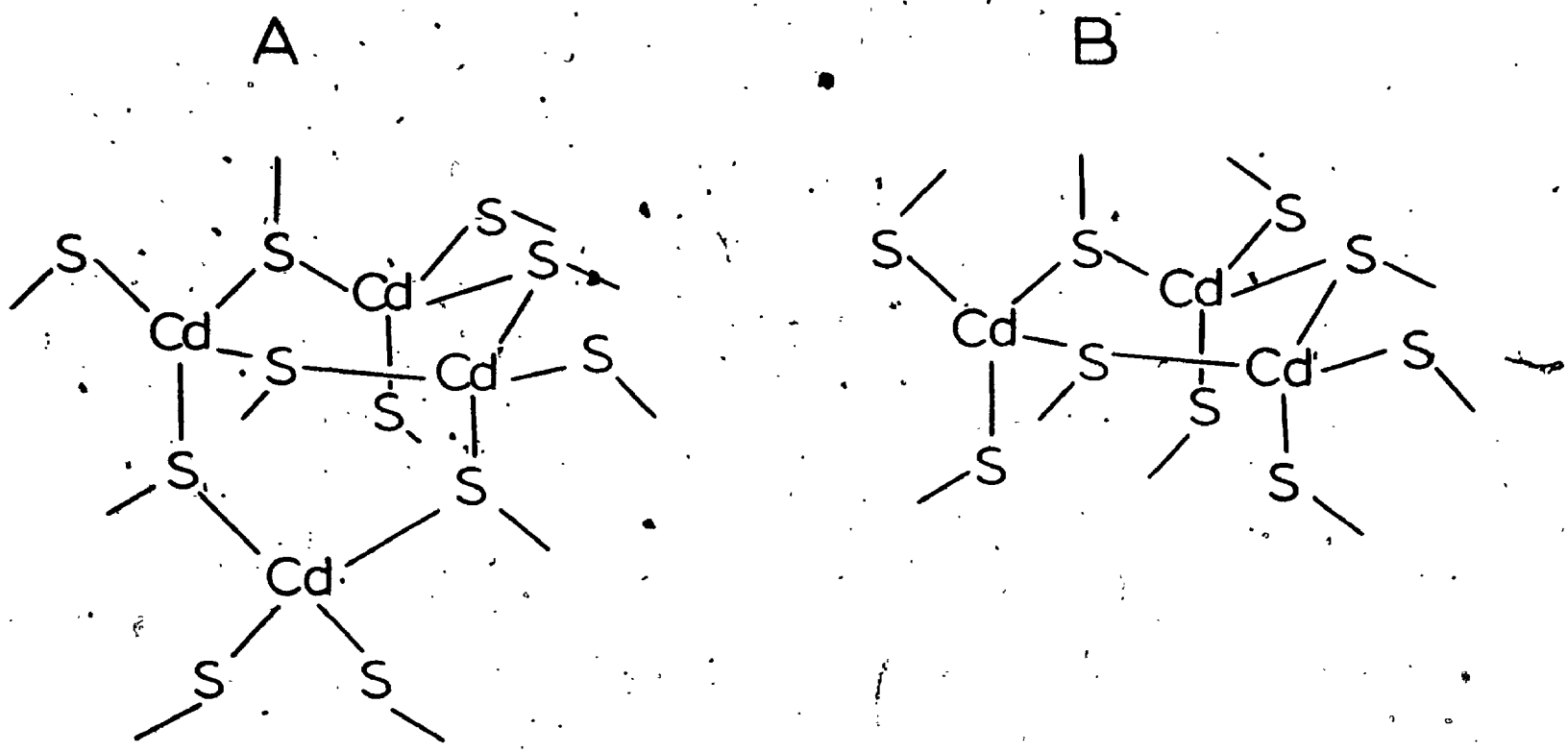

FIG. 2 Structures of the alpha (A) and beta (B) clusters in metallothionein, from ref. (98)

coordination of the metal ions, but there is a considerable distortion in the geometry.

Although ^{113}Cd nmr studies have established the binding of a total of 7 moles of metal ions in the two metal clusters in metallothionein, the majority of the data reported to date (for both the native and metal-reconstituted MT) has indicated a Cd^{2+} and Zn^{2+} content that ranges from 4.2 to 6.5. The discrepancies in the metal contents in the native proteins, where metallation takes place in vivo, probably results from both the loss of the less tightly bound Zn^{2+} ions during the isolation process and the inaccuracy in the measurement of the protein concentration. Different methods were used to estimate the protein concentration and, therefore, it became extremely difficult to correlate results from different laboratories.

The accurate measurement of protein and metal concentrations is very important in metal replacement studies for the elucidation of the stoichiometry of metal binding in MT. A variety of methods have been suggested for the estimation of metallothionein levels by a number of research groups and they are summarized in Table III. Kagi & Vallee (79) and Pulido et al. (84) determined an extinction coefficient at 250 nm for the Cd^{2+} chromophore from the difference spectrum of the native metallothionein (at pH 7) and the thionein (at pH 2). Since the 250 nm shoulder absorption arises from the S -> Cd charge transfer transitions, solutions containing the same protein concentration but with a different Cd^{2+} to Zn^{2+} ratio, will undoubtedly exhibit different absorbances at 250 nm (44). Therefore, this method of estimation should only be applied to protein samples that contain solely Cd^{2+}.

TABLE III

Different methods for determination of metallothionein concentrations

Method	References
1. Cd-heme	110,115
2. ^{109}Cd isotope	111
3. Extinction coefficient	78
4. ^{203}Hg saturation	112-114
5. Polarography	117
6. Radioimmunoassay	120-121
7. ^{203}Hg modified method	116
8. Thiol groups determination (DTNB)	118,119

Other protein concentration estimations make use of the different affinities of metal ions towards the sulfhydryl groups (Hg>Cd>Zn). In the Cd-heme method, excess Cd^{2+} is used to displace the bound Zn^{2+} ions and the protein concentration was then estimated by assuming that 6 Cd^{2+} ions are bound per protein molecule (110).

Radionuclides such as ^{109}Cd (111) and ^{203}Hg (112-114) have also been used as markers for the determination of protein concentration. The ^{203}Hg added displaces all the Cd^{2+} and Zn^{2+} that are bound to the protein initially. However, the metal displacement method using ^{203}Hg suffers from many drawbacks. It tends to overestimate the protein concentration due to the poor separation of the bound and unbound ^{203}Hg as well as due to the presence of other small molecules that bind to ^{203}Hg (115). Recently, a modified ^{203}Hg binding assay method was reported (116) in which the unbound ^{203}Hg were removed on a Sephadex G-10 column. Nevertheless, the detailed binding properties of Hg^{2+} to metallothionein have not been thoroughly investigated and the manner in which the Hg displaces the Cd^{2+} and Zn^{2+} and the subsequent binding of the Hg^{2+} to the protein is not well understood. In addition, the stoichiometry of Hg^{2+} binding has not been well established. Hence, the use of bound metal ions, in particular Hg^{2+}, as a marker for the estimation of protein concentration may result in considerable error at this time. Until the binding properties of these metal ions have been thoroughly characterized, one must be cautious in the assessment of the protein concentration based solely on metal replacement data.

The estimation of MT concentration using the polarographic technique was proposed by Olafson & Sims (117). It is based upon the heat

stability properties of the protein's thiol groups. The results obtained from this method appear to correlate well with the Cd-heme method (115). However, the polarographic method gives a consistently higher concentration for MT. Recently, the quantitation of the thiol groups in metallothionein has received much attention (118). One method, first introduced by Ellman (119), has proved to be a simple procedure for the estimation of protein concentration when the amino acid composition has been determined.

Though considerable structural information has been accumulated thus far, detailed studies on the metal binding properties of metallothionein have not been reported, and in particular, no data are available for MT containing metal ions other than Cd^{2+} and Zn^{2+}. Since Zn^{2+} is the major component in naturally occurring MT in liver and Cd^{2+} predominates in the MT induced by Cd^{2+} injection, the question that remains to be answered is: does the Cd^{2+} induce the synthesis of apo-MT and bind to this subsequently, or does it simply replace the Zn-containing MT already present *in vivo*? Detailed *in vitro* binding and metal replacement studies may help to answer this question. Moreover, a better understanding of the Cu^{+} and Hg^{2+} binding properties of metallothioneins is necessary in order to probe the binding sites involved in mixed-metal metallothioneins (e.g. Hg,Cd-MT and Cd,Cu-MT) synthesized *in vivo*. It is important to study how the Cu^{+} and Hg^{2+} are distributed between the two metal binding domains in MT.

The two metal clusters in MT appear to have different metal binding properties. Results from ^{113}Cd nmr experiments (98,122) have shown that in Cd,Zn-MT induced by Cd^{2+}, the Cd^{2+} is bound predominantly in the 4-metal alpha cluster (123), while Zn^{2+} is present in the 3-metal

beta cluster. On the other hand, Cu,Zn-MT isolated from calf liver was found to contain 3 Cu^{+} ions in the beta sites with the alpha sites occupied exclusively by Zn^{2+} (73).

The order of Cd^{2+} binding to apo-MT reported recently (124) suggests that Cd^{2+} incorporation in MT takes place in a cooperative manner, with the selective formation of the alpha cluster structure prior to the binding of Cd^{2+} to the beta cluster. However, a different mechanism for the reconstitution of Co-MT from apo-MT was suggested from ESR studies (108). These results indicate a stepwise reaction in which magnetically non-interacting high spin complexes were formed when up to 4 Co^{2+} ions were added, and the magnetically interacting cluster structures were formed upon further addition of Co^{2+} (108).

The recent isolation of the alpha cluster from rat liver MT (123,125) makes it possible to study the spectroscopic properties of this fragment independently and also to investigate if the 3-metal cluster affects the metal binding properties of the 4-metal cluster.

In this work, metallothioneins obtained from three different sources: rat liver, guinea pig liver, and crab have been characterized using absorption, circular dichroism (CD) and magnetic circular dichroism (MCD) techniques. The three metallothionein proteins are compared with respect to their reactions with protons as well as with metal ions (Chapter 3). The absorption and MCD spectra of a series of model compounds of Cd^{2+}, Hg^{2+} and Cu^{+} with 2,3-dimercaptopropanol (BAL) that mimic the binding site of MT are described in Chapter 4. Finally, metal replacement studies with Hg^{2+}, a toxic nonessential metal and Cu^{+}, an essential, but potentially, toxic metal, are described in chapters 5 and 6. A sample of alpha fragment obtained

from rat liver MT was also studied to determine its metal binding properties and to probe the changes in the Cd^{2+} cluster binding upon metal replacement.

CHAPTER 2: GENERAL EXPERIMENTAL

2.1. PROTEIN PREPARATIONS

Sprague Dawley rats were obtained from Canadian Breeders (Montreal, Quebec) weighing about 150-200g. They were kept in a galvanized steel cage, in a temperature-controlled room with a 12-hour light and dark cycle adjustment and with free access to food and water (Purina rat chow, Ralston Purina Co., St. Louis, MO). All the rats were kept for 1 week before the Cd^{2+} injections were started. They were injected with an aqueous $CdCl_2$ solution prepared by dissolving $CdCl_2.2.5\ H_2O$ in triply distilled water (3 mg Cd/mL). The rats were injected subcutaneously every other day at a dose rate of 3 mg Cd/kg body weight. A total of 11 injections were given and the rats were sacrificed about 12 hours after the last injection by using Nembutal (60 mg/kg body weight). The livers were removed and perfused in a normal manner with 0.9% NaCl solution and then chilled to 0^{o} C. The livers were weighed and cut into small pieces and homogenized with an equal volume of 0.25 M sucrose/Tris buffer at pH 7.4. The homogenates were then centrifuged at 12,000 rpm (at 5^{o} C) for 15 mins. The supernatant was removed and the pellets recentrifuged in an equal volume of the same buffer. The pooled supernatant was applied to a Sephadex G-75 column (Pharmacia, 2.5 cm x 95 cm) and eluted with a 30 mM Tris-HCl buffer, pH 8.0. The fractions were collected using a Buchler Fractomette Alpha 200 fraction collector at a rate of 15 drops/min. A total of 100 tubes (5 mL volume) were collected and the metallothionein fractions were determined by atomic absorption analysis for the presence of both Cd^{2+} and Zn^{2+}. The Sephadex G-75 elution pattern is depicted in FIG. 3. The appropriate fractions were

FIG. 3 Typical elution profile of metallothionein on a Sephadex G-75 column. The supernatant was applied to the column (2.5 cm x 95 cm, Pharmacia), which had been equilibrated with 30 mM Tris/HCl buffer, pH 8.0. The protein fractions were eluted with the same buffer solution. The Cd^{2+} and Zn^{2+} content of each fraction was determined by atomic absorption spectrophotometry. The absorption spectrum of each fraction was also recorded to monitor the changes in A_{250}. The metallothionein fraction (tubes # 64-86) was freeze dried for further purification.

Elution profile of Cd,Zn–MT on a G75 Sephadex column

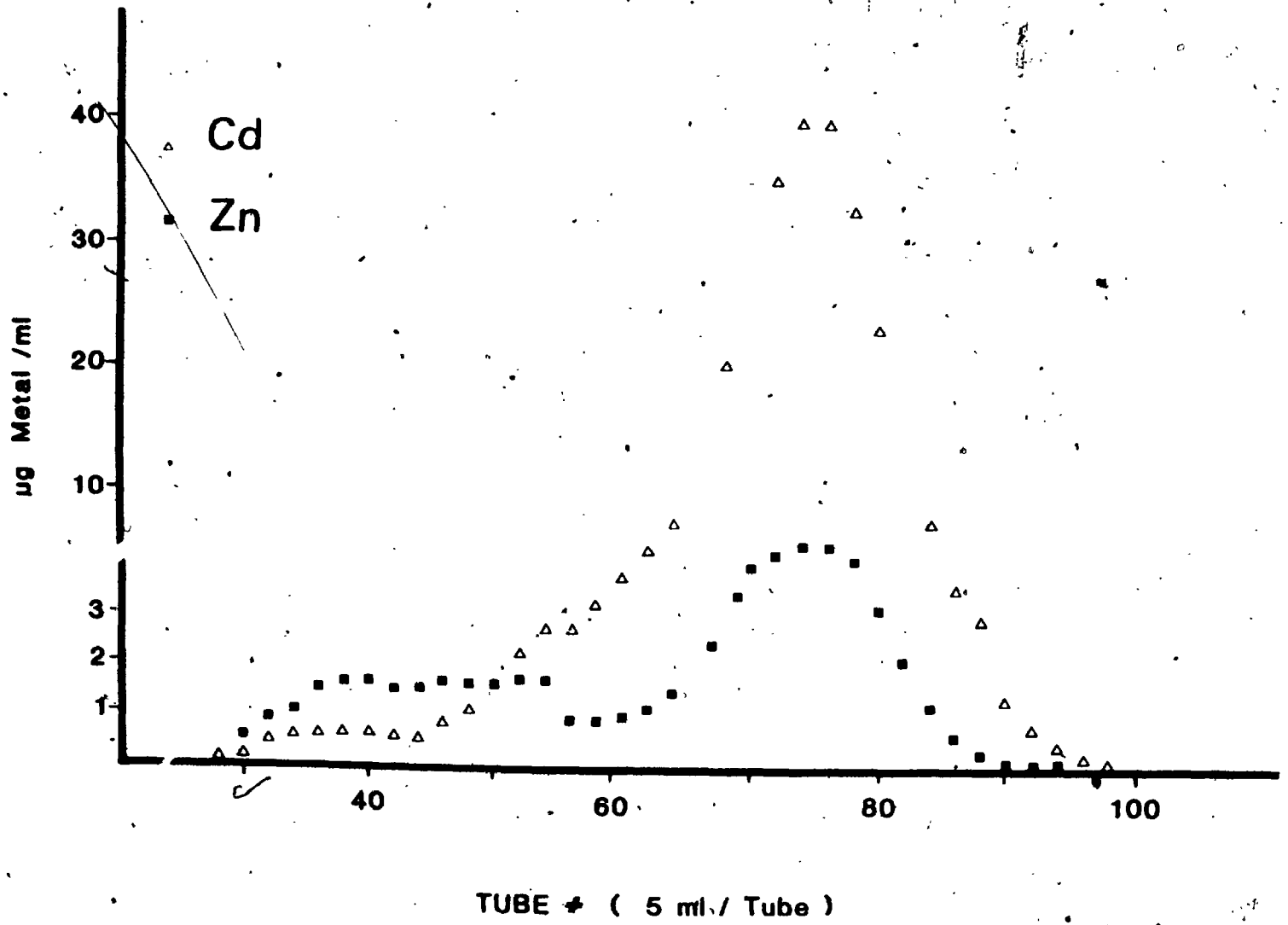

then freeze dried and reapplied on a second Sephadex G-75 or G-75 superfine (Pharmacia) column of the same dimension and eluted using the same Tris buffer solution as the previous column. The freeze dried protein was then applied to a Sephadex G-50 column (2.0 cm x 60 cm), which had been equilibrated with triply distilled water, in order to remove the Tris buffer from the protein. Some of the samples used were further purified using a DEAE column, or by gel electrophoresis, in order to separate the two isoforms of metallothionein, designated MT 1 and MT 2.

The Cd,Zn-MT 1 and 2 used in some of the metal replacement studies were gifts from Dr. Jadwiga Szymanska, Lodz, POLAND. The preparation and purification of this protein has been described previously (126). Crab Cd,Zn-MT 1 was a gift from Dr. R. Olafson (15) and the guinea pig Cd,Zn-MT 2 was prepared by Dr. E. Lui (127). The rat liver alpha fragment sample was prepared by Dr. A. Zelazowski according to Winge & Miklossy (123) with some modifications. Full details of the preparative procedure will be published shortly (125).

2.2. METAL CONCENTRATION DETERMINATION

Metal concentration analysis for most metallothionein solutions was carried out on a Varian 875 equipped with a PC 55 autosampler (flame mode with an air/acetylene flame). The concentration mode was used and the direct readout of the metal concentration (ppm) was recorded. At least two determinations were carried out for each protein solution. All calibration solutions were prepared in triply distilled water, at pH 2. All certified Atomic Absorption 1000 ppm standard solutions were obtained from Fisher. The protein samples were diluted in a pH 2 solution and assayed directly into the flame or graphite furnace

without prior preparation. The flameless mode, Varian GTA 95 equipped with an autosampler, was used to analyse solutions in which the metal concentrations were in the ppb range.

Mercury concentrations were determined using the hydride generation method (Perkin Elmer 5000 atomic absorption spectrometer equipped with the hydride generation accessary, or a home-made glass cell and reaction vessel adapted to the Varian 875). Fresh standard solutions were prepared in 1.5 % H_2SO_4; 100 µL of the protein solution were diluted into 10 mL of a 1.5 % H_2SO_4 solution and 100 µL of a 3 % $NaBH_4$ solution were used as the reducing agent. The mercury concentration in solution was then determined from a calibration curve obtained with the standard solutions.

2.3. PROTEIN CONCENTRATION DETERMINATION

Protein concentrations were determined by the quantitative measurement of the titratable thiol groups (119). Solutions of 6 M-guanidine hydrochloride/50 mM EDTA, pH 8.0 and 50 mM 5,5'-dithiobis-(2-nitrobenzoic acid) [DTNB] in 50 mM sodium phosphate buffer, pH 7.5, were prepared (118). 1.5 mL of the 6 M guanidine solution and 100 µL of the DTNB solution were put into a 1 cm quartz cell with a magnetic stirrer. The solution was mixed by stirring and the absorption spectrum obtained. 100 µL of the protein solution was then added to this mixture and stirred before the absorption spectrum was recorded one hour later. The solution developed a yellow colour. An extinction coefficient, $\varepsilon_{412} = 13600\ L\ mol^{-1}cm^{-1}$, was used to calculate the concentration of the thiol groups. Since the protein contains 20 thiol groups per mole of protein, its concentration in solutions can then be determined. However, for the earlier experiments, the protein

concentrations were calculated using ε_{250}= 57100 L $mol^{-1}cm^{-1}$, a value determined specifically for rat liver Cd,Zn-MT (128). A sample of the Cd,Zn-MT was subjected to several cycles of purification and freeze drying until a constant weight of the protein was obtained. The absorption spectrum of a solution containing a known amount of this protein was measured and the extinction coefficient determined.

2.4. OPTICAL MEASUREMENTS

All absorption spectra were recorded on a Cary 219 spectrophometer using a 1 cm path length quartz cell, unless indicated otherwise. The CD spectra were measured using a JASCO J5 with either one of the following two modifications: (a) JASCO J5 modified to S-20 specifications, (b) modified using an Ithaco 391 Lock-In amplifier, Morvue photoelastic modulator, Hamamatsu R375 phototube and a JASCO J500 programmed power supply. The MCD spectra were recorded at 5.5 T field (using an Oxford Instruments, SM2 magnet). The CD spectrometer was calibrated using a d-10-camphor sulfonic acid solution with $[\theta]_{289}/\varepsilon_{290}$= 226 (129) and the MCD intensity was calibrated with an aqueous solution of $CoSO_4$, with $[\theta]_M$(505 nm) = -61.6 deg cm^2 $dmol^{-1}$ T^{-1} or $\Delta\varepsilon_{505nm}$= -1.876 X 10^{-2} L mol^{-1} cm^{-1} T^{-1}.

All data were digitized directly from the amplifier. Each MCD spectrum reported here has had the zero field CD spectrum subtracted from it. The majority of the spectra presented here are direct computer plots. Some of them are retraced computer plots.

2.5. OTHER MEASUREMENTS AND CHEMICALS

All pH measurements were made at 25° C on a CORNING 125 pH meter using a FISHER microprobe combination electrode. Purified FISHER buffer solutions (pH 2,7 and 10) were used to standardize the pH meter.

CHAPTER 3: SPECTROSCOPIC PROPERTIES OF METALLOTHIONEINS

3.1. INTRODUCTION

A number of spectroscopic techniques has been utilized to probe the binding site structure and metal binding properties of MT. Among the techniques used, the most successful in providing structural information on the MT binding sites is the ^{113}Cd nmr, from which the two metal cluster structures with tetrahedrally coordinated metal ions were proposed for the binding site structure in MT (97-99). An Early study on the characterization of MT using absorption and CD spectroscopies was reported by Rupp & Weser (82). The spectral changes in the CD spectrum of Zn-MT in the presence of a high concentration of protons and Cd^{2+} ions have been described (82). Early studies using MCD spectroscopy have also established the potential of this technique in probing the metal binding sites in metalloproteins (106,107,130,131). Hence in addition to absorption and CD spectroscopies, MCD can provide further information on the physicochemical properties of metallothionein. Furthermore, MCD spectroscopy can be used to monitor the changes in the binding site geometry during metal replacement experiments.

In this chapter, 3 metallothioneins isolated from different sources (rat guinea pig and crab) are characterized using absorption, CD and MCD spectroscopies. The metal binding properties of each metallothionein protein in the presence of high proton, Cd^{2+} and Zn^{2+} concentrations were studied. In addition, ^{113}Cd nmr was also used to monitor the release of Cd^{2+} from the binding sites and the reconstitution of the apo-MT.

3.2. EXPERIMENTAL

3.2.1. Protein Preparation

All protein preparations were carried out as described in Chapter 2.

3.2.2. pH Experiments

All protein solutions were prepared in triply distilled water. The pH of the solution was adjusted by the addition of μL aliquots of concentrated HCl and NaOH solutions directly into a 1 cm cuvette and the solution was mixed immediately.

3.2.3. Cd^{2+} and Zn^{2+} Loading Experiments

The Cd^{2+} solution was prepared by dissolving $CdCl_2.2.5H_2O$ in triply distilled water, with a concentration of 1.0×10^{-2} M. $ZnCl_2$ was used to prepare a solution with a concentration of 0.94 M for the Zn^{2+} loading experiment. The addition of Cd^{2+} and Zn^{2+} into the Cd,Zn-MT solution contained in a 1 cm cuvette was carried out using calibrated μL Finnpipettes (variable volume, 0-5 μL and 5-50 μL, precision, ± 5%).

3.2.4. ^{113}Cd nmr experiment

3.2.4.1 Preparation of ^{113}Cd,Zn-MT

^{113}CdO (96.3% ^{113}Cd, from Oak Ridge National Laboratory) was converted to $^{113}CdCl_2.1.5H_2O$ using concentrated HCl. A solution prepared with a concentration of 2.8 mg Cd/mL was used for 9 subcutaneous injections into Sprague Dawley rats. The protein contafning ^{113}Cd was isolated and purified as reported earlier. The freeze dried protein (420 mg) was then dissolved in 1.5 mL of 10% D_2O solution, giving a Cd^{2+} concentration of 6.3 mM.

3.2.4.2. nmr spectra

This experiment was carried out in collaboration with Dr. P.A.W. Dean (Chemistry Department, U.W.O). All nmr spectra were recorded by

Dr. Dean.

The 88.7 MHz ^{113}Cd nmr spectra at ambient temperature were obtained with broad band proton decoupling using a Bruker WH400 nmr spectrometer. The spectrum of the native protein (at pH 7.9) in a 10 mm od nmr tube was measured with 13600 90° (39μs) pulses at 25 min^{-1} and a spectral width of 20 kHz and that of the reconstituted protein with 11700 90° pulses at 8 min^{-1} and a spectral width of 62.5 kHz. The spectrum of the acidified protein required 20 45° pulses at 3 min^{-1} with a spectral width of 50 kHz. The spectra were referenced to 4 M $Cd(NO_3)_2$ (aq) by sample interchange and converted to 0.1 M $Cd(ClO_4)_2$ as reference using δ(0.1 M $Cd(ClO_4)_2$) = δ(4 M $Cd(NO_3)_2$)-65 ppm; chemical shifts to lower shielding than the reference were taken as positive. The spectrum shown in FIG. 11 has 20 Hz line broadening. A few of the ^{113}Cd nmr spectra of free Cd^{2+} were measured using an XL-100 spectrometer system operating at 22.2 MHz. No proton decoupling was used and typically ca. 18000 30° (24 μs) pulses at 17 min^{-1} with a spectral window of 10 kHz gave an adequate signal:noise for a 0.08 M sample of "cold" $CdCl_2$ in a 12 mm od sample tube.

3.2.5. Apo-MT experiments

3.2.5.1. Dialysis experiments

Preliminary dialysis experiments were carried out to determine the length of time required for the complete removal of all metal ions from Cd,Zn-metallothionein to give the apo-MT.

(i) ^{109}Cd-MT

7 solutions of ^{109}Cd-MT (2.5 mL) in a pH 7, 0.05 M phosphate buffer were dialysed against triply distilled water at pH 2.2 for 0.5, 1.25, 3, 6, 7, 8 and 24 hours, respectively. Dialysis tubing with a molecular

weight cutoff of 3500 was used. The ^{109}Cd content of each solution after dialysis were determined by Gamma counting (Searle Instrument).

(ii) Cd,Zn-MT

Aliquots of a Cd,Zn-MT solution (2.5 mL) were dialysed in a similar manner as described above for the ^{109}Cd-MT experiment. The Cd^{2+} and Zn^{2+} contents for each solution was measured using a Jarrel Ash 810 spectrometer (flame mode).

(iii) $CdCl_2$

A series of $CdCl_2$ solutions were dialysed at pH 2.2 for up to 6 hours. The Cd^{2+} concentration in each of the dialysed solution was determined as described above.

3.2.5.2. Preparation of apo-MT by dialysis at low pH and the reconstitution of apo-MT.

The apo-MT was prepared by dialysing a rat liver Cd,Zn-MT 1 (2.5 mL) solution in 900 mL of deaerated, triply distilled water at pH 1 (dialysis tubing with molecular cutoff of 3500 was used) for 24 hours, with 2 changes of solution. AAS measurements for the apo-MT sample showed that there was no Cd^{2+} or Zn^{2+} present. The Cd^{2+} solution was added under nitrogen and μL aliquots of a 2 M Tris solution were used to raise the pH of the solution up to 7.3.

3.2.5.3. Preparation of apo-MT by proton displacement method and the reconstitution of apo-MT.

The apo-MT was prepared by the addition of concentrated HCl to a deoxgyenated solution. The apo-MT solution obtained at pH 2.3 was then reneutralized to pH 7.9 to study the rebinding of Cd^{2+}.

3.2.5.4. Preparation of apo-MT using a gel column.

A Sephadex G-25F (Pharmacia, 2 cm x 17 cm) column was equilibrated

with a pH 0.9 solution. The Cd,Zn-MT protein solution was acidified before it was applied on the column and the protein fractions were eluted with a pH 0.9 solution. The column separation was monitored by the changes in the intense UV absorption edge near 220 nm. The rebinding of Cd^{2+} to the apo-MT was studied by adding 5×10^{-7} moles of Cd^{2+} to a 2 mL aliquot of the apo-MT solution from the column. The absorption and CD spectra of the solution at pH 0.9 were recorded. The pH of this solution was raised to 7.2 with a μL aliquot of a NaOH solution. The absorption and CD spectra of the solution at pH 7.2 were obtained.

3.2.6. Cd^{2+} loading and dialysis experiments

Dialysis experiments were carried out in triply distilled water (dialysis tubing with a molecular weight cutoff of 3500 was used) for a total dialysis time of 9 hours with two changes of water. All solutions were degassed with nitrogen and the dialysis water was bubbled with nitrogen throughout the dialysis.

3.2.7. Cd^{2+}- red blood cell (RBC) hemolysate experiment

2 mL volumes of Cd,Zn-MT 2 in Tris/HCl, pH 8.6 solutions and containing different amounts of added Cd^{2+} were prepared. The solutions were allowed to equilibrate for 5 mins. 0.2 mL aliquots of Red Blood Cell (RBC) hemolysate were then added and the solutions were heat treated (in a boiling water bath at about 100^{o} C) for 1 min. After centrifuging for 5 mins, the solutions were filtered to remove the precipitates that were formed during the heating process. The metal concentrations were measured both before the addition of the hemolysate and after heat treatment and filtration. This procedure follows closely that outlined by Onosaka & Cherian (115).

3.2.8. Optical spectra

As previously described in Chapter 2

3.3. RESULTS

3.3.1. Absorption, CD and MCD spectra of metallothioneins

FIG. 4A and 4B show the absorption, CD and MCD spectra for the rat liver Cd,Zn-MT 1 and an alpha fragment sample prepared from the same species. Both species exhibit remarkably similar absorption, CD and MCD spectra. The absorption shoulder for the alpha fragment is significantly better resolved, possibly due to the absence of the S -> Zn charge transfer transition. Both the CD spectra show the characteristic, derivative-shaped signal: 258 nm(+), 238 nm(-) and 225 nm(+). The 225 nm CD band in the alpha fragment sample exhibits a much higher intensity than that observed for the Cd,Zn-MT 1 at a similar wavelength. The MCD spectrum is characterized by a near-symmetrical band with the negative trough in the 240 nm - 260 nm region.

FIG. 5A and 5B show the absorption, CD and MCD spectra of the guinea pig Cd,Zn-MT 2 and crab Cd,Zn-MT 1, respectively. Though the absorption, CD and MCD spectra of the rat liver and guinea pig MT's resemble each other closely, it is clear that the crab Cd,Zn-MT 1 exhibits a significantly different CD spectrum as shown in FIG. 5B. It is characterized by two positive bands, at 258 nm and 234 nm. This suggests that the spatial arrangement of the amino acid residues in the metal binding-sites are quite different in the crab protein.

3.3.2. pH experiments

In order to understand better the biological sequence of events that result in the formation of Cd,Zn-MT following an increase in the Cd^{2+} content in liver, it is important to study the uptake and release of

FIG. 4 (A) The absorption, CD and MCD spectra for native rat liver Cd,Zn-MT 1. (B) The absorption, CD and MCD spectra for a rat liver alpha fragment solution. All spectra were measured in a 1 cm cuvette, at 25° C. The units for ε and $\Delta\varepsilon$ are L mol^{-1} cm^{-1}. The units for $\Delta\varepsilon_M$ are L mol^{-1} cm^{-1} T^{-1}. The majority of the absorption, CD and MCD spectra reported in this work was replotted directly by the computer. In the absorption spectrum the noise level is equivalent to the pen width. The error associated with the CD and MCD spectra is small in the 350–240 nm region, while it is slightly higher below the 240 nm region due to the increase in absorbance.

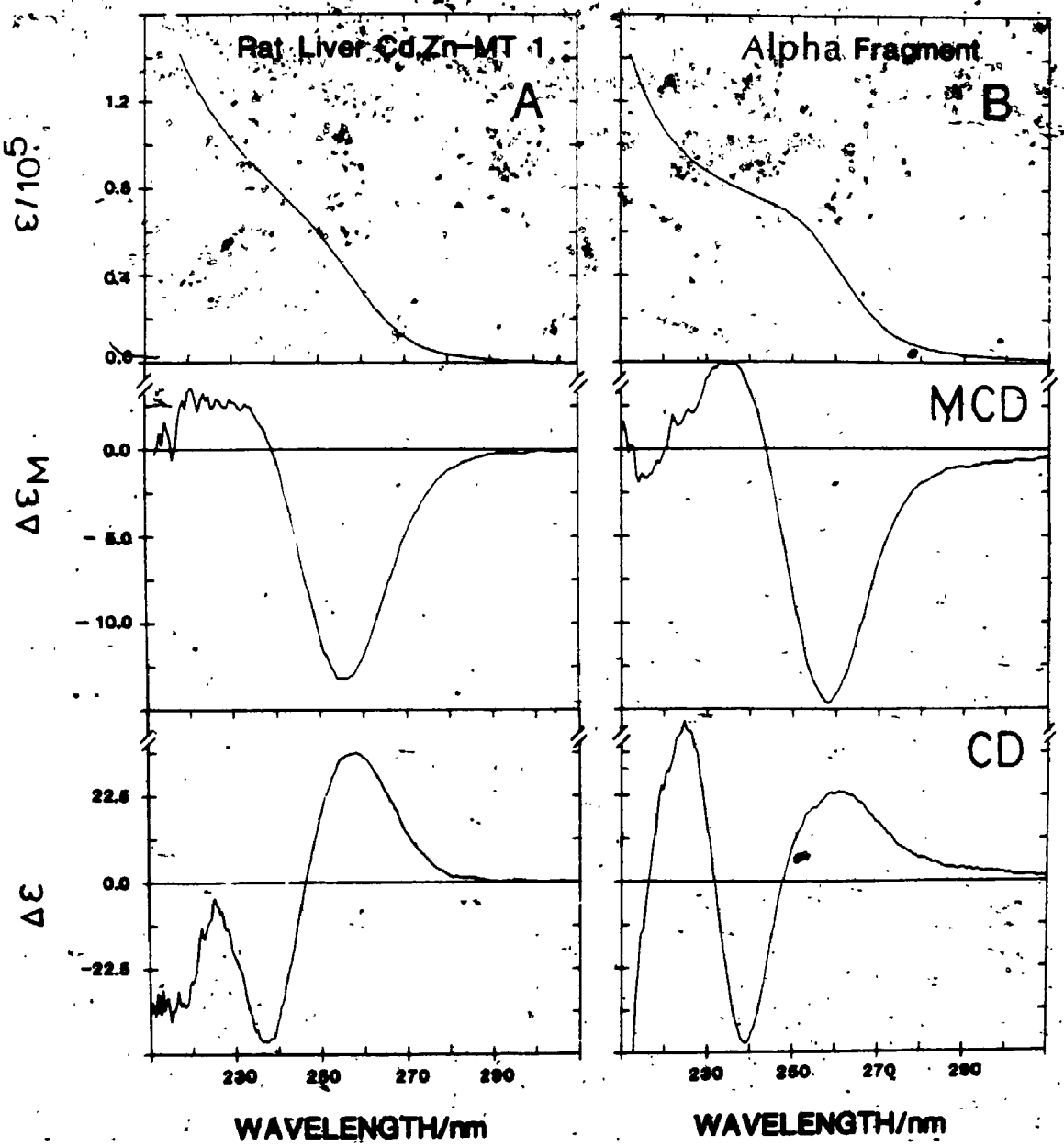
Rat Liver Cd,Zn-MT 1
A
Alpha Fragment
B
MCD
CD
ε/10^5
ΔεM
Δε
1.2
0.8
0.4
0.0
0.0
- 5.0
- 10.0
22.5
0.0
-22.5
230
250
270
290
WAVELENGTH/nm

FIG. 5 . (A) The absorption, CD and MCD spectra for native guinea pig Cd,Zn-MT 2. (B) The absorption, CD and MCD spectra for native Scylla Serrata crab Cd,Zn-MT 1. The units for ε and $\Delta\varepsilon$ are L mol^{-1} cm^{-1}. The units for $\Delta\varepsilon_M$ are L mol^{-1} cm^{-1} T^{-1}.

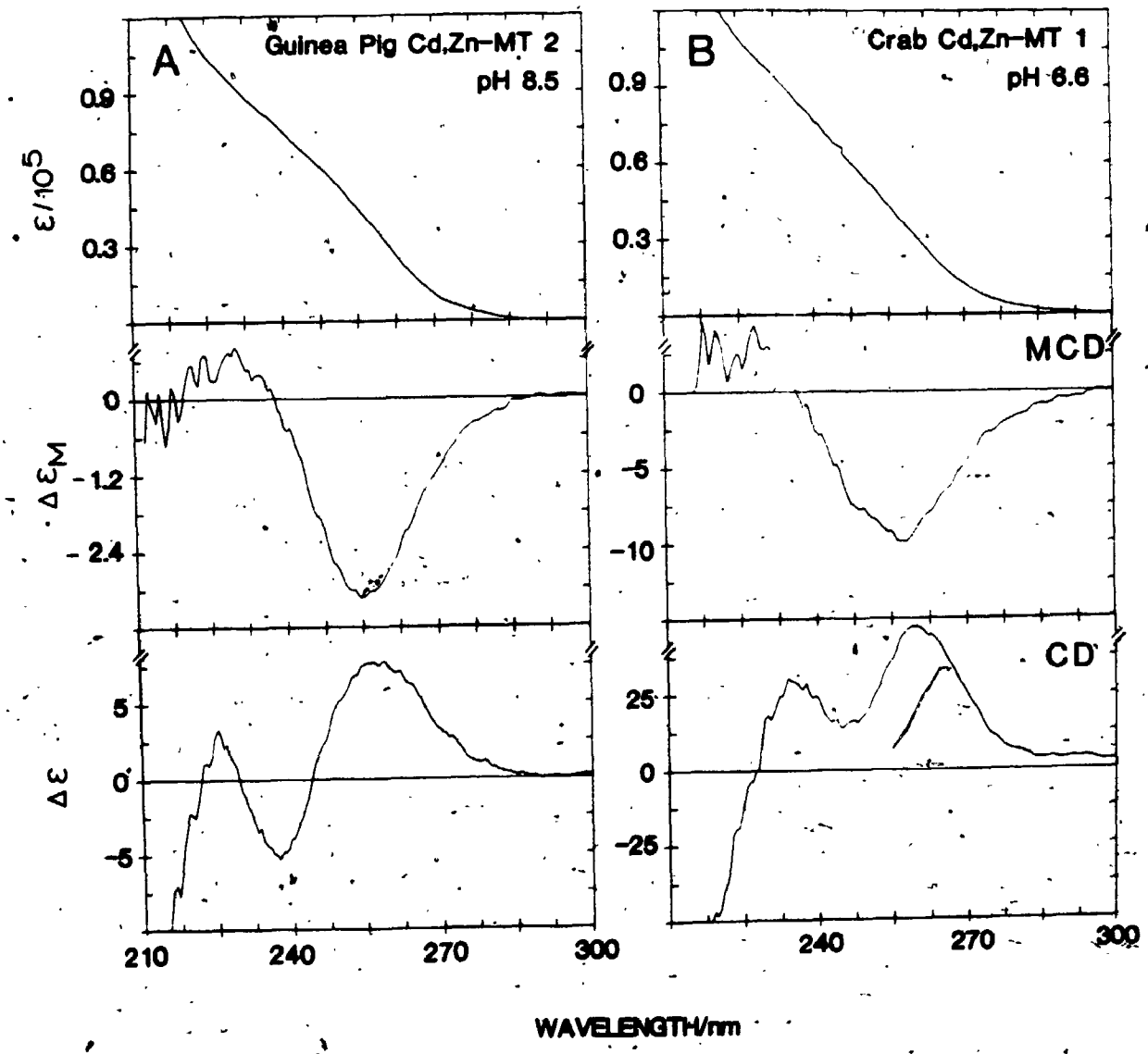
A
Guinea Pig Cd,Zn-MT 2
pH 8.5
B
Crab Cd,Zn-MT 1
pH 6.6
ε/10^5
0.9
0.6
0.3
MCD
Δε_M
0
-1.2
-2.4
0
-5
-10
CD
Δε
5
0
-5
25
0
-25
210
240
270
300
240
270
300
WAVELENGTH/nm

Cd^{2+} from metallothionein. The effect of pH on the binding of metal ions to metallothionein was studied for the three MT species (rat liver, guinea pig liver and crab). Results from these pH experiments demonstrate the stability of the protein at different pH values and also indicate if there are any changes in the stereochemistry of the metal binding sites as the metal ions are displaced from the native protein. TABLE IV shows the amino acid composition for each protein species. The crab MT has a smaller number of cysteine residues when compared to the rat and guinea pig MT's.

3.3.2.1. Rat liver Cd,Zn-metallothionein

FIG. 6 shows the results of a pH titration study of rat liver MT. No significant change in the absorption spectrum is observed until the pH is below 5. The large decrease in the intensity of the S->Cd charge transfer absorption band observed when the pH is taken below 5 suggests that the sulfur atoms have been protonated and dissociation of the metal ions has occurred. The final spectrum, obtained at pH 1.5, represents the apo-MT. The overall CD signal decreases in intensity as the proton concentration increases. During the early stage of the pH changes, it is observed that the 225 nm band in the CD is more susceptible to the effects of protonation than the rest of the spectrum. The MCD band envelope, which is sensitive to the geometry of the metal binding sites, shows a drop in intensity that follows the pH changes. As observed earlier for the absorption spectrum, the decrease in the MCD intensity becomes more significant below pH 5. Furthermore, a red-shift in the MCD band centre becomes apparent. The MCD spectrum at pH 4.2 gives a derivative-shaped signal and the negative band centre shows a red-shift of 4 nm. At pH 1.5, the MCD spectrum is

TABLE IV

AMINO ACID COMPOSITIONS OF METALLOTHIONEINS

Amino acid	Crab Cd,Zn-MT 1 (134)	Rat liver Cd,Zn-MT 1. (126)	Cd,Zn-MT 2	Guinea Pig Cd,Zn-MT 2 (127)
ASP	1	4	5	4
THR	3	3	3	2
SER	7	10	5	11
GLU	5	2	4	4
GLY	5	6	4	4
ALA	2	3	5	6
VAL	1	2	1	2
MET	0	0	0	1
ISOLEU	1	0	1	0
GLN	1	0	0	0
ASN	1	0	0	0
PHE	0	0	0	0
HIS	0	0	0	0
ARG	1	0	0	1
PRO	4	3	4	7
CYS	18	21	20	20
LYS	8	7	11	7

(# EXPRESSED AS RESIDUES PER MOLECULE CALCULATED FROM AMINO ACID ANALYSIS)

FIG. 6 The effect of pH on the absorption, CD and MCD spectra of rat liver Cd,Zn-MT. The pH of the solution in a cuvette was adjusted by adding μL aliquots of a concentrated HCl solution. The pH of the native protein was 7.5. The spectrum at pH 1.5 represents the apo protein. The units for ε and $\Delta\varepsilon$ are L mol^{-1} cm^{-1}. The units for $\Delta\varepsilon_M$ are L mol^{-1} cm^{-1} T^{-1}.

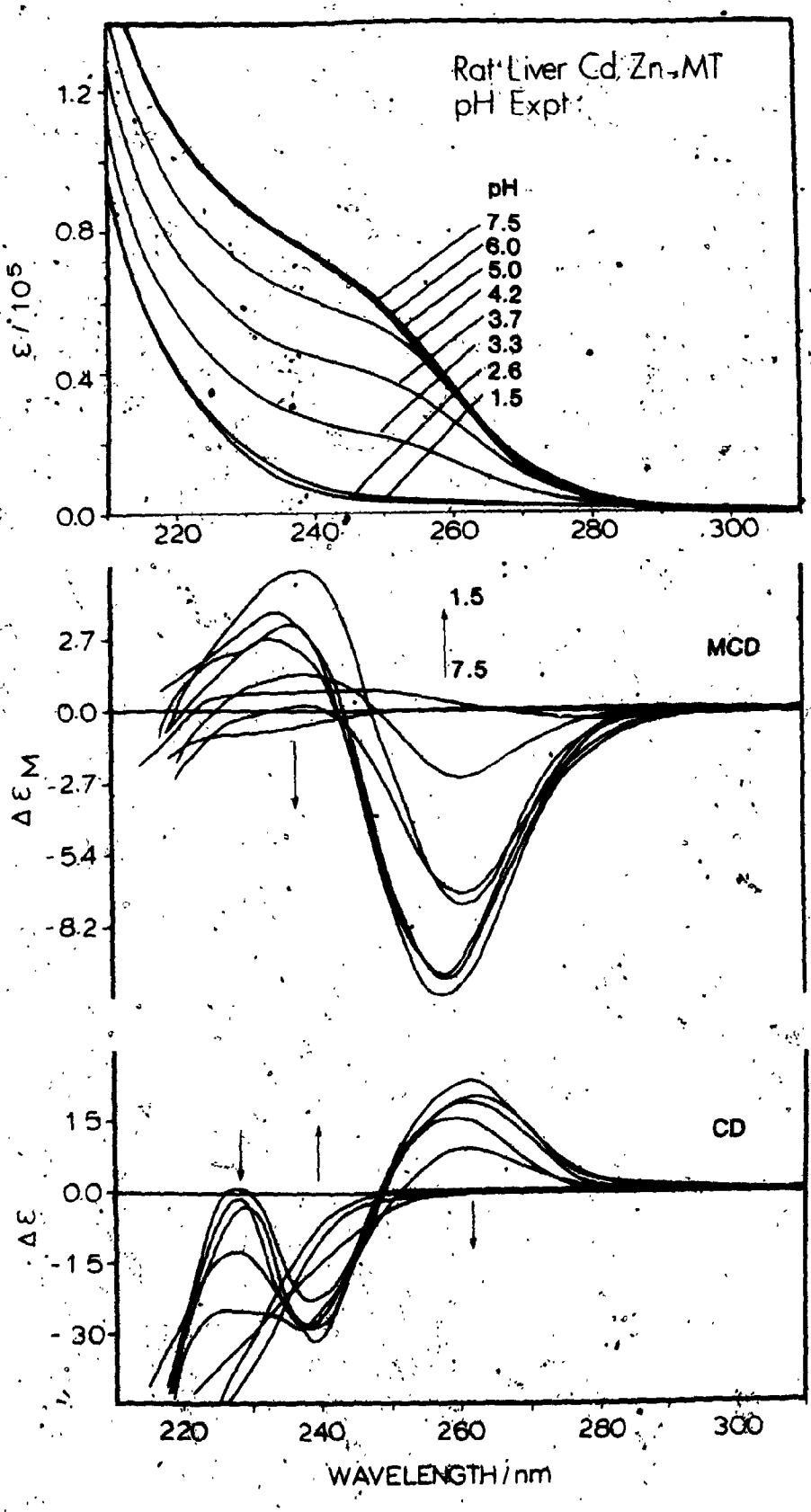
Rat Liver Cd, Zn-MT
pH Expt.
pH
7.5
6.0
5.0
4.2
3.7
3.3
2.6
1.5
ε / 10⁵
1.2
0.8
0.4
0.0
220
240
260
280
300
1.5
7.5
MCD
2.7
0.0
-2.7
-5.4
-8.2
Δε M
CD
1.5
0.0
-1.5
-3.0
Δε
WAVELENGTH / nm

featureless while the CD shows a flat region around 260 nm followed by a intense negative band which is due to the protein backbone.

3.3.2.2. Guinea Pig Cd,Zn-metallothionein

FIG. 7 shows the titration of the guinea pig MT with concentrated HCl. The experiment was carried out in the same manner as in the rat liver MT titration. The native guinea pig MT 2 has absorption, CD and MCD spectra that closely resemble that of the rat liver MT. The spectral characteristics of guinea pig MT include the 250 nm absorption shoulder, the derivative-shaped CD signal and the MCD envelope centred at 238 nm, with 231 nm(+) and 255 nm (+). The effect of pH on the absorption, CD and MCD spectra of the guinea pig MT 2 is very similar to that observed for the rat liver MT. No significant differences are seen in the spectra when the pH is lowered from 7.8 to 5.9. A further decrease in pH to 3.7 results in a drop in the 250 nm shoulder which signifies the protonation of the sulfur atoms on the cysteine residues. A corresponding decrease in both the MCD and CD spectra is apparent. A more significant change is the complete collapse of the 225 nm positive band in the CD spectrum at pH 3.7. The MCD band centre also shows a red-shift of 4 nm at this pH. Further reduction in the pH (to 3.1 and 2.3) results in the loss of intensity in the remaining bands in the absorption, CD and MCD spectra. The spectrum obtained at pH 2.3 represents that of the apo-MT.

3.3.2.3. Crab Cd,Zn-metallothionein

FIG. 8 shows the pH titration of a solution of crab Cd,Zn-MT 1. The crab native protein gives absorption and MCD spectra which are very similar to that of the rat and guinea pig MTs . In particular, in the MCD spectrum, the band shape and position (a negative trough at 252

FIG. 7 The effect of pH on the absorption, CD and MCD spectra of guinea pig Cd,Zn-MT 2. The pH of the native protein was 7.8. The pH of the solution was adjusted by adding μL aliquots of a concentrated HCl solution. The units for ε and $\Delta\varepsilon$ are L mol^{-1} cm^{-1}. The units for $\Delta\varepsilon_M$ are L mol^{-1} cm^{-1} T^{-1}.

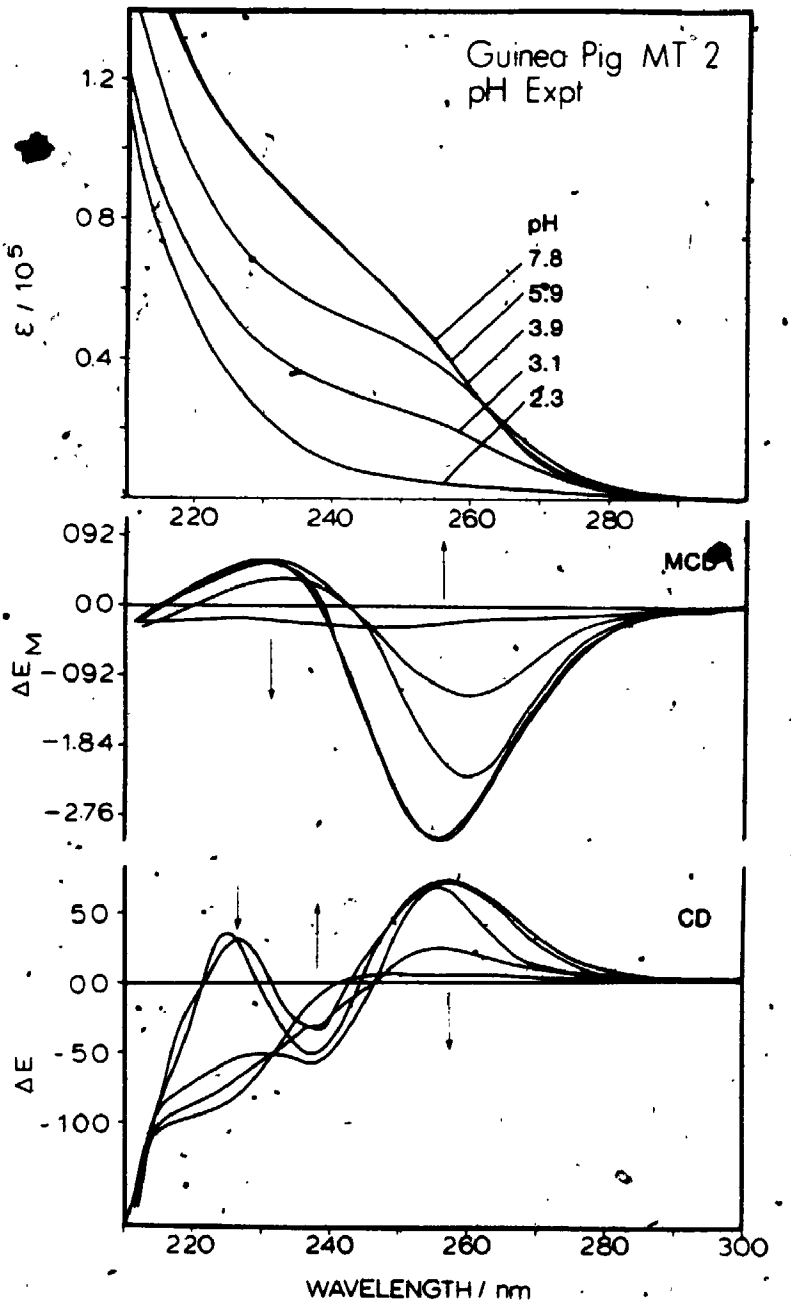
Guinea Pig MT 2
pH Expt
pH
7.8
5.9
3.9
3.1
2.3
ε / 10⁵
1.2
0.8
0.4
220
240
260
280
MCD
092
00
-092
-1.84
-2.76
ΔE_M
CD
50
00
-50
-100
ΔE
220
240
260
280
300
WAVELENGTH / nm

FIG. 8 The effect of pH on the absorption, CD and MCD spectra of Scylla Serrata crab Cd,Zn-MT 1. The pH of the native protein was 6.6. The pH of the solution was adjusted by concentrated HCl. The units for ε and $\Delta\varepsilon$ are L mol^{-1} cm^{-1}. The units for $\Delta\varepsilon_M$ are L mol^{-1} cm^{-1} T^{-1}.

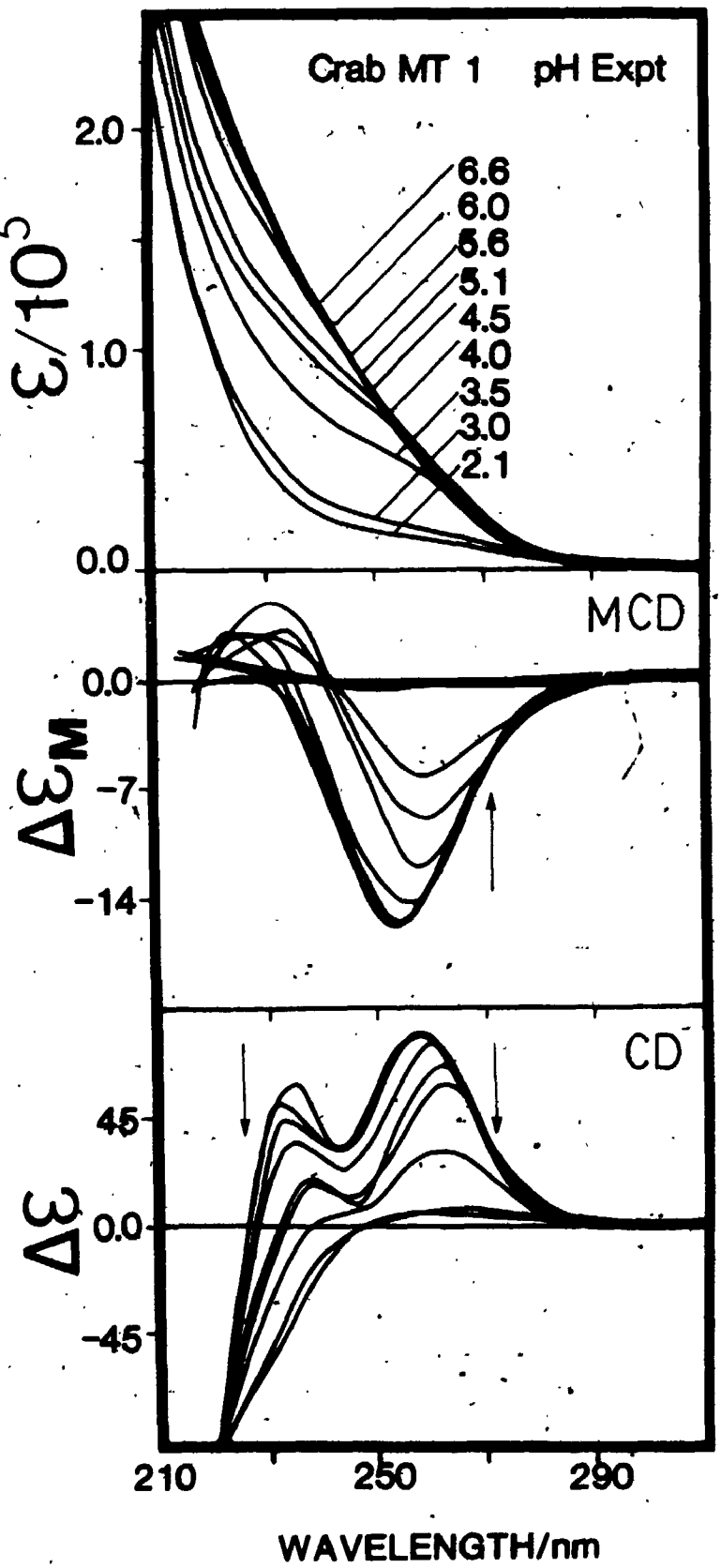
Crab MT 1 pH Expt
6.6
6.0
5.6
5.1
4.5
4.0
3.5
3.0
2.1
2.0
1.0
0.0
ε/10^5
MCD
0.0
-7
-14
Δε_M
CD
45
0.0
-45
Δε
210
250
290
WAVELENGTH/nm

nm, with the cross-over points at 241 nm and a positive peak at 232 nm) are the same. This suggests that the geometry of the Cd^{2+} binding sites in the crab is quite similar to that of rat and guinea pig MT's. However, a different CD spectrum is observed for the crab protein. It is characterized by 2 positive bands at 258 nm and 234 nm and the spectrum does not cross the centre line. The different CD spectrum observed for the crab protein suggests that there is a considerable difference in the arrangement of the cysteine residues around the Cd^{2+} binding sites. Nevertheless, the crab MT does behave in a similar manner to the effects of low pH as do other MT's. As observed earlier with the rat and guinea pig MT's, the higher energy CD band is more sensitive to the effects of protonation. The 234 nm band in the crab decreases in intensity when the pH of the solution is lowered from 6.6 to 5.6, while the 258 nm band remains fairly constant. A similar red shift of about 4 nm is clearly observed in the MCD envelope when the pH is lowered to 4.5.

3.3.3. Apo-MT experiments

While the pH experiments provide information on the relative stability of the metal ions bound to metallothionein, it is also important to study the uptake of Cd^{2+} in apo-MT. Zn-MT is known to occur naturally in tissues of organs such as the liver. The fact that Zn^{2+} is always present in Cd^{2+}-induced hepatic MT suggests that Zn^{2+} may be bound to apo-MT prior to the binding of Cd^{2+}. It has not been established whether the Cd,Zn-MT synthesized *in vivo* is made by the displacement of Zn^{2+} by Cd^{2+} in the existing Zn-MT or as a result of the binding of Cd^{2+} to apo-MT. The following experiments serve to provide information on the stability of apo-MT and the conditions for

the rebinding of metal ions. The apo-MT can be prepared by a number of methods: proton displacement (79,82,132), dialysis at low pH (87) and by the gel filtration method (133).

3.3.3.1. Cd^{2+} binding to apo-MT prepared by proton displacement.

FIG. 9 shows the absorption, CD and MCD spectra of a native Cd,Zn-MT at pH 8.5. When the pH of the solution is lowered to 2.3 by the addition of concentrated HCl, the 250 nm absorption band loses all its intensity as the sulfur atoms on the cysteine residues are protonated and the metal ions dissociate. Both the CD and MCD spectra at pH 2.3 show little intensity which further demonstrates the loss of Cd^{2+} from the MT binding sites. The absorption spectrum recorded after the pH of the solution has been raised from 2.3 to 7.9 shows the reappearance of the 250 nm shoulder. This suggests that the Cd^{2+} is once again bound to the thiolate groups resulting in a remetallated protein. The slight increase in the resolution of the 250 nm absorption is associated with a reproducible red-shift of approximately 4 nm in the MCD band. The CD intensity decreases slightly and there is no significant change in the overall CD envelope. This indicates that although the change in the conformation of the protein is apparently small following the pH cycle, the greater resolution of the 250 nm shoulder in the absorption is due to a shift to longer wavelengths rather than an increase in intensity.

3.3.3.2. ^{113}Cd nmr experiments

In addition to the optical techiques, ^{113}Cd nmr has been shown to be a very useful probe for monitoring the binding and release of the Cd^{2+} in these pH experiments. However, one drawback with the nmr technique is that a very high concentration of the protein sample (about $10^{-2}M$.)

FIG. 9 The effect of pH on the absorption, CD and MCD spectra of rat liver Cd,Zn-MT and the reconstituted apo-MT. The absorption, CD and MCD spectra of the native protein at pH 8.5 (————); the solution acidified to pH 2.3 (•• •• •• ••); spectra after the pH of the solution has been raised from 2.3 to 7.9 (—• —•—• —•).

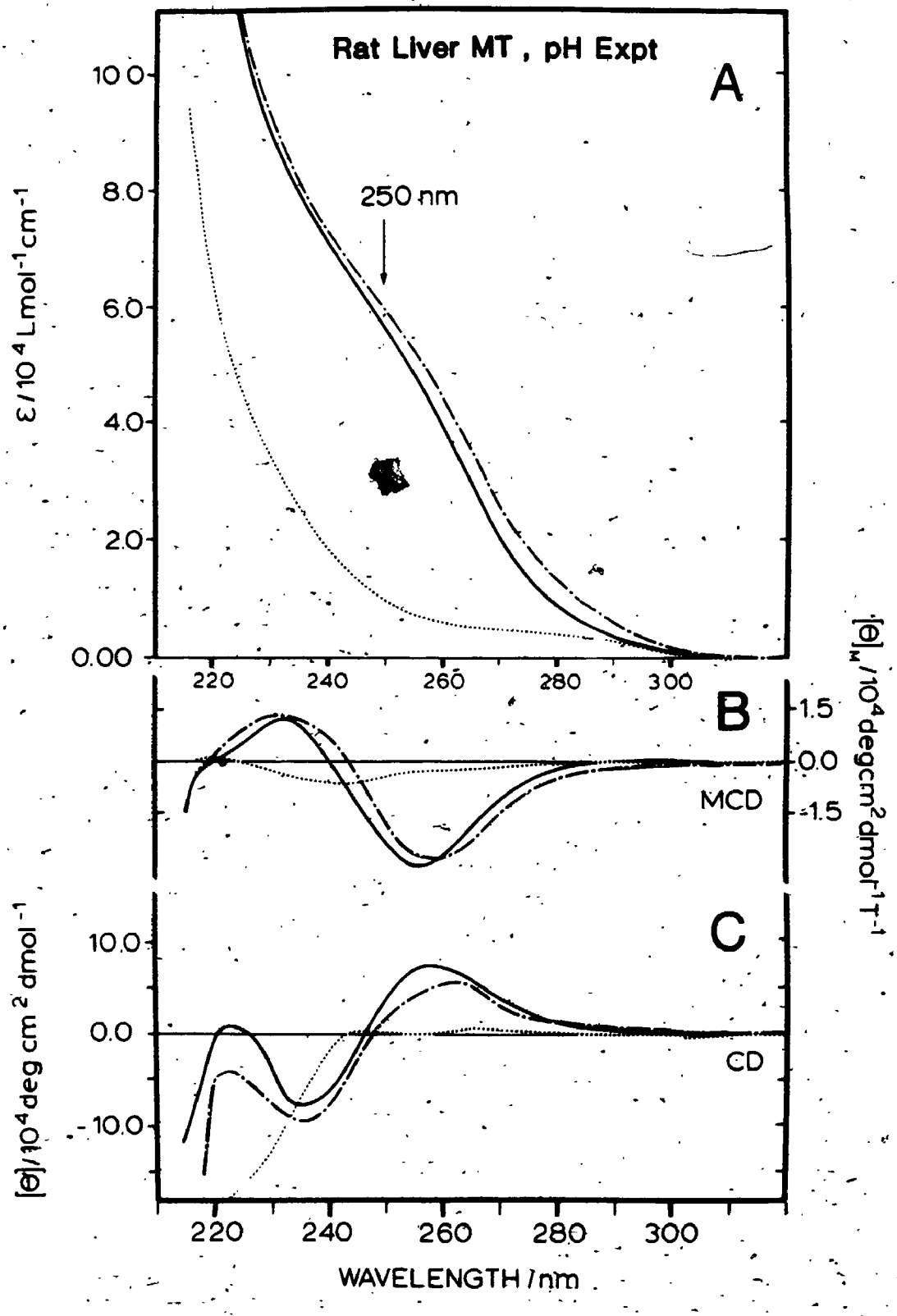
Rat Liver MT , pH Expt
A
250 nm
10.0
8.0
6.0
4.0
2.0
0.00
ε / 10⁴ Lmol⁻¹cm⁻¹
220
240
260
280
300
B
MCD
1.5
0.0
-1.5
[θ]M / 10⁴ degcm²dmol⁻¹T⁻¹
C
CD
10.0
0.0
-10.0
[θ]/10⁴deg cm² dmol⁻¹
WAVELENGTH / nm

is required to carry out the experiment. On the other hand, a 10^{-5} M solution is sufficient for optical measurements. In the following experiment, ^{113}Cd nmr was used to monitor the release of Cd^{2+} at low pH and the subsequent rebinding of the metal to MT when the pH was returned to about 7. FIG. 10 shows the absorption and CD spectra of native Cd,Zn-MT at pH 7.9 and the reconstituted protein at pH 7.6. The two spectra were obtained by diluting a μL aliquot of the concentrated nmr sample solution before and after the pH changes. They do not represent spectra of solutions with the same concentration and therefore should not be used for intensity comparisons. The absorption shoulder at 250 nm is observed for the native protein. The CD spectrum, however, contains only one positive band at about 260 nm followed by an intense negative band which is due to the protein backbone.

FIG. 11 shows the 88.7 MHz ^{113}Cd nmr spectra for the native protein and the reconstituted solution. The distinctive features are the nine areas of resonances centred on about 671, 665, 648, 639, 631, 626, 618, 612 and 602 ppm relative to 0.1 M $Cd(ClO_4)_2$. The apo-MT was obtained by acidification of the protein with aliquots of concentrated HCl to give pH 1.6, at which point a signal due to free Cd^{2+} was observed with a chemical shift of 186 ppm from 0.1 M $Cd(ClO_4)_2$. This shows that the dissociation of metal ions from the binding sites has taken place. Following neutralization of the protein solution to pH 7.6 with aliquots of concentrated NaOH, the absorption shoulder near 250 nm due to the S-> Cd charge transfer returns to approximately the same intensity as in the native MT. The return of the CD signal intensity (FIG. 10B) was also observed. More remarkable is the fact

FIG. 10 (A) shows the absorption and CD spectra of a native ^{113}Cd,Zn-MT solution at pH 7.9 and (B) shows the spectra recorded at pH 7.6 after the solution used for the pH 7.9 ^{113}Cd nmr spectra had been acidified to pH 1.6, and then reneutralized by the addition of aliquots of a concentrated NaOH solution. The solutions for the two sets of spectra were obtained by diluting μL aliquots of the concentrated protein solution used in the nmr experiment. Note that the absorbance values in (A) and (B) are different because two separate solution were used.

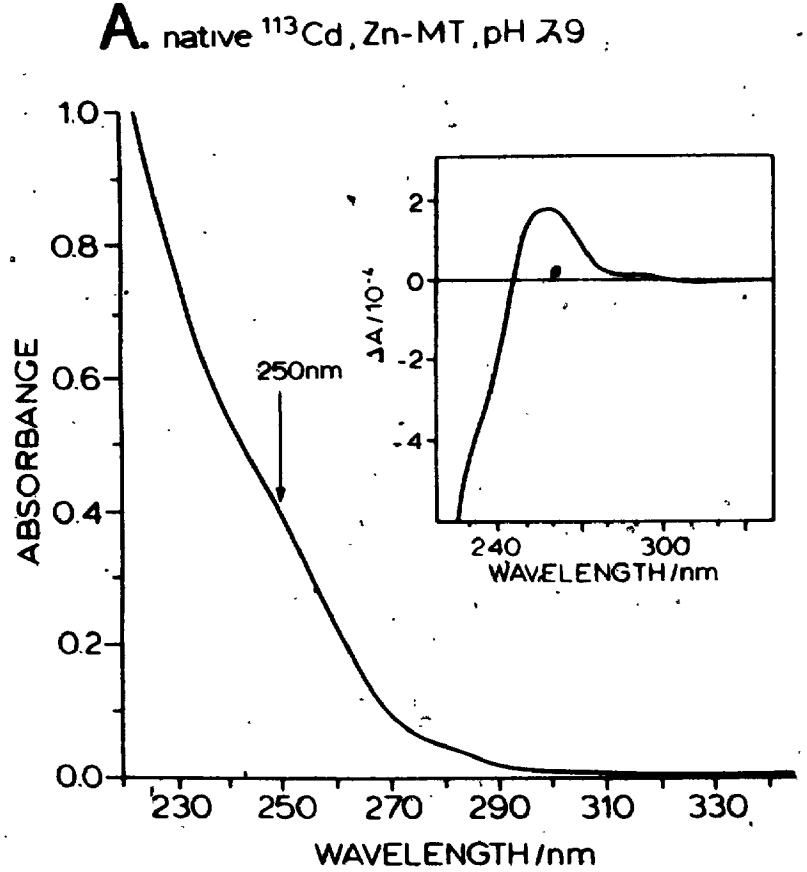
A. native ^{113}Cd, Zn-MT, pH 7.9
ABSORBANCE
1.0
0.8
0.6
0.4
0.2
0.0
250nm
230 250 270 290 310 330
WAVELENGTH/nm
ΔA/10^{-4}
2
0
-2
-4
240 300
WAVELENGTH/nm

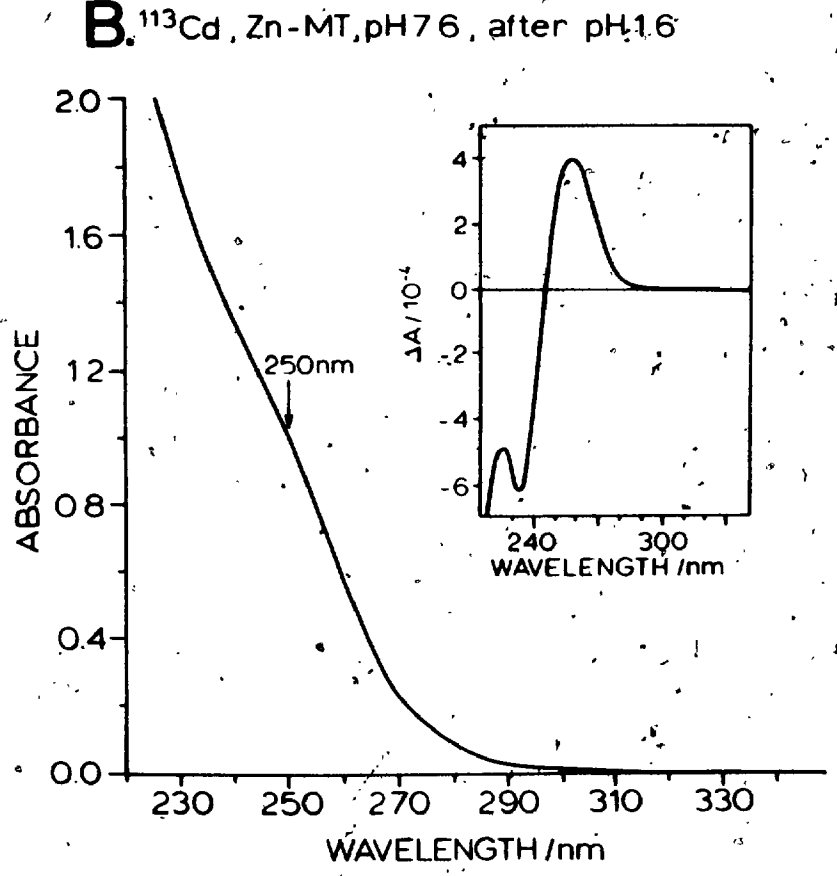
B. ^{113}Cd, Zn-MT, pH 7.6, after pH 1.6
ABSORBANCE
2.0
1.6
1.2
0.8
0.4
0.0
250nm
230 250 270 290 310 330
WAVELENGTH/nm
ΔA/10^{-4}
4
2
0
-2
-4
-6
240 300
WAVELENGTH/nm

FIG. 11 (A) shows the 88.7 MHz ^{113}Cd nmr spectrum of the native Cd,Zn-MT at pH 7.9 and (B) shows the spectrum of the reconstituted protein at pH 7.6, after the pH of the solution had been lowered to 1.6. The pH of the protein sample was adjusted using concentrated HCl and NaOH solutions. The spectra shown contain 20 Hz line broadening.

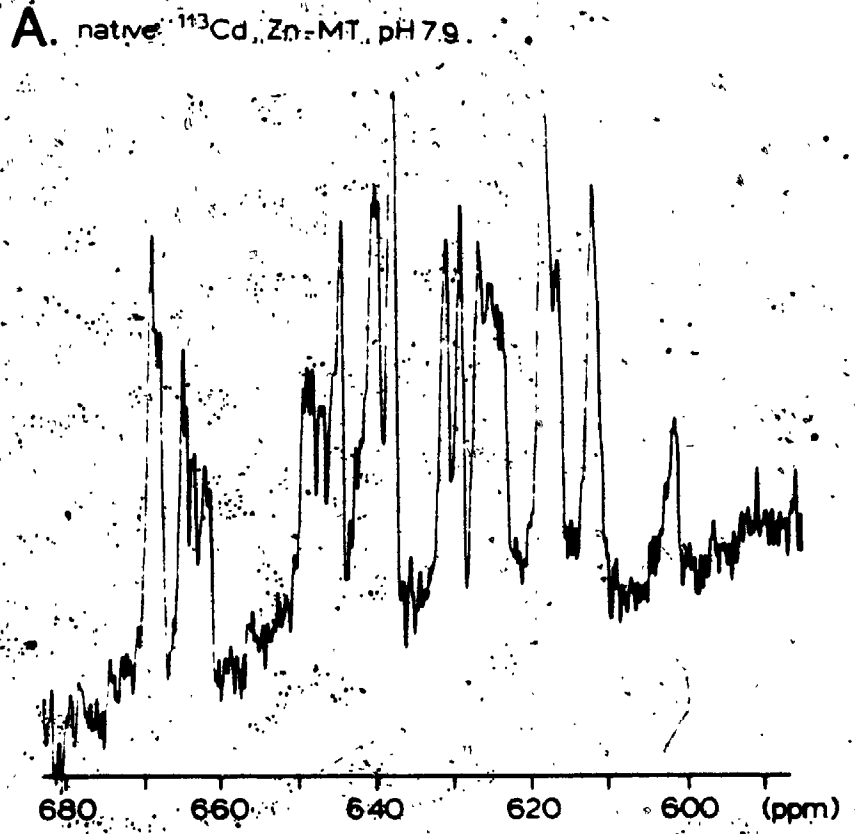
A. native ^{113}Cd, Zn-MT, pH 7.9
680
660
640
620
600
(ppm)

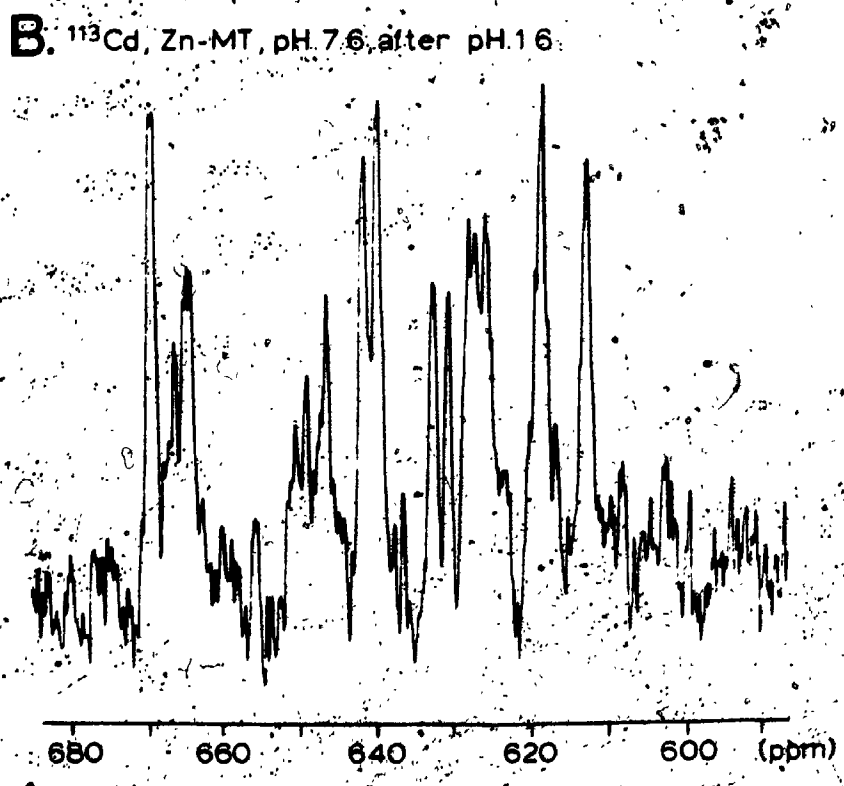
B. ^{113}Cd, Zn-MT, pH 7.6, after pH 1.6
680
660
640
620
600
(ppm)

that the ^{113}Cd nmr spectrum of the reconstituted protein resembles that of the native spectrum very closely.

The free-to-bound Cd^{2+} exchange was also studied by adding isotopically natural $CdCl_2$ to the reconsituted ^{113}Cd-MT at pH 6.6 (approximately 13,5 mol natural Cd/mol bound ^{113}Cd). The exchange between Cd^{2+} bound to MT and free Cd^{2+} was found to be facile, and within the time taken to record the ^{113} Cd nmr spectrum (18 hours) a complete scrambling between the pools of natural Cd^{2+} and ^{113}Cd has occurred.

3.3.3.3 The release of Cd^{2+} and rebinding to apo-MT.

FIG. 12 shows the effect of dialysis at pH 2 on the Cd^{2+} (and Zn^{2+}) content in MT. FIG. 12A shows the effect of dialysis of a MT labelled with ^{109}Cd. The release of Cd^{2+} after dialysis was monitored by ^{109}Cd gamma counting. The results show that more than 8 hours of dialysis at pH 2 is necessary to remove 95 % of the bound Cd^{2+}. An analogous experiment carried out with Cd,Zn-MT also shows similar behaviour (FIG. 12B). Moreover, it takes longer to remove Cd^{2+} than Zn^{2+} from MT which suggests that Cd^{2+} is bound more tightly than Zn^{2+}. A solution of $CdCl_2$ dialysed in the same manner shows that all Cd^{2+} are removed by about 6 hours.

3.3.3.4. Cd^{2+} binding to apo-MT prepared by dialysis

The Cd^{2+} rebinding properties of apo-MT were studied. The apo-MT was prepared by dialysis for 24 hours, at pH 1, to insure that all native Cd^{2+} ions were removed. All solutions were deaerated with nitrogen and the rebinding experiment was carried out under nitrogen to prevent air oxidation. FIG. 13 shows the absorption and CD spectra of the native protein before dialysis; the apo-MT at pH 1 and the solution after 7.6

FIG. 12 (A) A plot of the percentage of ^{109}Cd that remained in solutions of ^{109}Cd-MT after dialysis for different lengths of time. The ^{109}Cd concentrations were determined by Gamma counting. (B) Plot of the Cd^{2+} and Zn^{2+} content of a series of Cd,Zn-MT solutions after dialysis at pH 2.2. (C) Plot of the Cd^{2+} concentration of $CdCl_2$ vs dialysis time. The Cd^{2+} and Zn^{2+} concentrations were measured using a Varian 875 atomic absorption spectrometer.

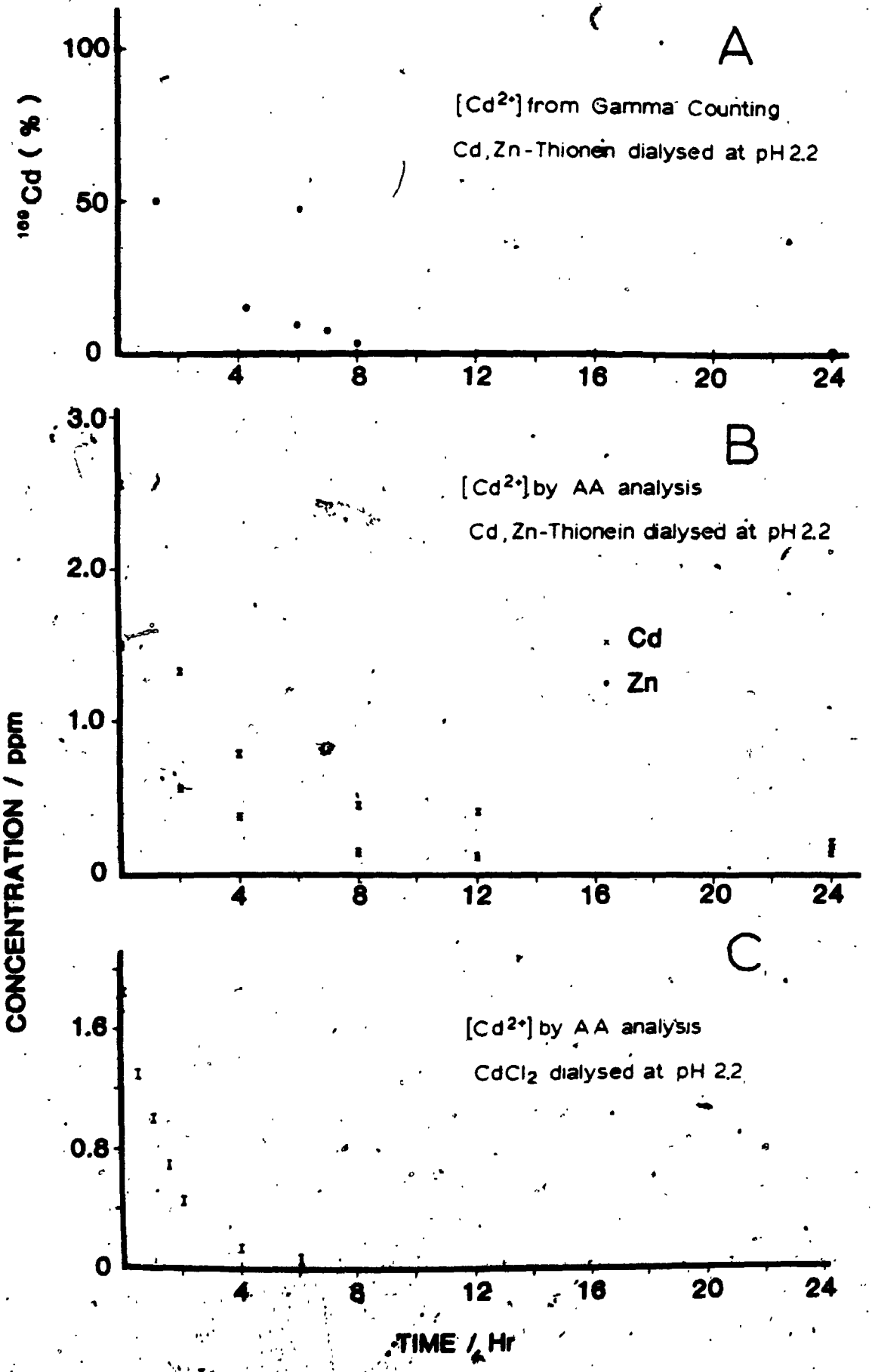
A
[Cd2+] from Gamma Counting
Cd, Zn-Thionein dialysed at pH 2.2
100
50
0
109Cd (%)
4
8
12
16
20
24
B
[Cd2+] by AA analysis
Cd, Zn-Thionein dialysed at pH 2.2
Cd
Zn
3.0
2.0
1.0
0
C
[Cd2+] by AA analysis
CdCl2 dialysed at pH 2.2
1.6
0.8
0
CONCENTRATION / ppm
TIME / Hr

FIG. 13 The effect of adding Cd^{2+} to apo-MT. The apo-MT was prepared by dialysing a rat Cd,Zn-MT solution at pH 1 for 24 hours. The absorption, CD and MCD spectra of the native protein (□ □ □); the apo-MT at pH 1 (△ △ △); after 7.6 mole equivalents of Cd^{2+} were added to the apo-MT solution at pH 1 and the pH of the solution was then raised to 7.1 using μL aliquots of a 2 M Tris solution (○ ○ ○). The units for ε and Δε are L mol^{-1} cm^{-1}. The units for $\Delta\varepsilon_M$ are L mol^{-1} cm^{-1} T^{-1}.

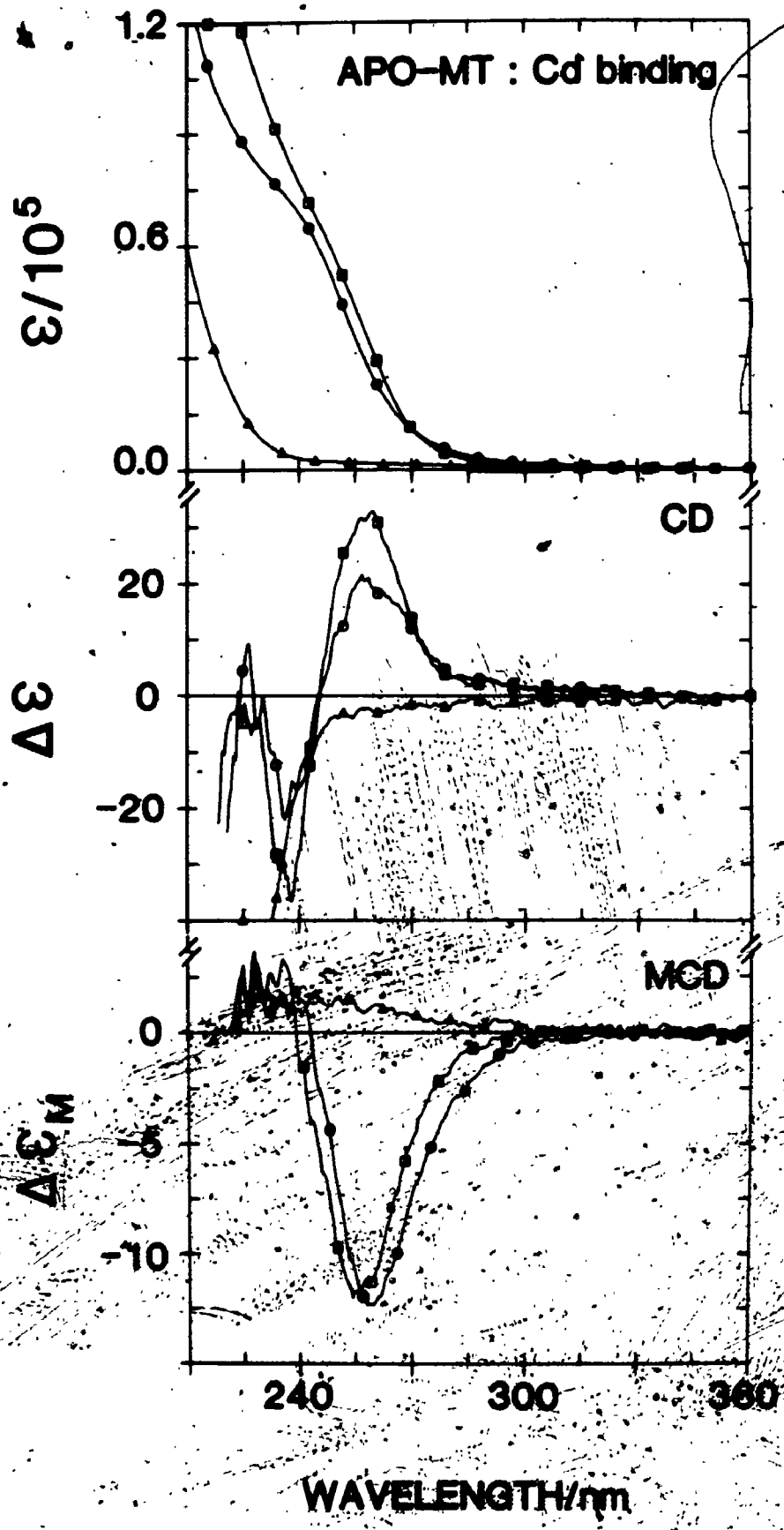
APO-MT : Cd binding
1.2
0.6
0.0
ε/10⁵
CD
20
0
-20
Δε
MCD
0
-5
-10
Δε_M
240
300
360
WAVELENGTH/nm

mole equivalents of Cd^{2+} had been added, and after the pH of the solution was raised to 7.1 using μL aliquots of 2 M Tris solution. The rebinding of Cd^{2+} was demonstrated by the reappearance of the 250 nm absorption shoulder as well as the distorted MCD signal. The MCD spectra of the native and reconstituted protein are remarkably similar which suggests that all the Cd^{2+} have rebound in sites which have a very similar geometry to those of the native protein. It is important to note the red-shift of the MCD band observed in the reconstituted protein. In another experiment where the apo-MT was prepared by passage through a acidified column, the addition of Cd^{2+} to the apo-MT followed by the neutralization of the pH to 7.2 also results in the reconstituted protein.

3.3.4. Cd^{2+} loading experiments

3.3.4.1. Rat liver Cd,Zn-MT-1: Cd^{2+} loading experiment

FIG. 14 shows the absorption, CD and MCD spectra of the titration of a Cd,Zn-MT 1 sample with Cd^{2+}. In these experiments the conformation of the protein around the metal binding sites is already determined by the Cd^{2+} and Zn^{2+} that are present, so the spectral changes indicate whether the Zn^{2+} is displaced by the Cd^{2+} and/or whether there is any change in the Cd^{2+} binding in the presence of excess metal ions above the normal seven per molecule. The binding of Cd^{2+} is shown to occur in two stages as indicated by the changes in these spectra. The protein sample used contained a total of 3.9 moles of Cd^{2+} and 1.9 moles of Zn^{2+} per mole of protein. When the Cd^{2+} concentration is increased to a total of 5.8 mole equivalents (which represents 3.9 mole of Cd^{2+} from MT, together with 2.0 moles of Cd^{2+} added, a value just greater than the 1.9 moles of Zn^{2+} initially present), an

increase in the absorption shoulder at 250 nm is observed (FIG. 14, lines 1-7). Addition of another 0.5 moles of Cd^{2+} does not further change the absorption spectrum. An isosbestic increase in the Cd-related envelope in the MCD spectrum is observed during this stage of the titration (lines 1-7). No difference in the MCD intensity is observed with 6.4 mole equivalents of Cd^{2+} added but the isosbestic point is lost. Both the zero cross-over point and the band centre of the negative trough in the MCD spectrum are red-shifted 4 nm and 3 nm, respectively, when the total Cd^{2+} concentration present is 6.4 mole equivalents. At this point the MCD spectrum (line 7) shows a 40% increase in the peak-to-trough amplitude.

The changes in the CD spectrum, however, are much more complicated during the first stage (i.e. addition of up to 2.5 mole equivalents of Cd^{2+}). The 258 nm band experiences a slight drop in intensity initially, but this is then followed by a blue-shift of the band centre as well as an increase in intensity. A more significant change is observed in the 225 nm band. It reaches its maximum peak intensity at 5.9 mole equivalents of Cd^{2+} but decreases in intensity at higher Cd^{2+} concentrations, while the 238 nm band remains unchanged. Addition of another 0.4 moles (to a total 6.8 mole equivalents of Cd^{2+}), results in a shift of the 258 nm to 255 nm but there is no further change in the 225 nm band intensity.

The next set of traces (lines 8-15) demonstrates the effect of adding Cd^{2+} in excess of the seven mole equivalents bound in the native protein. The absorption spectrum is characterized by a sharp isosbestic point at 258 nm, while the MCD spectrum shows a gradual decrease in the overall intensity. The 258 nm band in the CD spectrum

FIG. 14 The effect of adding Cd^{2+} on the absorption, CD and MCD spectra of a rat liver Cd,Zn-MT 1 solution. The native solution contained 3.9 mol eq Cd^{2+} and 1.9 mol eq Zn^{2+} (- - - -) based on protein concentration determined using the DTNB reaction. μL aliquots of an aqueous $CdCl_2$ solution were added to separate 3 mL volume of the protein solution. The mol eq Cd^{2+} contained in each solution was A: (1) 3.9 (native); (2) 4.4; (3) 4.6; (4) 5.1; (5) 5.3; (6) 5.9; (7) 6.4 B: (8) 6.8; (9) 7.4; (10) 8.3; (11) 14.2; (12) 26.7; (13) 40; (14) 53.4 and (15) 68. The units for ε and $\Delta\varepsilon$ are L mol^{-1} cm^{-1}. The units for $\Delta\varepsilon_M$ are L mol^{-1} cm^{-1} T^{-1}.

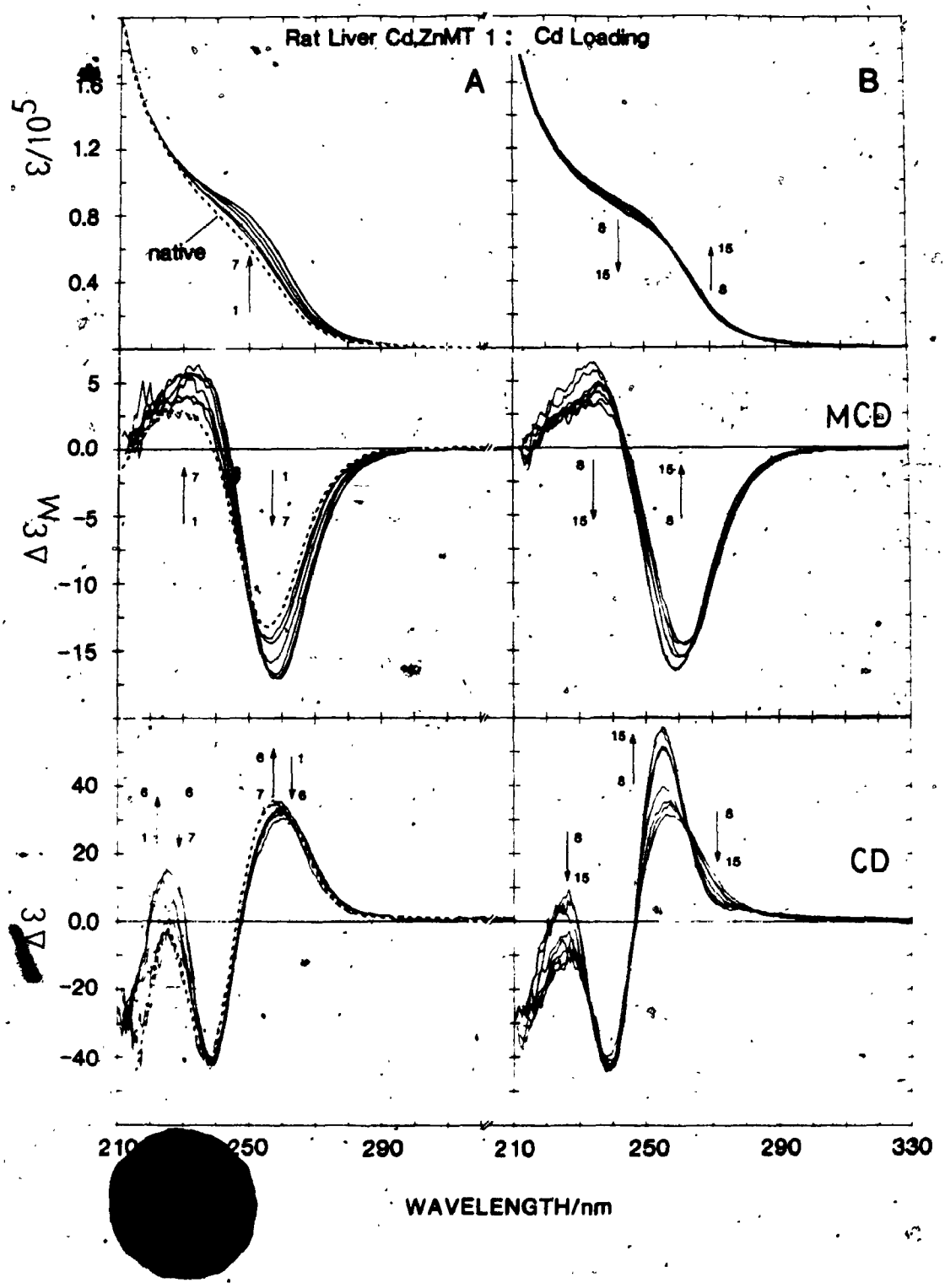
Rat Liver Cd,ZnMT 1 : Cd Loading
A
B
native
MCD
CD
$\Delta\varepsilon_{M}/10^{5}$
$\Delta\varepsilon_{M}$
$3\Delta\varepsilon$
1.6
1.2
0.8
0.4
5
0.0
-5
-10
-15
40
20
0.0
-20
-40
210
250
290
330
WAVELENGTH/nm

experiences a blue-shift which is accompanied by a decrease in band width. When the Cd^{2+} concentration has reached 7.4 mole equivalents, the 258 nm band shifts to 255nm and increases in intensity. The 225 nm CD band initially decreases but then remains constant after more than 15 mole equivalents of Cd^{2+} have been added. The MCD spectrum of the MT solution containing a total of 68 mole equivalents of Cd^{2+} is comparable to that of the native protein in overall intensity, but the entire envelope is shifted 6 nm to longer wavelengths.

3.3.4.2. Crab MT 1 - Cd^{2+} loading experiment

A similar titration experiment was carried out with crab Cd,Zn-MT 1. The spectral changes in the absorption, CD and MCD spectra are shown in FIG. 15. The protein solution used contained 3.1 moles of Cd^{2+} and 1.6 moles of Zn^{2+} per mole of protein. The protein concentration was calculated using the extinction coefficient of 57000 1 mol^{-1} cm^{-1}, which had been previously determined for rat MT (insufficient crab MT was available to measure its extinction coefficient). The second trace in the CD spectrum represents a solution containing 1.4 mole equivalents of added Cd^{2+}, which is very close to the Zn^{2+} concentration present in the native MT. There are three major spectral changes in the absorption and CD spectra at this point: (i) the absorption spectrum increases in intensity between 230 nm and 250 nm, (ii) the CD spectrum shows a decrease in the 233 nm band intensity, (iii) the 258 nm CD band shifts to 262 nm and is accompanied by an increase in intensity. Though the initial addition of Cd^{2+} results in non-isosbestic changes, further addition of Cd^{2+} gives rise to an isosbestic change with both the 233 nm and 262 nm CD bands diminishing in intensity, while a positive band develops at 245 nm. The overall

FIG. 15 Absorption and CD spectra of crab Cd,Zn-MT 1. $CdCl_2$ was added in μL aliquots to the protein solution at pH 7; these traces were recorded following the addition of (1) native; (2) 1.4; (3) 2.8; (4) 4.2; (5) 5.6; (6) 8.4; (7) 9.8; (8) 11.9; (9) 15.4 and (10) 18.9 mole equivalents of Cd^{2+}. The units for ε and Δε are L mol^{-1} cm^{-1}.

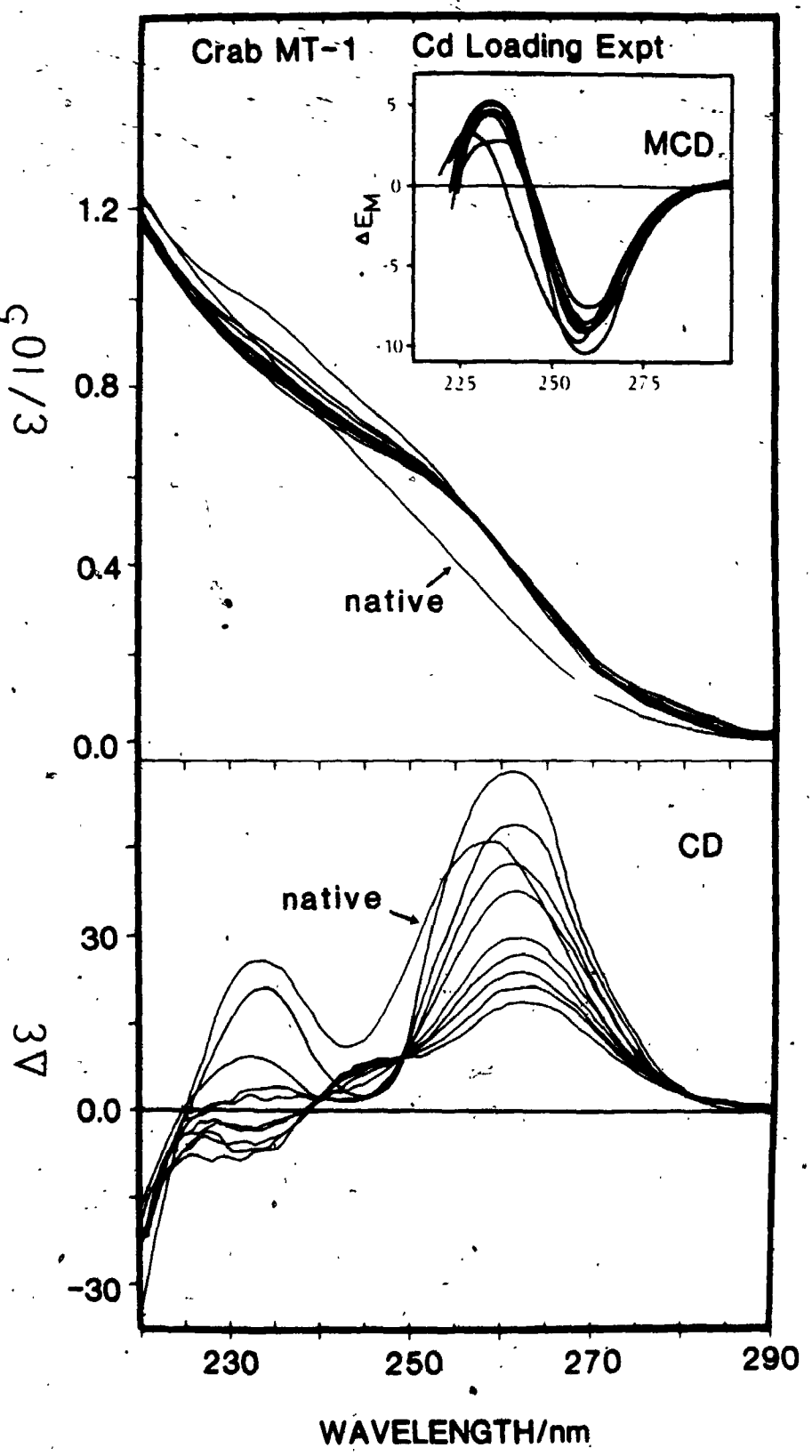
Crab MT-1
Cd Loading Expt
MCD
native
CD
native
ε/10^5
Δε
ΔE_M
1.2
0.8
0.4
0.0
30
0.0
-30
5
0
-5
-10
225
250
275
230
250
270
290
WAVELENGTH/nm

effect observed in the absorption spectrum is very similar to that seen in the Cd^{2+} loading experiment with rat MT. The red-shift of the S->Cd charge transfer transitions is illustrated in the MCD spectrum recorded in a separate experiment (insert). The red shift is also accompanied by an increase in the peak to trough intensity of the MCD envelope as the Zn^{2+} is displaced by the Cd^{2+}. Further addition of Cd^{2+} results in a drop in the overall intensity.

3.3.4.3. Cd^{2+} Loading and Dialysis Experiment

The results from the Cd^{2+} loading experiments in both the rat and crab MT indicate that significant structural changes occur in the presence of excess Cd^{2+}. In particular, in the crab (which contains two 3-metal clusters), a single, new species is formed which is related by two sharp isosbestic points. This strongly suggests that the excess Cd^{2+} can bind to the two 3-metal clusters beyond the saturation point of six moles of Cd^{2+}, normally expected for crab MT. A similar conclusion can also be drawn from the spectral changes observed in the rat liver MT Cd^{2+} titration experiments. However, it is not possible at this point to conclude whether the changes are resulted from the binding of Cd^{2+} to the 3-metal cluster exclusively.

In order to investigate further the origin of these spectral changes in the CD spectrum when high concentrations of Cd^{2+} are present in solution, and to determine the maximum number of moles of Cd^{2+} that can be bound to MT, the following loading and dialysis experiments were carried out with rat liver Cd,Zn-MT 2. Three 5 mL aliquots of a native Cd,Zn-MT 2 solution with different mole equivalents of Cd^{2+} added were dialysed with 3 changes of deoxygenated, triply distilled water. The dialysis solutions were deaerated with nitrogen throughout

the nine hours of the dialysis. The absorption and CD spectra of each sample were recorded. FIG. 16A-C shows the effects of added Cd^{2+} on the absorption and CD spectra. These data follow very closely those observed in the Cd^{2+} binding experiment with rat liver MT described earlier (FIG. 14). In FIG. 16A, the changes in the CD spectrum are dominated by the increase in the 225 nm band intensity and a slight red-shift of the 258 nm band. In solution B, the amount of Cd^{2+} added was equivalent to the Zn^{2+} concentration initially bound in the native protein. The CD spectrum resembles that of the native protein very closely in the 225 nm and 238 nm bands. This data set illustrates the importance of this detailed titration followed using CD spectroscopy, which makes it possible to note the initial spectral change that takes place in 225 nm region (FIG. 16A). In the presence of a large excess of Cd^{2+} (FIG. 16C), a blue-shift of the 258 nm CD band is now apparent with some loss of the 225 nm band intensity. The CD spectra for both solutions (A and B after dialysis) are very similar while a slightly lower CD intensity is observed for solution C. Table V shows the metal content of each solution before and after dialysis. The native protein used contained 4 mole equivalents of Cd^{2+} and 2.3 mole equivalents of Zn^{2+}. The data indicate that in the presence of excess Cd^{2+}, 8.6 moles of Cd^{2+} can be bound to the metallothionein. The amount of excess Cd^{2+} bound is about twice the Zn^{2+} concentration originally present in the native protein. Moreover, the similar CD spectrum observed when Cd^{2+} displaces Zn^{2+} isomorphously (solution B) suggests that the CD spectrum is dominated by the binding of Cd^{2+}.

3.3.4.4. Cd^{2+} loading and the effect of RBC binding

The fact that MT is capable of binding in excess of seven mole

FIG. 16 The effect of adding different amounts of Cd^{2+} to three Cd,Zn-MT 2 solutions. The solutions were then dialysed for 9 hours at 4° C. The absorption and CD spectra of the native protein (□ □ □); the solution after Cd^{2+} addition (○ ○ ○) and the same solution after dialysis (△ △ △). The units for ε and $\Delta\varepsilon$ are $L\ mol^{-1}\ cm^{-1}$.

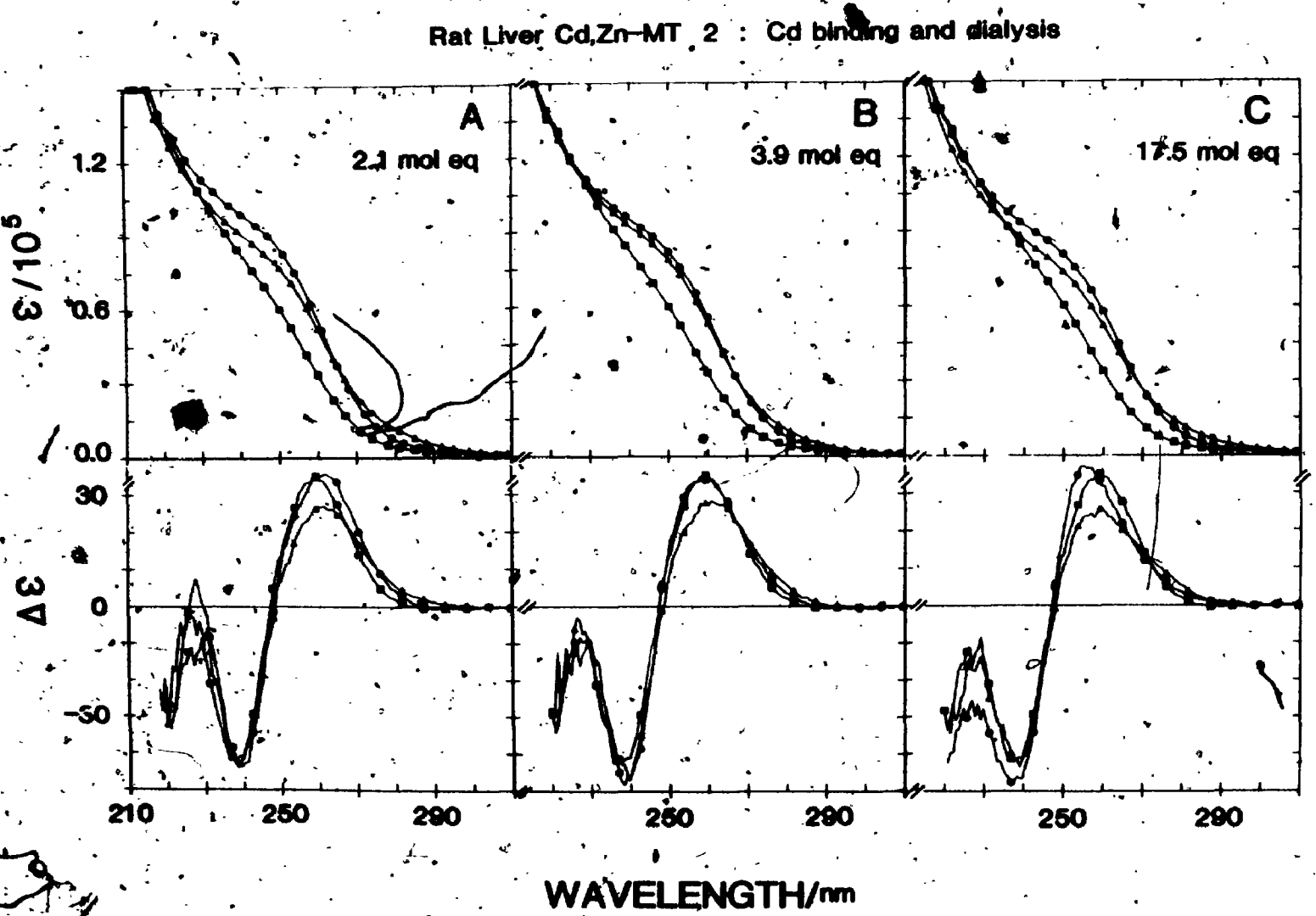
Rat Liver Cd,Zn-MT 2 : Cd binding and dialysis
A
2.1 mol eq
B
3.9 mol eq
C
17.5 mol eq
ε/10⁵
1.2
0.6
0.0
Δε
30
0
-30
210
250
290
250
290
250
290
WAVELENGTH/nm

TABLE V

The effect of dialysis on the number of moles of Cd^{2+} bound to metallothionein

	Cd^{2+}			Zn^{2+}	
	moles	mol. eq. (alpha)	(beta)[a]	moles	mol. eq. (beta)[a]
Cd,Zn-MT 2					
Before dialysis	6.2×10^{-8}	4	-	3.5×10^{-8}	2.3
After dialysis	6.1×10^{-8}	4	-	2.6×10^{-8}	2.0
Cd,Zn-MT 2 +3.2×10^{-8} mol Cd^{2+} after dialysis	8.5×10^{-8}	4	1.7	-	0
+6.0×10^{-8} mol Cd^{2+} after dialysis	10.4×10^{-8}	4	3	-	0
+27.2×10^{-8} mol Cd^{2+} after dialysis	12.9×10^{-8}	4	4.6	-	0

[a] refers to the two cluster model proposed by Otvos & Armitage (98). The values in this column have been normalized assuming 4 Cd^{2+} in the alpha cluster with 2.3 Zn^{2+} in the beta cluster.

equivalents of Cd^{2+} when exposed to high concentrations of cadmium salts raises questions regarding the validity of the methods of estimating MT concentration that are based on Cd^{2+} binding properties. One of the methods used for the estimation of MT levels is the Cd-saturation method introduced by Onosaka and coworkers (110). It is based upon the isomorphous replacement of Zn^{2+} by Cd^{2+} in the presence of excess Cd^{2+}. The unbound Cd^{2+} is subsequently removed by the addition of red blood cell (RBC) hemolysate which is known to be a good scavenger for free Cd^{2+}. There are two major assumptions: (i) while the RBC hemolysate does not affect the MT bound Cd, it does bind all excess Cd in solution, and (ii) that only six moles of Cd^{2+} bind to each mole of protein in the presence of excess Cd^{2+}.

The following experiment was used to study the efficiency of RBC hemolysate as a scavenger for the excess Cd^{2+} bound to MT. Two solutions, one containing 5.0×10^{-8} and the other 11.8×10^{-8} moles of Cd^{2+}, were treated with RBC hemolysate and the Cd^{2+} concentrations of the solutions before and after treatment were determined. The results are summarized in TABLE VI. It is clear that for the first solution the excess Cd^{2+} bound to this metallothionein corresponds to the Zn^{2+} concentration initially present. Even at the higher concentration (11.8×10^{-8} moles in solution 2), the amount of excess Cd^{2+} bound after the hemolysate treatment was found to be very close to the number of Zn^{2+} ions bound in native protein. FIG. 17 shows the effect of addition of Cd^{2+} and RBC hemolysate on the absorption and CD spectra. The CD spectrum of the MT solution containing 14.1 mole equivalents of Cd^{2+} added exhibits a blue shift of the 258 nm positive band together with a drop in intensity. A decrease in the intensity of

FIG. 17 The effect of adding Cd^{2+} to a sample of Cd,Zn-MT 2 (solution 2 in TABLE VI) and treating the solution with RBC hemolysate. The absorption and CD spectra of the native spectrum (————); after addition of 14.1 mol eq Cd^{2+} to the solution (— · — · —); the solution after addition of RBC hemolysate and followed by heating and filtration (- - - - -). The units for ε and $\Delta\varepsilon$ are L mol^{-1} cm^{-1}.

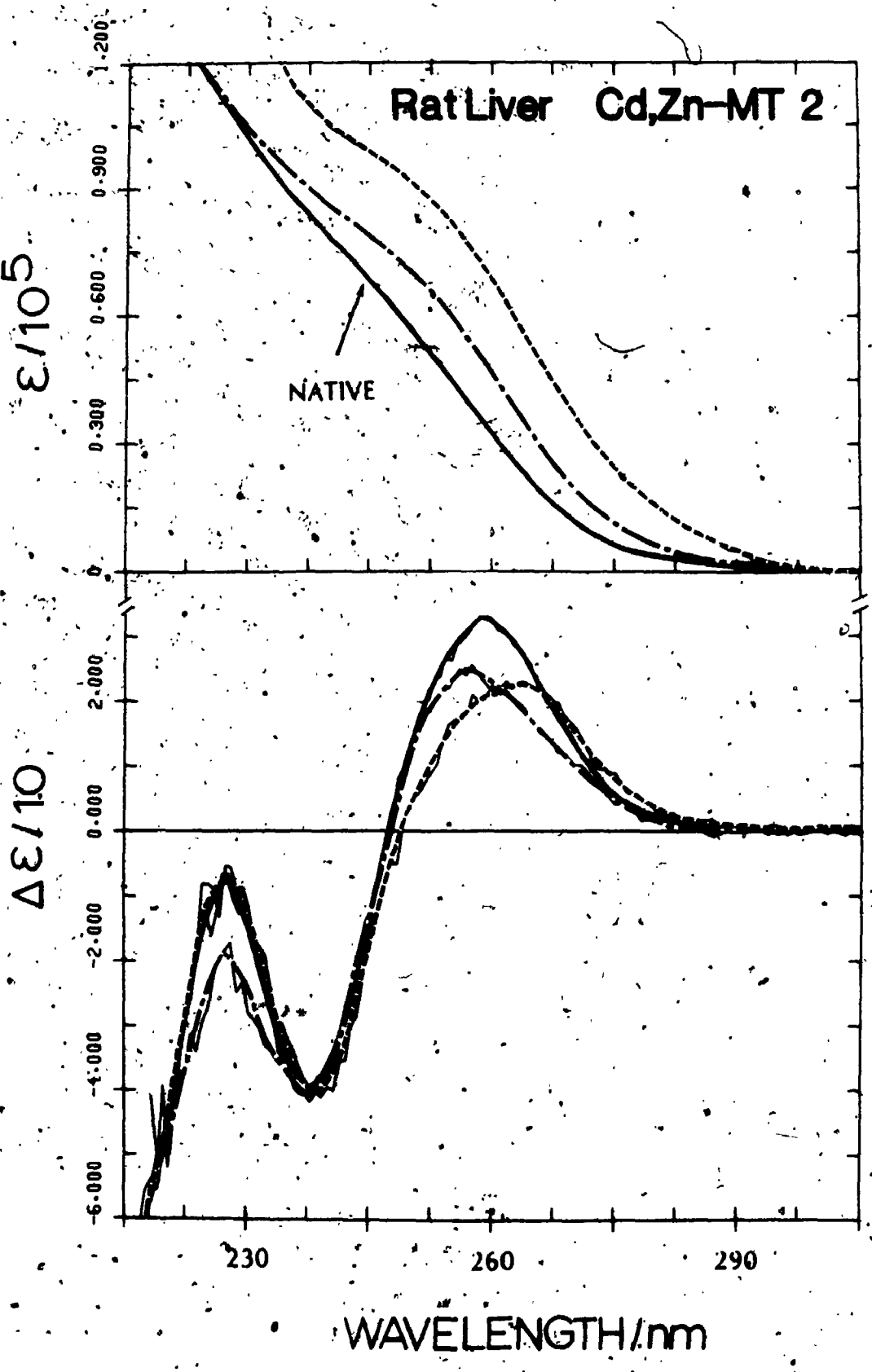
Rat Liver Cd,Zn-MT 2
NATIVE
ε/10⁵
Δε/10
1.200
0.900
0.600
0.300
0
2.000
0.000
-2.000
-4.000
-6.000
230
260
290
WAVELENGTH/nm

TABLE VI

The effect of RBC hemolysate on the removal of the excess Cd^{2+}. The native Cd,Zn-MT 2 contained 1.9×10^{-8} mol Cd^{2+} and 1.2×10^{-8} mol Zn^{2+} (for solution 1). The native protein in solution 2 contained 2.7×10^{-8} mol Cd^{2+} and 1.6×10^{-8} mol Zn^{2+}. An aliquot of Cd^{2+} was added to the protein solution (to give Cd^{2+} content before treatment with RBC hemolysate).

	Total Cd^{2+} concentration ($\times 10^{-8}$ moles)		
	Before treatment	After treatment	excess Cd^{2+} bound[a]
Solution 1	5.1	3.0	1.1 (~ [Zn])
Solution 2	11.8	4.3	1.6 (~ [Zn])

a. difference between total Cd^{2+} content after treatment and the Cd^{2+} content of the native protein. There was no Zn^{2+} present in the protein after RBC treatment.

the 225 nm band is also observed, while the 238 nm negative band does not change significantly. The absorption spectrum shows an increase of the 250 nm shoulder, which is characteristic of Cd^{2+} displacement of Zn^{2+}. After RBC treatment, the CD band at 256 nm now shifts back to a longer wavelength (262 nm). The 225 nm band regains its intensity which closely rsembles that observed originally in the spectrum of the native protein. Again the 238 nm CD band does not change significantly. However, the corresponding absorption spectrum shows a large increase in the overall intensity.

3.3.5. Zn^{2+} loading experiment

Since Zn^{2+} is present in the majority of metallothioneins isolated from tissues and it appears to be an integral component of MT, the binding of Zn^{2+} to Cd,Zn-MT was also studied to determine its effect on the MCD spectrum. As Zn^{2+} is known to have a much lower affinity than Cd^{2+} for the thiolate group on the cysteine ligand, the effect of a large excess of Zn^{2+} on the binding of Cd^{2+} in MT was investigated (FIG. 18). The protein sample contained 9.5×10^{-8} moles (3.4 mole equivalents) of Cd^{2+} and 1.8×10^{-9} moles (0.7 mole equivalents) of Zn^{2+}. The addition of a large excess (164 mole equivalents) of Zn^{2+} resulted in an overall reduction of the 250 nm absorption shoulder. A corresponding decrease in the MCD band with a small shift of the band centre to higher energy was observed. The CD spectrum shows a decrease in the band intensities at 260 nm and 225 nm. Addition of another 328 mole equivalents of Zn^{2+} (line 3) results in a further decrease in the absorption shoulder but an increase in the MCD band intensity. In the CD spectrum, the 260 nm band shifts to higher energy and broadens slightly while the 225 nm band loses much of its intensity. Further

FIG. 18 The effect of adding Zn^{2+} to a solution of Cd,Zn-MT. $A_{250\ nm}$ = 0.63. The protein sample contained 3.4 mol eq Cd^{2+} and 0.7 mol eq Zn^{2+} (based on protein concentration calculated using ε_{250} = 57100 l mol^{-1} cm^{-1}). The mole equivalent of Zn^{2+} added were : (1) 0 (native), (2) 164, (3) 328, (4) 652, and (5) 984. μL aliquots of a $CdCl_2$ solution were then added to the solution containing excess Zn^{2+} (line 5): (6) 11 mol eq and (7) 22 mol eq Cd^{2+} were added to the solution. The units for ε and Δε are L mol^{-1} cm^{-1}. The units for $\Delta\varepsilon_M$ are L mol^{-1} cm^{-1} T^{-1}.

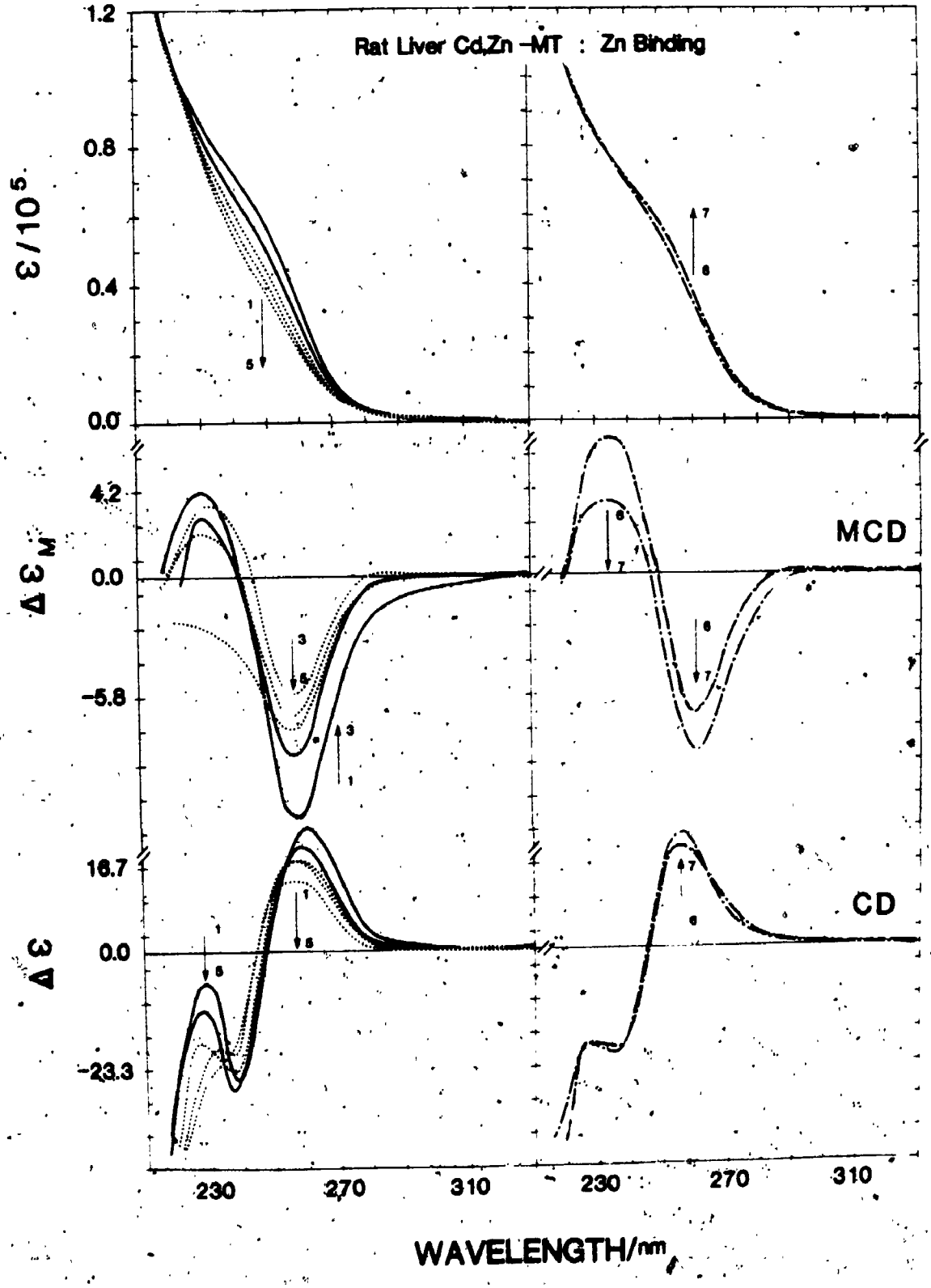
Rat Liver Cd,Zn –MT : Zn Binding
1.2
0.8
0.4
0.0
ε/10⁵
4.2
0.0
-5.8
Δε_M
MCD
16.7
0.0
-23.3
Δε
CD
230
270
310
230
270
310
WAVELENGTH/nm

addition of Zn^{2+} to this solution gives rise to an absorption spectrum which continues to decrease in intensity. The CD spectrum shows a complete loss of the 225 nm band intensity. The MCD now increases in intensity giving a near-symmetrical, derivative-shaped MCD signal (line 3). The last MCD spectrum shows a broad negative band with the loss of the positive lobe. Cd^{2+} was then added to this solution to see if the Cd^{2+} would rebind again in the same sites. When 11 mole equivalents were added, the 250 nm absorption shoulder, a characteristic of Cd^{2+} binding in MT, immediately returns. The CD band at 258 nm sharpened and shifted to higher energy. A hint of the return of the 225 nm band can also be observed. Again the MCD spectrum gives more dramatic evidence for the rebinding of Cd^{2+} in a tetrahedral environment. A symmetrical MCD band is now observed with the negative trough centred at a higher wavelength. The negative MCD band increases in intensity upon the addition of another 11 mole equivalents of Cd^{2+}. However, there is a loss in the intensity of the positive lobe.

3.5. DISCUSSION

Since its initial discovery in 1957, metallothioneins have been isolated from many different sources (52) and studied using a large number of spectroscopic techniques. In the majority of the early studies, the characterization of metallothionein was primarily based on the following properties: low molecular weight, high cysteine and metal content and a complete absence of aromatic amino acids. Since the number of MT's isolated from different sources increased dramatically in the past decade, it became apparent that a further criterion should be imposed on the assignment of a protein as belonging to the metallothionein class. In the earliest study (79) the

absorption spectrum obtained for MT showed a characteristic shoulder at 250 nm and this has since been used as an indicator for the presence of MT. In a later study, Rupp & Weser established the characteristic absorption and CD spectra for MT containing different Cd^{2+} and Zn^{2+} ratios and these spectral changes were found to be very sensitive indicators in metal replacement studies (82).

The absorption spectrum of the rat liver Cd,Zn-MT 1 (FIG. 4) shows the typical spectrum of a metallothionein. It is characterized by a broad absorption shoulder (at about 250 nm) on the side of a rapidly rising absorption edge. The 250 nm absorption is assigned to a S->Cd charge transfer transition (79,83). The S->Zn charge transfer band, which is at a much higher energy than that arising from the Cd^{2+} is masked by the broad absorption at lower energy. The CD spectrum exhibits a derivative-shaped signal in the 220 nm to 260 nm region, which has been shown to arise from the binding of Cd^{2+} in metallothionein (82). The MCD band is characterized by a distorted, derivative-shaped envelope under the charge transfer transition. Of the three techniques used here to characterize metallothionein, the absorption spectrum is the least informative. The absorption shoulder at 250 nm is indicative of Cd-S bond formation. However, the poor resolution of the charge transfer band means it is difficult to obtain any quantitative information. The CD spectrum intensity observed in this region results from the mixing of the chiral states on the coordinating cysteine residues into the absorption band due to the S -> Cd charge transfer transition. The MCD intensity may result from a combination of two factors. Firstly, it may arise from the degeneracy of the excited state in which case a symmetrical, derivative-shaped

signal, an MCD A term, is observed. Secondly, it may result from the field-induced mixing of states and hence a Gaussian signal of either sign, a MCD B term, is observed. In general, the MCD spectrum is known to be sensitive to the geometry of the metal binding sites.

A comparison of absorption and CD spectra of the three native metallothioneins and the sample of alpha fragment, have shown that they exhibit very similar spectral characteristics. In particular, there is striking resemblence between the rat liver MT 1 and the alpha fragment sample that was prepared from the same protein, which suggests that the CD spectrum of the Cd,Zn-MT is dominated by the CD signal due to the Cd^{2+} to alpha fragment. In other words, the binding of Cd^{2+} or Zn^{2+} in the beta site does not contribute much CD intensity. All three species exhibit the same broad absorption shoulder at 250 nm. The absorption shoulder observed for the alpha fragment solution is particularly well-resolved. This is probably due to the absence of the S->Zn charge transfer absorption at higher energy. Furthermore, a significant red-shift in the MCD trough is observed for the alpha fragment. The MCD spectra for all four protein samples show the near symmetrical envelope with the negative trough in the 240-260 nm region, which implies that the geometry of the metal binding sites is similar. A comparison of the MCD spectra of Cd,Zn-MT and a Cd-thiolate model compound (which will be described in Chapter 4) shows that the Cd^{2+} binding sites in MT have a tetrahedral symmetry (T_d). The only spectral difference between the rat liver, guinea pig and the crab MT with respect to the metal binding sites is observed in the CD spectrum. While the CD spectrum of both the rat and the guinea pig MT resemble one another closely, the CD spectrum for the crab MT

is quite different, which suggests that the chiral arrangement of the cysteine residues in the metal binding site is different in the crab MT. ^{113}Cd nmr studies have shown that the metal binding sites in mammalian metallothioneins studied thus far contain two metal clusters (one 3-metal cluster and one 4-metal cluster), where each metal ions is bound by a combination of bridging and terminal sulfur atoms (98,99). The structures of the two metal clusters A & B (the protein fragments containing these two clusters are designated alpha and beta fragment, respectively) are depicted in FIG. 2. Analysis of the amino acid sequence of the crab MT indicates that there are only 18 cysteine residues (134,135) and the ^{113}Cd nmr spectral data obtained for crab MT are consistent with only two 3-metal clusters (136). Therefore, the difference in the CD spectrum observed here may well reflect the variation in the amino acids in the immediate environment of the metal clusters. Thus the three techniques, absorption, CD and MCD together, can provide "fingerprinting" data of the metal binding sites in metallothioneins.

The data obtained in the pH titration experiments (FIGS 4-6) shows that the metal ions bound in metallothionein are released from the binding sites through competitive binding of protons to the sulfur atoms. All three species behave in a similar manner to the change in the proton concentration. As the proton concentration increases, protonation of the sulfur atoms is indicated by the loss of the absorption shoulder around 250 nm. The reproducible red-shift observed in the MCD spectra of all three MT's when the pH of the solution was lowered to about 4 signifies the loss of Zn^{2+} from the binding sites. The MCD envelope also shows the same red shift during metal

replacement with Cd^{2+}. This shift results from two factors: (i) the loss of a S -> Zn band near 240 nm which distorts the MCD spectrum in the Cd,Zn-MT and (ii) the loss of Zn^{2+} from the binding sites results in a change in the energy of the S -> Cd charge transfer band.

Besides the release of metal ions from MT, the uptake or rebinding properties of the apo-MT are also important. The apo-MT prepared by the proton displacement method was monitored by the absorption, CD and MCD techniques. After neutralization of the acidified protein solution, the return of the 250 nm absorption shoulder and the derivative-shaped CD and MCD spectra, suggest that reconstitution of the apo-MT has occurred. The close resemblence between the MCD spectra of the native and the reconstituted solution implies that the metal ions have rebound at sites that possess a similar geometry as in the native protein. More importantly, the reappearance of the CD signal demonstrates that the arrangement of the cysteine residues around the metal ions has not changed. The release and rebinding of the Cd^{2+} was also followed using ^{113}Cd nmr. The ^{113}Cd nmr spectrum obtained for the native protein is very similar to those observed for native Cd,Zn-MT from rabbit liver and rat liver (97,98,100,102). This suggests that the binding sites in the rat and rabbit liver MT's are essentially the same. The majority of the resonances exist as multiplets which result from the ^{113}Cd-^{113}Cd spin coupling through the two-bond interactions between adjacent ^{113}Cd ions. The large number of groups of resonances observed here reflect the heterogeneity of the protein used (98,102). A signal which is due to free Cd^{2+} appeared when the pH of the protein solution is adjusted to 1.6 suggests that the dissociation of the metal ions has occurred. The remarkable similarity between the spectra

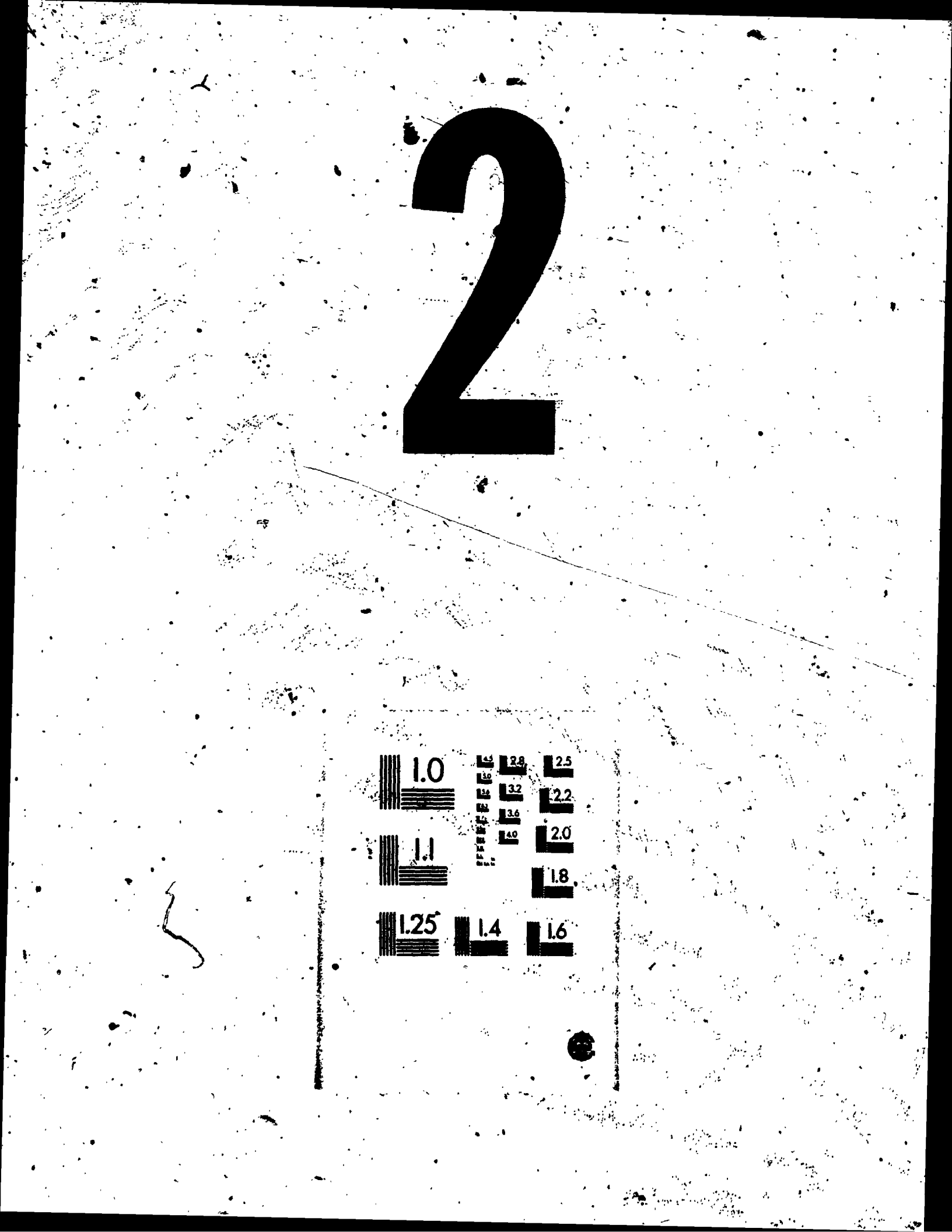
2
1.0
1.1
1.25
1.4
1.6
1.8
2.0
2.2
2.5
2.8
3.2
3.6
4.0

of the native and the reconstituted ^{113}Cd nmr provides further support for the conclusion that the Cd^{2+} rebinds to the apo-MT in sites that are very similar to that used in the native protein. The only major difference between the nmr spectra of the native and reconstituted proteins is the absence of the resonance at 602 ppm in the reconstituted protein spectrum. A similar effect was also observed in the rabbit liver metallothionein when in vitro displacement of Zn^{2+} by Cd^{2+} had taken place (98). The marked similarity between the ^{113}Cd nmr spectrum of the reconstituted protein and the Cd^{2+} saturated protein spectrum suggests that on reconstitution, Zn^{2+} does not rebind to the apo-MT and that Cd_7-MT is formed preferentially. In a recent study, Nielson & Winge (124) have demonstrated the order of remetallation of the apo-MT with Cd^{2+}. The results indicate specific binding of Cd^{2+} to give the saturated alpha fragment containing 4 Cd^{2+} ions which was then followed by the formation of the beta cluster.

The ability of the Cd^{2+} to bind to apo-MT in vitro has special significance. The implication is that such binding reactions may occur in vivo, thus providing evidence that the Cd^{2+}-metallothionein may be synthesized from the apo-MT that may be present in vivo. Another outstanding question concerning the in vivo synthesis of metallated MT is whether Zn-MT, a naturally occurring protein, functions as a precursor for the synthesis of Cd,Zn-MT. In order to answer this question, it was necessary to study the metal substitution reactions in metallothionein, namely, the replacement of Zn^{2+} by Cd^{2+}. Metal replacement experiments were used to demonstrate the ability of metallothioneins to accommodate metal substitution without degradation of the cluster structure. Recently, a number of other metals such as

Co^{2+}, Ni^{2+}, Bi^{3+} and Pb^{2+} have been shown to bind to metallothionein *in vitro* (23,106-108). However, it has not been possible to ascertain whether these metals induce any changes in the quaternary structure of the protein. In other words, is the native protein structure maintained after the binding of these metal ions? As none of these metals has been shown to induce the synthesis of MT, no direct comparison between the structure of the native protein containing these metals and the metal-substituted MT can be carried out. In the case with the Bf-induced Zn-MT, however, titration studies with Cd^{2+} did give rise to the characteristic CD and MCD signals due to the Cd-thiolate chromophore in MT which suggests that the metal exchange between the Cd^{2+} and Zn^{2+} occurs readily (137).

Results from the Cd^{2+} loading experiments with both the rat liver and crab MTs suggest that a considerable structural change has occurred when Cd^{2+} in excess of 7 mole eqivalents for rat MT and 6 mole equivalents for crab MT are titrated into the protein solution. The initial addition of up to 2 mole equivalents of Cd^{2+} represents the displacement of Zn^{2+} by Cd^{2+}, as evidenced by the absorption and MCD data. Changes in the CD spectrum are significant only in the 225 nm region where the positive CD band increases in intensity. The dramatic changes observed in both the CD and MCD spectra when the Cd^{2+} concentration is greater than 7 mole equivalents provide strong evidence that Cd^{2+} binding continues beyond this concentration. The excess Cd^{2+} bound to MT appears to result in a change in the protein conformation which is flagged by the changes in the CD spectrum. A slight decrease in the Cd-related MCD envelope suggests that some of the Cd^{2+} may have lost its near-tetrahedral symmetry. The MCD band

intensity observed for the final spectrum resembles the native MCD envelope in overall intensity but differs in the band centre wavelength, which suggests that the Cd^{2+} originally present in the alpha cluster is not significantly affected by the excess Cd^{2+} present in either the solution or bound to the protein.

Results from a Cd^{2+} loading experiment with a sample of alpha fragment (prepared by the proteolytic cleavage of the rat liver MT which leaves the four-metal cluster intact) did not show any significant changes in the CD spectrum even in the presence of 7 mole equivalents of excess Cd^{2+} (125). This demonstrates the remarkable stability of the 4-metal cluster with respect to excess Cd^{2+}. In view of the dramatic changes in the CD spectrum of the crab, and comparatively minor changes in the rat CD spectrum, a difference in the Cd^{2+} binding properties and stability of the two different metal clusters in metallothionein may be postulated. A similar conclusion has been suggested from ^{113}Cd nmr data reported previously (98,99). The decrease in the Cd^{2+} bound with a tetrahedral symmetry, in addition to the changes in the CD spectrum suggests that the new species formed involves two-fold Cd-thiolate coordination, and eventually groups containing Cys-S-Cd-X units may be formed.

In the crab CD spectrum, the isosbestic changes observed upon addition of Cd^{2+} suggest that a single species is being formed. The last trace containing 19 mole equivalents of Cd^{2+} presumably contains $Cd(S)_2$ units as suggested earlier with the rat liver protein.

The dialysis of protein solutions containing different amounts of added Cd^{2+} was used to determine the maximum number of moles of Cd^{2+} that were bound to the protein. The data obtained (FIG. 16) suggest

that the binding of Cd^{2+} to the beta site in MT does not contribute signficantly to the CD intensity. In the presence of a large excess of Cd^{2+}, only about 8.6 mole equivalents of Cd^{2+} can be bound to MT. Based on the fact that the alpha site is resistent to excess Cd^{2+}, the extra Cd^{2+} bound on the MT represents twice the Zn^{2+} content present in the native protein. This implies that each Zn^{2+} site in the beta cluster can accommodate a maximum of 2 Cd^{2+} ions. The fact that MT can bind an extra 4.6 moles of Cd^{2+}, an amount that is twice the initial Zn^{2+} concentration present in the beta site, poses questions regarding the mode of binding for the excess Cd^{2+}. To simplify the answers to these questions we will assume that the 2.3 mole equivalents of Zn^{2+} represent the partially filled beta cluster. Furthermore, we will interpret the data in terms of a filled beta cluster unit containing 3 moles of metal ions. This means that a total of 6 extra moles of Cd^{2+} can be bound to give $Cd_4(\alpha),Cd_6(\beta)$-MT. There are several schemes that will account for the binding of the excess Cd^{2+} in the beta sites: (i) the 3-metal cluster remains intact while the extra three Cd^{2+} bind on the three terminal cysteines forming cys-S-Cd-X units; (ii) the 3-metal cluster structure collapses and all 6 Cd^{2+} bind with a different coordination geometry and a new arrangement of the cysteine residues, or (iii) the excess Cd^{2+} acts as a bridging ligand between two MT proteins, thus forming dimeric or polymeric species. The low concentration of the protein solutions used in optical experiments means that aggregation reactions are rather unlikely. Moreover, when a solution of MT containing excess Cd^{2+} was eluted through a Sephadex G-25 (fine) column at pH 7, dimer formation was not indicated. Our MCD data obtained in the Cd^{2+} titration study (FIG. 14) show an initial

increase in the MCD band intensity when the added Cd^{2+} replaces the Zn^{2+}, while further addition of the Cd^{2+} beyond the saturation point gives a gradual decrease in the overall MCD envelope. This suggests that the tetrahedral geometry of some of the Cd^{2+} is no longer maintained. This also implies that the cluster structure of the beta site may not be intact and that the binding of Cd^{2+} probably involves a different geometry and arrangement of the cysteine residues.

Since the MT is capable of binding three extra Cd^{2+} ions, the validity of MT estimation methods that are based solely on the Cd^{2+} binding properties is challenged. In particular, the heme-saturation method introduced by Onosaka and coworkers (115) which is based upon the isomorphous replacement of Zn^{2+} by Cd^{2+}, and the ability of RBC hemolysate to remove the excess Cd^{2+} ions in solution. Therefore, it is necessary to reexamine the procedure used and to study the efficiency of the RBC hemolysate in removing the excess bound Cd^{2+} from the protein. The results shown in TABLE VI suggest that the excess Cd^{2+} bound corresponds to the Zn^{2+} initially present. These results demonstrate that the Cd^{2+} bound in excess have a much lower binding constant than those of the first seven Cd^{2+} bound. The RBC hemolysate can successfully compete with MT for the Cd^{2+} bound in excess of 7 moles per mole of protein. Thus the Cd-saturation method does estimate the protein concentration accurately when based on the complete loading of all metal binding sites in MT. The CD spectrum of the solution after hemolysate treatment is similar to that obtained in the dialysis experiment. It is interesting to speculate that the efficiency of the competition by the RBC hemolysate for the excess Cd^{2+} in the Cd_{10}-MT may represent a mechanism by which MT accommodates

Cd^{2+} during acute exposure in which the excess Cd^{2+} may be redistributed to newly synthesized MT at a later time.

The replacement of Zn^{2+} in Cd,Zn-MT by Cd^{2+} results in a red shift in the MCD envelope. This shift may arise from two factors: (i) the change in the protein geometry that takes place when zinc is replaced by the larger cadmium ion and (ii) the lack of a S->Zn band near 240 nm which distorts the MCD spectrum of the native Cd,Zn-MT. An MCD study of a Zn^{2+} titration of metallothionein provides some insights into the contribution of Zn-related transitions in the MCD spectrum observed for Cd,Zn-MT. It also probes the origin of the red shift in the MCD band envelope when Cd,Zn-MT is titrated with Cd^{2+}. Rupp and Weser have reported the CD spectrum for Zn-MT (82) and the MCD spectrum was published recently (47). Stillman & Szymanska have reported the absorption, CD and MCD spectra of a Bi-induced Zn-MT isolated from rat liver and kidneys (138). The data presented in FIG. 18 suggests that the Cd-S bonds are broken in the presence of high concentrations of Zn^{2+}. The CD spectrum for the solution containing a high concentration of Zn^{2+} closely resembles that observed previously for Zn-MT (86). The decrease in the intensity of the MCD band envelope is accompanied by a blue-shift of the band centre. Furthermore, an increase in the negative MCD intensity at the new band centre is observed when more Zn^{2+} is added. Hence these data suggest that the MCD spectrum obtained for a mixed-metal metallothionein containing both Cd^{2+} and Zn^{2+}, consists of two derivative-shaped bands arising from both the S-> Zn and S->Cd charge transfer transitions. The characteristic red shift in the Cd^{2+}-loaded MT indicates a change in the metal binding sites involving the Zn^{2+}. In addition, this shows

that the assymmetric decrease in the MCD band intensity noted during the early stages of the pH experiments reflects the removal of the Zn^{2+} prior to the removal of the Cd^{2+} from the binding sites.

The results from these metal replacement studies using Cd^{2+} and Zn^{2+} suggest that *in vitro* metal replacement in metallothionein can occur readily. This is important as it implies that the same type of reaction can effectively occur *in vivo*, upon exposure to Cd^{2+}. The naturally-occurring Zn-MT present *in vivo* can be transformed into Cd,Zn-MT, which may then functions as a storage site for Cd^{2+}.

Although the involvement of MT in the metabolism or detoxification of other metals, in particular, copper, has been suggested previously, the binding properties of Cu^{+} to MT have not been well established. In addition Hg^{2+}-containing MTs have received relatively little attention. In Chapters 5 and 6, the Cu^{+} and Hg^{2+} replacement of Cd^{2+} and their subsequent binding to MT are described. A model compound study of Cd^{2+}, Hg^{2+} and Cu^{+} with 2,3-dimercaptopropanol (BAL) will be described in Chapter 4.

CHAPTER 4: MODEL COMPOUNDS STUDIES

4.1. INTRODUCTION

Since it has been established that metal binding in metallothioneins involves the thiol groups on the cysteine residues, it is of interest to study the coordination geometry of complexes containing group IIB metals with simple thiol ligands which mimic the metal binding sites in metallothionein.

Metal-sulfur interactions have been well established in a number of biological systems, in particular the iron-sulfur and "blue" copper proteins (139,140). A tremendous amount of work has been done on model compounds of iron and copper which mimic the metal binding sites in these proteins. Recent advances in the use of sulfur-containing compounds such as BAL (2,3-dimercaptopropanol) and penicillamine as therapeutic agents for heavy metal poisoning have stimulated further interest in the study of metal-thiolate compounds.

BAL has been used in the treatment of Hg^{2+} poisoning in humans (141). *in vivo* chelation studies of Cd^{2+} with BAL has shown that BAL could successfully mobolize Cd^{2+} ions from the liver (142,143). A more recent study on a series of mono-, di- and trithiols have also established that BAL is the most effective ligand for the mobilization of Cd^{2+} via biliary excretion (144). Despite the reported interactions of BAL with metals *in vivo*, little is known regarding the structure and mode of binding of this ligand with Cd^{2+} or other metal ions. Two recent reviews have covered the complexation of Cd^{2+} and Hg^{2+} ions with thiolate ligands, as well as with sulfur-containing amino acids (145,146). Carson et al. (93) have reported a study of a series of alkylthiolate complexes of Cd^{2+} using MCD and ^{113}Cd nmr

techniques. One of the ligands studied was BAL. However, no MCD data for the complexes of BAL with either Hg^{2+} or Cu^{+} have been reported and hence BAL was chosen for the model compound study in this work.

A survey of the Cd-thiolate complexes studied thus far shows that they form a range of molecular structures. Table VII lists some of the thiolate complexes of Cd^{2+} that have been characterized structurally. The tendency of the thiolate ligand to act as a bridging ligand and the ease of Cd^{2+} to form cluster and polymeric species has been amply demonstrated in the majority of these complexes. Some examples of thiolate complexes of Hg^{2+} and Cu^{+} are also shown in TABLE VIII and TABLE IX, respectively.

In this chapter, the absorption and MCD spectra of complexes of BAL with Cd^{2+}, Hg^{2+} and Cu^{+} are described.

4.2. EXPERIMENTAL

The BAL solution was prepared by diluting stock BAL solution (Sigma Chemical Co.) in a pH 10.2 $Na_2CO_3/NaHCO_3$ buffer. All solutions were deaerated and prepared under nitrogen. The BAL solution concentration was determined using an extinction coefficient, $\varepsilon_{234} = 4800$ L mol^{-1} cm^{-1}. The $Cu(CH_3CN)_4ClO_4$ was prepared according to Hemmerich & Sigwart (147). The Cu^{+} solution was prepared under N_2 in a CH_3CN/H_2O (1:3 vol/vol) solution to stabilize the Cu^{+} ions. The Hg^{2+} and Cd^{2+} solutions were made by dissolving $Hg(NO_3)_2$ and $CdCl_2 \cdot 2.5H_2O$ in triply distilled water, respectively; the final concentrations of both solutions were of the order 10^{-2} M. The addition of the metal ion solution was carried out using a μL Finnpipette (variable volume, 0-5 μL range).

The absorption spectra were obtained using a Gary 219.

spectrophotometer and 1 cm quartz cells. The MCD spectra were recorded on a JASCO J5 spectrometer modified using an Ithaco 391 Lock-In amplifier, Morvue photoelastic modulator, Hamamatsu R375 phototube and a JASCO J500 programmed power supply. The MCD spectra were measured using an Oxford Instruments SM2 superconducting magnet, operating with a field of 5.5 T. The MCD intensity was calibrated using an aqueous solution of $CoSO_4$; $[\theta]_M$ (505 nm) = -61.6 deg cm^2 $dmol^{-1}$ T^{-1}. The absorption spectra are reported as ε with units of L mol^{-1} cm^{-1}. The MCD spectra are reported as $\Delta\varepsilon$ with units of L mol^{-1} cm^{-1} T^{-1}. Both the absorption and MCD data were digitized directly and the data presented here are retraced computer plots.

4.3. RESULTS

FIG. 19 shows the absorption and MCD spectrum of BAL at pH 10.2. The absorption spectrum of BAL is characterized by a relatively well-resolved band at about 234 nm on the edge of an intense UV absorption, with an extinction coefficient of 4800 L $mol^{-1}cm^{-1}$ at 234 nm. The MCD spectrum of BAL itself at pH 10 exhibits a near symmetrical, derivative-shaped band which crosses the zero line at about 237 nm.

4.3.1. Cadmium-BAL

FIG. 19 shows the effect of titrating aliquots of Cd^{2+} into a BAL solution on the absorption and MCD spectra. The absorption spectrum clearly shows a red shift of the absorption shoulder at 234 nm and the formation of a well-resolved band as the BAL/Cd^{2+} mole ratio in the solution decreases. The new absorption band at 245 nm reaches its maximum intensity when the BAL/Cd^{2+} ratio is 4.5. Two isosbestic points, at 232 nm and 238 nm, are observed. The MCD spectrum also shows a characteristic red shift and the formation of a distorted

derivative-shaped envelope where the zero cross-over point corresponds roughly to the band peak position in the absorption spectrum. Moreover, isosbestic points are also observed in the MCD data at 235 nm and 249 nm. The absorption and MCD spectra remain unchanged upon addition of more Cd^{2+} up to a BAL/Cd^{2+} mole ratio of 2.7. When the BAL/Cd^{2+} ratio in the solution is adjusted to 2.3, both the absorption and the MCD band are observed to decrease in intensity.

4.3.2. Mercury-BAL

FIG. 20 shows the absorption and MCD spectra obtained for a titration of BAL with Hg^{2+}. The formation of a new band in both the absorption and MCD spectra is more distinct than in the case with the Cd^{2+}-BAL complex. The new absorption band is red-shifted further and it is centred at 284 nm. A distorted, derivative-shaped MCD band develops as more Hg^{2+} is added to the BAL solution. The MCD band due to BAL completely disappears when the BAL/Hg^{2+} mole ratio is 3.5. Two isosbestic points at 239 nm and 281 nm can clearly be observed in the MCD spectra. When the BAL/Hg^{2+} mole ratio is changed from 3.5 to 1.4, a decrease in the intensity of both the absorption and MCD bands is observed.

4.3.3. Copper-BAL

FIG. 21 shows the absorption and MCD spectra during the formation of the Cu^{+}:BAL complexes (with BAL/Cu^{+} mole ratios of 9.7, 5.2, 4, 3.4, 2.3, 1.3 and 0.6). Unlike the cases with Hg^{2+} and Cd^{2+} where near symmetrical MCD envelopes and well-resolved absorption bands are observed, the absorption and MCD spectra of the species formed in solution containing Cu^{+} and BAL are characterised by multiple bands. The initial addition of Cu^{+} to the BAL solution results in a weak,

FIG. 19 A titration of a solution of 2,3-dimercaptopropanol (BAL) in a $Na_2CO_3/NaHCO_3$ buffer at pH 10.2 with $CdCl_2$. The molar ratios of BAL:Cd are 27.0, 13.7, 9.1, 6.8, 5.5, 4.5, 3.5, 2.7, and 2.3. The absorption and MCD spectra for the last three solutions are not shown. The units for ε are L mol^{-1} cm^{-1}. The units for $\Delta\varepsilon_M$ are L mol^{-1} cm^{-1} T^{-1}.

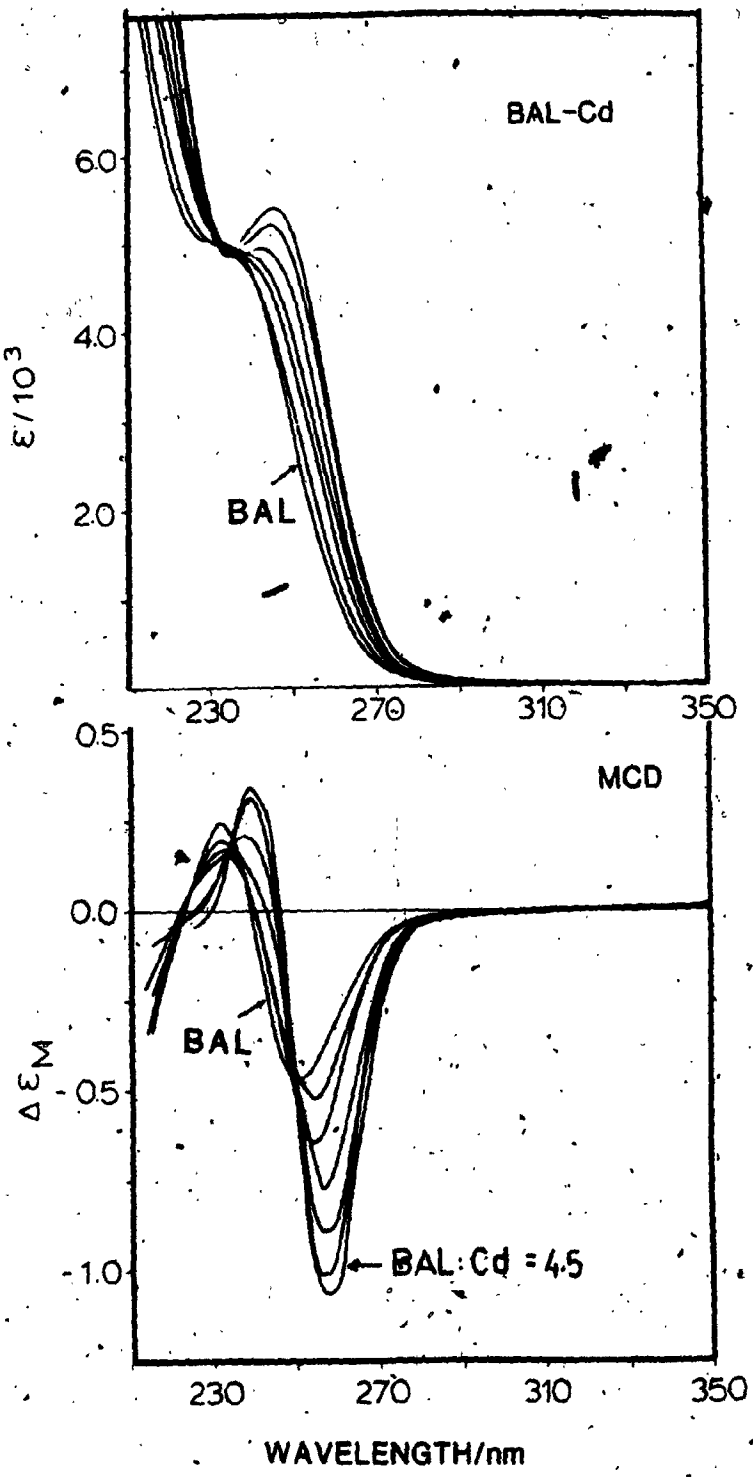
BAL-Cd
6.0
4.0
2.0
ε/10³
BAL
230
270
310
350
0.5
0.0
-0.5
-1.0
MCD
BAL
Δε_M
BAL:Cd = 4.5
230
270
310
350
WAVELENGTH/nm

FIG. 20 A titration of a solution of 2,3-dimercaptpropanol (BAL) in a $Na_2CO_3/NaHCO_3$ buffer at pH 10.2 with $Hg(NO_3)_2$. The molar ratios for BAL:Hg are 27.7, 13.8, 9.2, 6.9, 4.6, 3.5 and 1.4 (last trace not shown). The units for ε are L mol^{-1} cm^{-1}. The units for $\Delta\varepsilon_M$ are L mol^{-1} cm^{-1} T^{-1}.

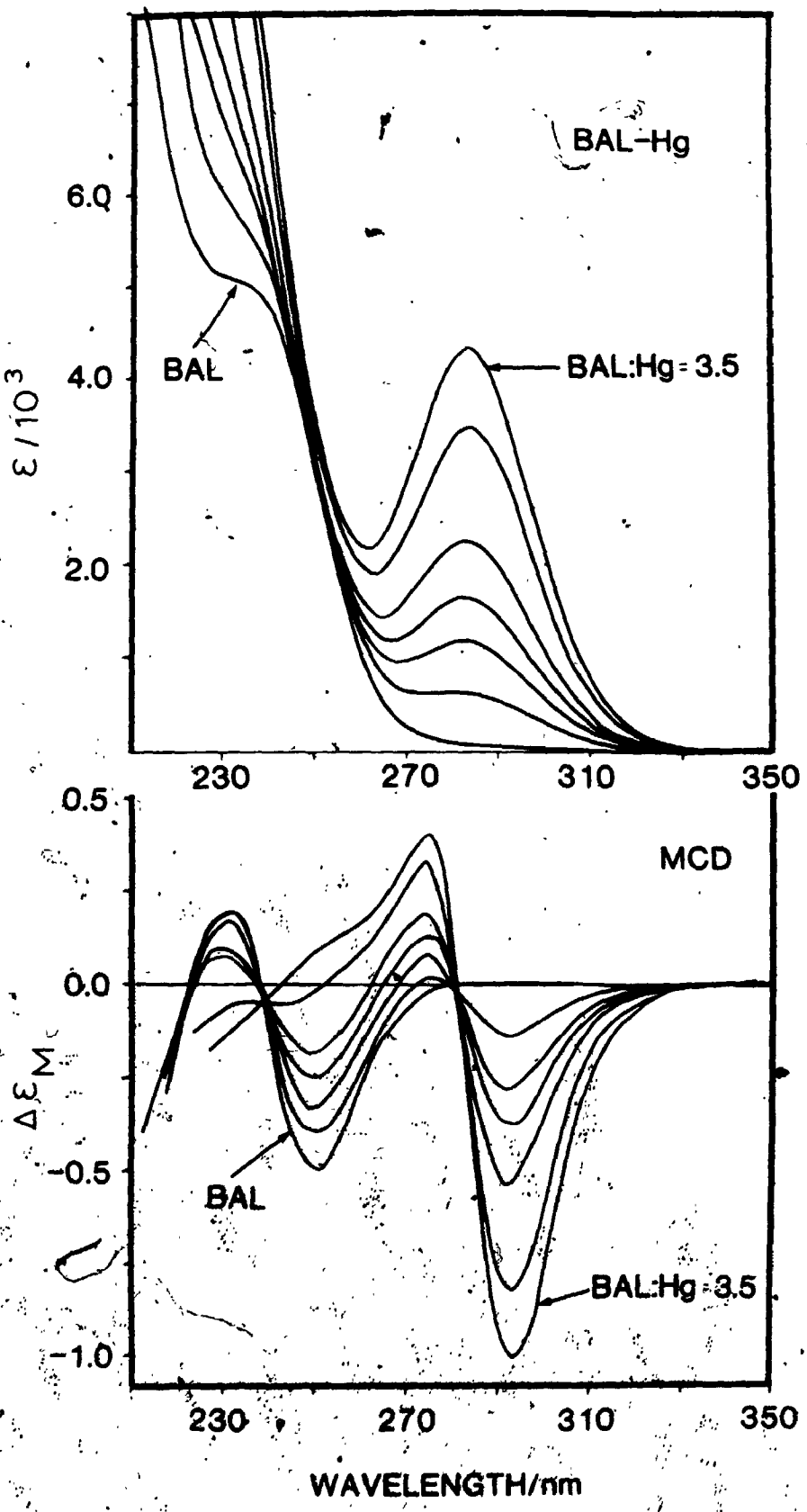
BAL-Hg
BAL
BAL:Hg = 3.5
6.0
4.0
2.0
ε / 10³
230
270
310
350
MCD
0.5
0.0
−0.5
−1.0
Δε_M
BAL
BAL:Hg = 3.5
230
270
310
350
WAVELENGTH/nm

FIG. 21 A titration of a solution of 2,3-dimercaptopropanol (BAL) in a $Na_2CO_3/NaHCO_3$ buffer at pH 10 with $Cu(CH_3CN)_4CLO_4$. The absorption and MCD spectra of the BAL solution (- - - - -). The molar ratios for BAL:Cu^+ are (1) 0 (BAL solution), (2) 9.7, (3) 5.2, (4) 4.0, (5) 3.4, (6) 2.3, (7) 1.3, (8) 0.6. The units for ε are L mol^{-1} cm^{-1}. The units for $\Delta\varepsilon_M$ are L mol^{-1} cm^{-1} T^{-1}.

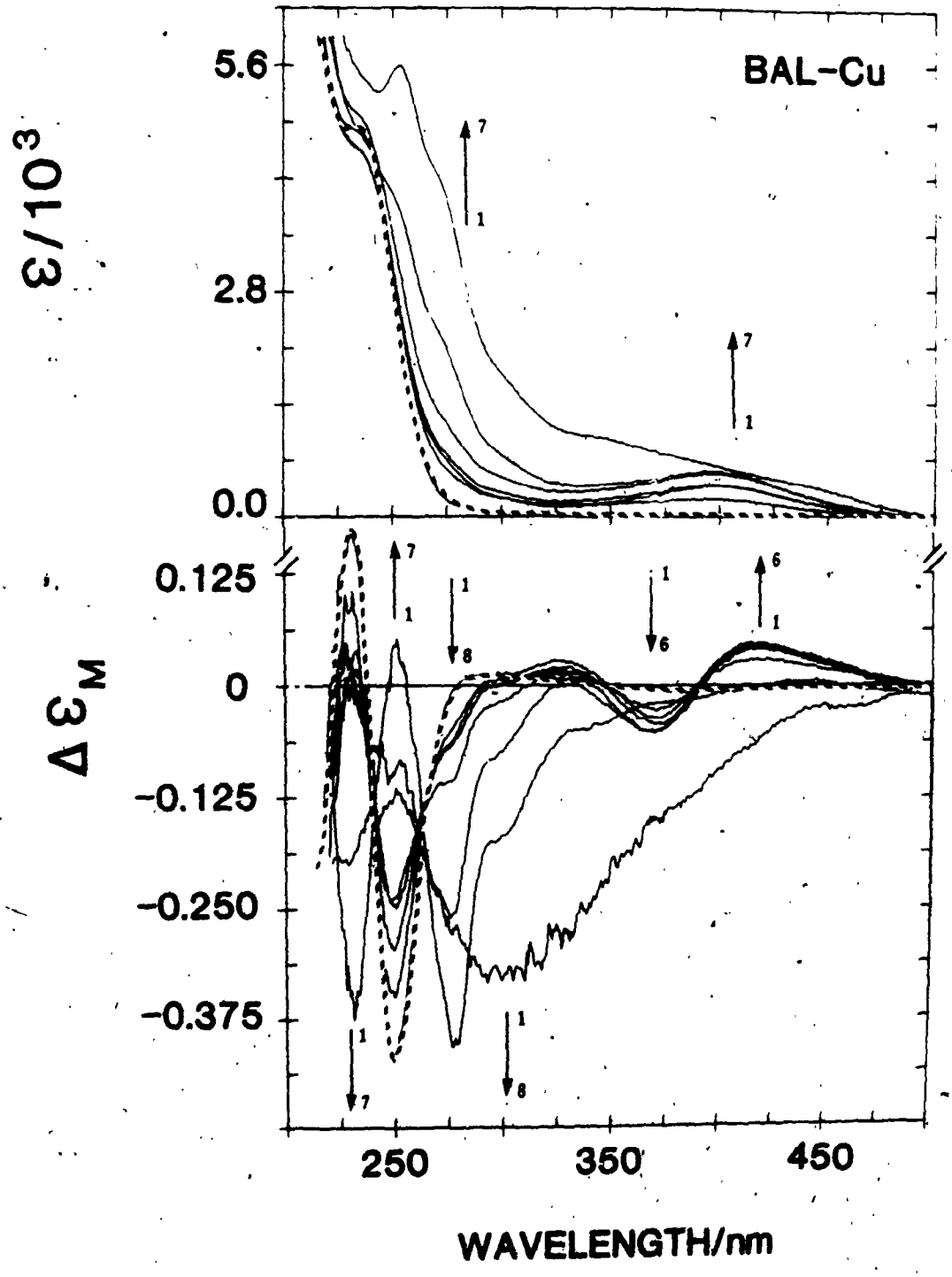
BAL-Cu
5.6
2.8
0.0
ε/10³
0.125
0
-0.125
-0.250
-0.375
Δε_M
250
350
450
WAVELENGTH/nm

broad absorption band at about 395 nm and a corresponding derivative-shaped band is observed in the MCD spectrum. This absorption band reaches a maximum when the BAL/Cu^+ mole ratio is 4.0 and remains constant while two other absorption shoulders with higher extinction coefficients are observed at 275 nm and 300 nm. Negatively-signed MCD envelopes corresponding to these absorption shoulders are also observed. The solution develops a yellow colour upon addition of Cu^+ which intensifies as the Cu^+ concentration in the solution increases. The complete collapse of the MCD band due to BAL is observed when the BAL/Cu^+ mole ratio reaches 1.3. Further increase in the concentration of Cu^+ (BAL/Cu^+=0.6) results in a species which displays a broad, negative MCD signal at 305 nm. At this point, a small amount of precipitate is observed in the solution. In a separate experiment in which a Cu^+ solution was titrated with BAL, the MCD spectra observed for the solution containing a very low BAL/Cu^+ ratio is characterized by a broad negative band, which is very similar to the last trace in FIG. 21 (line 8). Further addition of BAL to this solution results in an increase in the band intensity.

4.4. DISCUSSION

In general, mononuclear complexes predominate when the ligand is present in excess, while polynuclear or cluster compounds involving bridging ligands are more important in solutions containing a low ligand to metal ratio. Cd^{2+} has been shown to form a number of cluster compounds with terminal and bridging thiolate ligands. In the complexes shown in TABLE VII, tetrahedral coordination of Cd^{2+} is the most commonly observed with Cd-S bond lengths that range from 2.45 - 2.62 Å.

The presence of the two isosbestic points in the absorption and MCD spectra during the titration of Cd^{2+} into a BAL solution suggests that a single species is formed in the reaction. The distorted, derivative-shaped MCD envelope is centred roughly about the band maximum in the absorption spectrum. The absorption and MCD spectra observed for the complex formed between Cd^{2+} and BAL correlate well with that reported previously (93). In their recent report, Carson et al. examined a series of thiolate complexes of Cd^{2+} in solution, in order to elucidate the relationship between structure and MCD spectral characteristics. Their results showed that a 1:1 BAL-cadmium complex exhibits a negative MCD band quite different from that observed for the 2:1 complex which is characterized by a distorted, Faraday A term. This shows that MCD spectroscopy can be used to monitor the changes in the geometry of Cd^{2+} complexes formed in solution. The new band in the absorption spectrum has been suggested to result from ligand to metal charge transfer transition which arises from a combination of 3p(S) -> 5s and 5p(Cd) transitions (93). The Faraday A term observed in the MCD spectrum results from the degeneracy in the excited states which most likely arises from a tetrahedral arrangement of sulfur around the Cd^{2+} ions. This derivative-shaped MCD signal resembles very closely that observed in Cd-MT which suggests sthat the metal binding sites in MT contain tetrahedrally coordinated Cd^{2+} ions. The fact that the derivative MCD band is distorted suggests that there is an additional B term present.

The formation of the Faraday A term when Cd^{2+} is titrated into a BAL solution suggests that the species formed involves a tetrahedral arrangement of BAL ligands. The fact that the MCD cross-over point did

not shift when the BAL/Cd^{2+} mole ratio was changed, strongly implies that a single species is formed. The absorption and MCD intensities obtained for this species reach a maximum when the BAL/Cd^{2+} mole ratio is about 4.5. This indicates that under these conditions the BAL does not form a chelate complex and the species formed is probably $[Cd(BAL)_4]^{2-}$. The band width and band position of the MCD signal is very similar to that observed for other Cd^{2+}-thiolate complexes (93).

Further increase in the Cd^{2+} concentration (i.e. as the BAL/Cd^{2+} ratio decreases from 4.5 to 2.7) does not change the intensity of either the absorption or MCD spectrum, which implies that the tetrahedral symmetry is still maintained even in the presence of a high concentration of Cd^{2+}. The decrease in both the absorption and MCD bands intensity when the BAL/Cd^{2+} mole ratio is 2.3 (not shown) indicates that the coordination goemetry around the Cd^{2+} has changed.

The titration of BAL with Hg^{2+} is characterized by the formation of a well-resolved absorption band that is red shifted about 35 nm from the absorption shoulder due to BAL. A near-symmetrical band develops in the MCD spectrum and it is related by two isosbestic points with the cross-over point corresponding roughly to the band centre in the absorption spectrum. The presence of the isosbestic points suggests that only one species is formed in solution. Crystal structures obtained for simple thiolates $Hg(SR)_2$ where SR= Me (174), Et (175) and Bu^t (176) have shown the formation of either linear monomers or polymeric chains involving tetrahedral Hg^{2+}. Reactions of $HgCl_2$ with L-cysteine give rise to $[Hg(cysteine)Cl_2]^-$ species with tetrahedral Hg^{2+} and bridging sulphurs, while $Hg(cysteine)_2HCl.1/2H_2O$ which contains linear coordination of Hg^{2+} was formed in neutral or slightly

acidic conditions (157).

In an early MCD study of a series of tetrahalo complexes of Hg^{2+}, the derivative-shaped MCD band observed was assigned to an np(X^-) -> 6p (Hg) degenerate transitions (177). This is based on the assumption that the derivative-shaped band represents a Faraday A term rather than two B terms of opposite signs. Hence a tetrahedral symmetry around the Hg^{2+} was suggested. The MCD spectrum obtained for the BAL-Hg^{2+} species formed here closely resembles that observed for the $[HgX_4]^{2-}$ chromophore, in that there is the derivative band shape with the positive lobe at higher energy to the band centre. Hence the MCD band obtained here may be assigned as an A term arising from 3p (S) -> 5p (Hg) charge transfer transition.

The decrease in the absorption and MCD band intensity when the BAL/Hg^{2+} mole ratio is adjusted from 3.5 to 1.4 suggests that the tetrahedral geometry around the Hg^{2+} is lost. It is quite possible that a linear-coordinated Hg^{2+} species may be formed at this point.

Studies of the coordination chemistry of Cu^+ with sulfur containing ligands have revealed the tendency of Cu^+ to form multinuclear aggregates. These cluster units exist in a wide variety of composition and structures. Some of the basis core units that have been characterized structurally are Cu_4S_6, Cu_4S_8, Cu_5S_6, Cu_5S_7, Cu_8S_{12}. Non-chelating ligands favour the formation of the Cu_4S_6 "adamantane" unit when the Cu:S ratio is 2:3 (165,,178). More importantly, compounds with the same stoichiometry are often found to have different coordination geometries. Tris(thiourea)copper(I)tetrafluoroborate, [Cu-$(tu)_3$]BF_4, and tris(N,N'-dimethylthiourea)copper(I)tetrafluoroborate, [Cu$(s\text{-}dmtu)_3$]BF_4, consist of dimeric species with

tetrahedral Cu^+ and bridging sulphurs (162); while tris(ethylene-thiourea)copper(I)sulphate and tris(tetramethythiourea)copper(I)-tetrafluoroborate are monomers involving trigonal planar coordinated Cu^+ (160). Hence the prediction of coordination geometry based solely on the ligand/Cu^+ ratio is not reliable.

The absorption and MCD spectra of the Cu-BAL complex formed during the early stage of the titration is characterized by a broad absorption band at about 395 nm with a corresponding derivative-shaped MCD signal which suggests a tetrahedrally-coordinated complex. The most likely species formed in the presence of excess ligand is $[Cu(BAL)_4]^{3-}$, as suggested from the BAL titrations with Cd^{2+} and Hg^{2+}. In addition, $[Co(SPh)_4]^{2-}$ is formed when an excess of SPh^- is used while the adamantane like cluster predominates when the Co:S ratio is 1:3 (179,180). $[M(SPh)_4]^{2-}$ complexes were also isolated from reactions between SPh and Cd^{2+} and Zn^{2+} (105). Monomeric and dimeric species containing tetrahedral Cu^+ with thiourea and its derivatives have been observed and characterized structurally. With tetramethylbenzenethiolate, the Cu^+ coordination is found to be linear (173). Cu^+ involving trigonal planar coordination is also commonly found in polynuclear or cluster compounds. A list of some of the thiolate complexes of Cu^+ that have been characterized structurally are shown in TABLE IX.

As the BAL/Cu^+ mole ratio decreases below 4.0, the appearance of new absorption shoulders at 255 nm, 275 nm and 300 nm suggests that new species are being formed in solution. Negative MCD signals corresponding to these absorption shoulders are also observed. The absorption spectrum of a Cu^+ complex with a cyclic tetrathiaether also

exhibits a broad absorption band at about 400 nm and a much more intense peak at 265 nm (181) which suggests that these absorption bands probably arise from S->Cu charge transfer. It is important to note that Cu-MT isolated from yeast and Neurospora crassa both display similar absorption shoulders in the 250-270 nm region which has been used as an indicator of Cu-S interaction (12,182,183). The derivative-shaped MCD signal at 395 nm collapses completely when the BAL/Cu^+ ratio is 1.3. The intensification of the yellow colour of the solution is most probably indicative of $Cu(I)_xS_y$ cluster formation (165,169,170). A more dramatic change in the coordination around the Cu^+ is observed when the BAL/Cu^+ ratio is changed from 1.3 to 0.6. The dramatic change observed in the MCD spectrum suggests that the coordination geometry of the species in solution has changes. In another experiment, a similar MCD spectrum is observed when BAL is titrated into a Cu^+ solution at a Cu^+/BAL mole ratio of 7.6 (or a BAL/Cu^+ of 0.13). Addition of more BAL (Cu^+/BAL mole ratio of 3.8) at this point results in an increase in the intensity of the negative MCD signal which suggests that only one species is formed in the presence of excess Cu^+.

The MCD spectra recorded during this titration with Cu^+ provide information on the band positions and intensities of Cu-related transitions in thiolate compounds. Until the MCD spectra of a series of Cu-thiolate complexes of known structure can be measured and the relationship between structure and MCD spectral characteristics determined, it will not be possible to analyse systematically the many bands observed in the Cu-BAL MCD spectrum.

With Cd^{2+} and Hg^{2+}, BAL favors the formation of a tetrahedrally

coordinated species, $[M(BAL)_4]^{2-}$ in which the BAL probably acts as a monothiolate rather than a chelating ligand. The derivative-shaped MCD signal assigned as a Faraday A term is indicative of the tetrahedral symmetry. On the other hand, a mixture of complexes appears to be formed when BAL is titrated with Cu^+.

TABLE VII

Thiolate complexes of Cd^{2+}

Compounds	Coordination Geometry	Cd-S bond (Å)	Reference
$[Cd(SPh)_4]^{2-}$	tetrahedral	2.535(3) 2.517(3) 2.540(4) 2.546(4)	105
$[Cd_4(SPh)_{10}]^{2-}$	tetrahedral	2.467(9) 2.56(2)	148
$[Cd(\mu\text{-}SCH_2COOCH_2CH_3)_2]$	tetrahedral/ tetracapped tetrahedral	2.53 2.62	149
$[ICd_8(SCH_2CH_2OH)_{12}]^{3+}$	trigonal bipyramid	2.5	150
$[Cd_{10}(SCH_2CH_2OH)_{16}]^{4+}$	tetrahedral/ trigonal bipyramid/ octahedral	2.51/ 2.52/ 2.56	151
$[Cd(SC_5H_9NHMe)_2^{2+}]_n$	tetrahedral	2.546(9) 2.550(9)	152
$[S_4Cd_{10}(SPh)_{16}]^{4-}$	tetrahedral	S_{br} 2.566 S_t 2.459	153
$[Cd(SCH_2CH_2OH)_2]_n$	tetrahedral/ trigonal bipyramid	S_{av} 2.56	154
$[Cd_2(SC_5H_9NHMe)_2X_4]H_2O$	tetrahedral		155

TABLE VIII

Thiolate complexes of Hg^{2+}

Compound	Coordination Geometry	Hg–S bond (Å)	Reference
$HgCl_2[SCH_2CH(NH_3)COOH]$	tetrahedral	2.490(4)	157
$Hg[SCH_2CH(NH_3)COO]_2HCl.1/2H_2O$	linear	2.355(3) 2.355(5)	157
$(HgCl_2[SC(CH_3)_2CH(NH_3)COOH]2H_2O$	tetrahedral	2.822(5) 2.356(5)	158
$Hg_2(SC_5H_9NHMe)_2)X_4]H_2O$	tetrahedral		155
$[HgBr_2(S_2CNEt_2)Hg(S_2CNEt_2)]_n$	tetrahedral/digonal	2.552(10) 2.569(10) 2.385(11) 2.365(10)	156

TABLE IX

Thiolate complexes of Cu^+

Compounds	Coordination Geometry	Cu-S bond (A)	Reference
$Cu(tu)_3Cl$	tetrahedral		159
$Cu(ethylene\text{-}tu)_3SO_4$	trigonal planar	2.27-2.28	160
$Cu(tetramethyl\text{-}tu)_3BF_4$	trigonal planar	2.258-2.238	160
$Cu(N,N'\text{-}dimethyl\text{-}tu)_3Cl$	tetrahedral	2.360-2.460	161
$Cu(tu)_3BF_4$	tetrahedral	2.295-2.429	162
$Cu(s\text{-}dimethyl\text{-}tu)_3BF_4$	tetrahedral	2.328-2.461	162
$Cu(tu)_2Cl$	trigonal planar		163
$[Cu_4(ethylene\text{-}tu)_9(NO_3)_4].6H_2O$	tetrahedral	2.290-2.348	164
$[Cu_4(SPh)_6]^{2-}$	trigonal planar	2.29	165
$[Cu(S_2P_2Me_4)][CuCl_2]$	tetrahedral	2.244-2.486	166
$Cu_4[SC(NH_2)_2]_6^{2+}$	trigonal planar	2.32-2.48	167
$Cu_4[SC(NH_2)_2]_9^{4+}$	trigonal /tetrahedral	2.30-2.42	167
$[R_4N]_2[Cu_5(SPh)_7]$	trigonal planar /linear	2.23-2.33	168,169
$[Cu_5(\mu_2\text{-}SBu^t)_6]^-$	trigonal/linear		170
$[Cu_4(\mu_2\text{-}SPh)_6]^{2-}$	trigonal planar	2.29	171
$Cu_{10}[S_2CCH(COO\text{-}t\text{-}C_4H_9)_2]_6[S_2CC(COO\text{-}t\text{-}C_4H_9)_2]_2$	trigonal planar	2.656-2.888 (3.438)	172
$[N(n\text{-}Pr_4)][Cu(SC_{10}H_{13})_2]$	linear digonal		173

tu= thiourea

CHAPTER 5: Hg binding to MT

5.1 INTRODUCTION

Though hepatic MT containing Cd^{2+} and Zn^{2+} has received the most attention in the past decade, emphasis has recently been placed on MT containing other metal ions such as Cu^{+} and Hg^{2+}. Jabubowski et al. were the first to demonstrate using gel chromatography that more than 50% of the Hg^{2+} injected into rats was present in a fraction containing compounds with a molecular weight similar to that of metallothionein (184). Subsequent reports by this group and others (21,185-188) have confirmed the presence of Hg^{2+} in the MT fraction. It was only recently that these Hg-containing metallothioneins, isolated from rat kidney, were characterized. Their amino acid compositions, molecular weights and metal contents (31) have recently been reported. In addition to Hg^{2+}, a significant amount of Cu^{+} was also found to be bound to the MT. The total metal content (Hg^{2+} and Cu^{+}) ranges from 4.2 to 5.6 mol eq based on the molecular weight calculated from amino acid analysis. These proteins have been classified as Hg,Cu-MTs. The results from these studies raise questions regarding the mode of Hg^{2+} binding in native Hg-containing MTs and whether these proteins contain the alpha and beta clusters that have now been well established for Cd,Zn-MTs (98).

Despite the number of papers suggesting the presence of Hg^{2+} in the MT fraction, relative little is known about the stoichiometry of Hg^{2+} binding and the geometry of the Hg^{2+} binding sites in MT. Sokolowski et al. (189) have reported the <u>in vitro</u> preparation of Hg-MT. Their X-ray photoelectron study indicated a considerable shift in the binding energy of the $2p_{1/2, 3/2}$ levels of the sulfur atom, thus this

confirmed the involvement of the cysteine sulfurs in the Hg^{2+} binding sites. They also suggested that dramatic structural changes in the protein occurred upon the complete displacement of Cd^{2+} and Zn^{2+} by Hg^{2+}.

Recently, Vasak and Kagi have reported the CD and MCD spectra of a Hg-MT prepared by the reconstitution of rabbit apo-MT with stoichiometric amounts of Hg^{2+} (23,47). However, no spectra showing the growth of these spectral bands with amounts of less than 7 mole equivalents were presented. We have shown previously in Chapter 3 that in titration studies of rat and crab Cd,Zn-MTs with Cd^{2+}, the spectral changes that take place during metal replacement reaction reflect the changes in metal binding in the alpha and beta clusters. Since Hg^{2+} has a higher affinity for sulfur than either Cd^{2+} or Zn^{2+}, detailed spectral studies of the titration of Cd,Zn-MT with Hg^{2+} will give information on the order of metal replacement in the alpha and beta clusters and the eventual location of the Hg^{2+} within the protein and provide evidence for the possible mode of binding.

In this study, Cd,Zn-MT isolated from rat liver was used in a titration with Hg^{2+} and the changes in the metal binding sites were monitored using absorption, CD and MCD spectroscopies. In addition, the binding of excess Hg^{2+} to apo-MT prepared by dialysis was also studied.

Besides Cd^{2+}, Zn^{2+} and Hg^{2+}, other metal ions have also been shown to bind to metallothionein <u>in vitro</u> (e.g. Cu, Ni, Co). Of these metal ions, we have studied the binding of Co^{2+} in this work. It was of interest to investigate the binding of Co^{2+} to MT largely because its paramagnetic properties and its d-d transitions are very sensitive to

the changes in the coordination geometry of the complex formed. Furthermore, Co^{2+} has been shown to substitute for Zn^{2+} in a number of Zn^{2+} metalloproteins without any significant change in the overall protein structure or protein-related functions (190). Therefore, Co^{2+} substitution in MT can be used to probe the geometry of the binding sites in the native protein. Co-MT was first prepared by Vasak and Kagi (106,107) by the reconstitution of rabbit apo-MT. The CD and MCD spectra observed revealed spectral characteristics which are consistent with a tetrahedral symmetry around the Co^{2+} ions (130,131,191).

In this chapter, the binding of Co^{2+} to rat liver Cd,Zn-MT will also be described. Several different methods for the preparation of Co-MT have been investigated in an attempt to understand the Co^{2+} binding characteristics of MT.

5.2. EXPERIMENTAL

Rat liver Cd,Zn-MT 1 was used in the Hg^{2+} titration experiment.

5.2.1. Hg^{2+} Experiment

(i) Hg^{2+} titration experiment

The protein sample was prepared in triply distilled water. The metal contents of the native protein were: Cd^{2+}= 3.3 mole equivalents and Zn^{2+}= 2.0 mole equivalents. The Hg^{2+} solution was prepared by dissolving $Hg(NO_3)_2$ in triply distilled water. The concentration of the Hg^{2+} solution was 8.9×10^{-3} M. The Hg^{2+} additions were carried out using a variable volume Finnpipette (0-5 μL range). The volume of sample used was 5 mL. The solution was mixed immediately after each addition and the spectrum was recorded. The pH of each MT solution containing added Hg^{2+} was maintained at about 7.8 by the addition of

μL aliquots of a NaOH solution.

(ii) Hg^{2+} Dialysis Experiment

A series of rat liver Cd,Zn-MT 1 solutions (2.5 mL) containing different amounts of Hg^{2+} were dialysed in triply distilled water at pH 8, with one change of water after 4 hours. The total dialysis time was 8.5 hours. The metal content of the solutions after dialysis were measured using atomic absorption spectrophotometry (AAS).

(iii) Hg^{2+} binding to apo-MT

The apo-MT was prepared by dialysing a solution of rat liver Cd,Zn-MT 1 (2.5 mL) in 900 mL of deaerated, triply distilled water at pH 1, (dialysis tubing with molecular cutoff of 3500 was used) for 24 hours, with 2 changes of water. AAS measurements for the apo-MT sample showed that there was no Cd^{2+} or Zn^{2+} present. The Hg^{2+} solution was added under nitrogen and μL aliquots of a 2 M Tris solution were used to raise the pH of the solution up to 7.3.

(iv) ^{119}Hg nmr experiment

^{199}HgO (85.3% ^{199}Hg, from Merck Sharp and Dohme Canada Ltd.) was converted to $HgCl_2$ by evaporation to dryness with concentrated HCl. The Hg^{2+} saturated metallothionein solution was prepared by dissolving 2.4 mg of both isoforms of horse kidney metallothionein in 1.5 mL of 10% D_2O solution followed by the addition of $^{199}HgCl_2$ (2.8 mg). ^{199}Hg NMR spectrum was recorded three hours later. A second spectrum was obtained after the addition of another 2.8 mg $^{199}HgCl_2$, four hours later.

5.2.2 Co^{2+} binding experiments

(i) In vitro binding of Co^{2+} to Cd,Zn-MT

Rat liver Cd,Zn-MT was dissolved in triply distilled water. The Co^{2+}

solution was prepared by dissolving $CoSO_4$ in triply distilled water. 27 mol eq of Co^{2+} were added to this protein solution and the absorption and CD spectra were recorded immediately after Co^{2+} addition and again 24 hours later. The pH of the solution was 7.1. The solution was then acidified to pH 2.2 with a concentrated HCl solution. The pH of the solution was subsequently raised to 7.3 with µL aliquots of NaOH solution.

(ii) Co^{2+} column experiment

A G-50F (Pharmacia, 15 cm x 2.5 cm) column was equilibrated with a 0.98 M $CoSO_4$ solution. A Cd,Zn-MT solution that had been acidified to pH 2.5 was applied to the column and eluted with triply distilled water. The Co^{2+} was eluted off the column with the protein sample. The protein fractions eluted were analysed by AAS.

(iii) Equilibrium dialysis

A Cd,Zn-MT solution was dialysed in 500 mL of a deoxygenated, 0.2 M $CoSO_4$ solution for a total of 96 hours. Dialysis tubing with a molecular weight cutoff of 3500 was used. The absorption spectra of the solution was recorded after dialysis.

(iv) Reconstitution of apo-MT

A concentrated Cd,Zn-MT solution (2.5 mL) was prepared at pH 7 and deaerated with nitrogen. 50 µL of this solution was diluted 51 times and the absorption spectrum of the diluted native solution was recorded. The concentrated protein sample was then dialysed in 900 mL of pH 1 solution, with one change of solution after 4 hours. The total time of dialysis was 8 hours. All solutions were purged with nitrogen before use. 18.6 mole equivalents of Co^{2+} were added to the apo-MT under nitrogen. The pH of the solution was raised to 7.0 using a 2 M

Tris solution. The absorption and MCD spectra were recorded immediately after the pH change.

5.2.3. Spectra

As previously described in Chapter 2. The MCD spectrum for the visible region was recorded on a modified Cary 14 spectrometer using a 1 cm path length quartz cell. The MCD spectrum in the UV region was measured using the JASCO J5 modified as described in the previous Chapter. A 0.2 cm path length quartz cell was used.

5.3. RESULTS

5.3.1. Hg^{2+} binding to Cd,Zn-MT

FIG. 22 shows a Hg^{2+} titration with Cd,Zn-MT 1 monitored using absorption, CD and MCD spectroscopies. The protein solution used contained 3.3 moles of Cd^{2+} and 2.0 moles of Zn^{2+} per mole of protein. Two stages in the binding of Hg^{2+} to metallothionein are clearly demonstrated in the absorption spectrum. The initial addition of Hg^{2+} results in an apparent increase in the absorption at 250 nm. It has been suggested that this increase results from a shift in the S->Cd charge transfer transition energy due to the removal of Zn^{2+} from the binding sites. FIG. 22A illustrates this early effect of Hg^{2+} on the absorption, CD and MCD spectra. The absorption shoulder reaches its maximum intensity when 1.7 mole equivalents of Hg^{2+} have been added (line 3 in FIG 22A). A broad band in the 290 nm region is also observed to grow in intensity. The effects of Hg^{2+} addition on the MCD spectra are characterized by a red shift in the negative MCD envelope, together with a loss in intensity. At the same time, a broad, negative band centred at about 300 nm, which corresponds to the 290 nm absorption band, is formed. This new MCD band also attains its maximum

FIG. 22 The effect of Hg^{2+} binding to rat liver Cd,Zn-MT 1 on the absorption, CD and MCD spectra. The sample contained 3.3 mol eq Cd^{2+} and 1.6 mol eq Zn^{2+} (based on protein concentration determined using the DTNB reaction). Mole equivalents of Hg^{2+} were: (1) 0 (native), (2) 0.86, (3) 1.7, (4) 2.3, (5) 3.0, (6) 4.0, (7) 5.3 (spectra illustrated with a thick line), (8) 6.6, (9) 8.0, (10) 9.3. The units for ε and $\Delta\varepsilon$ are L mol^{-1} cm^{-1}. The units for $\Delta\varepsilon_M$ are L mol^{-1} cm^{-1} T^{-1}.

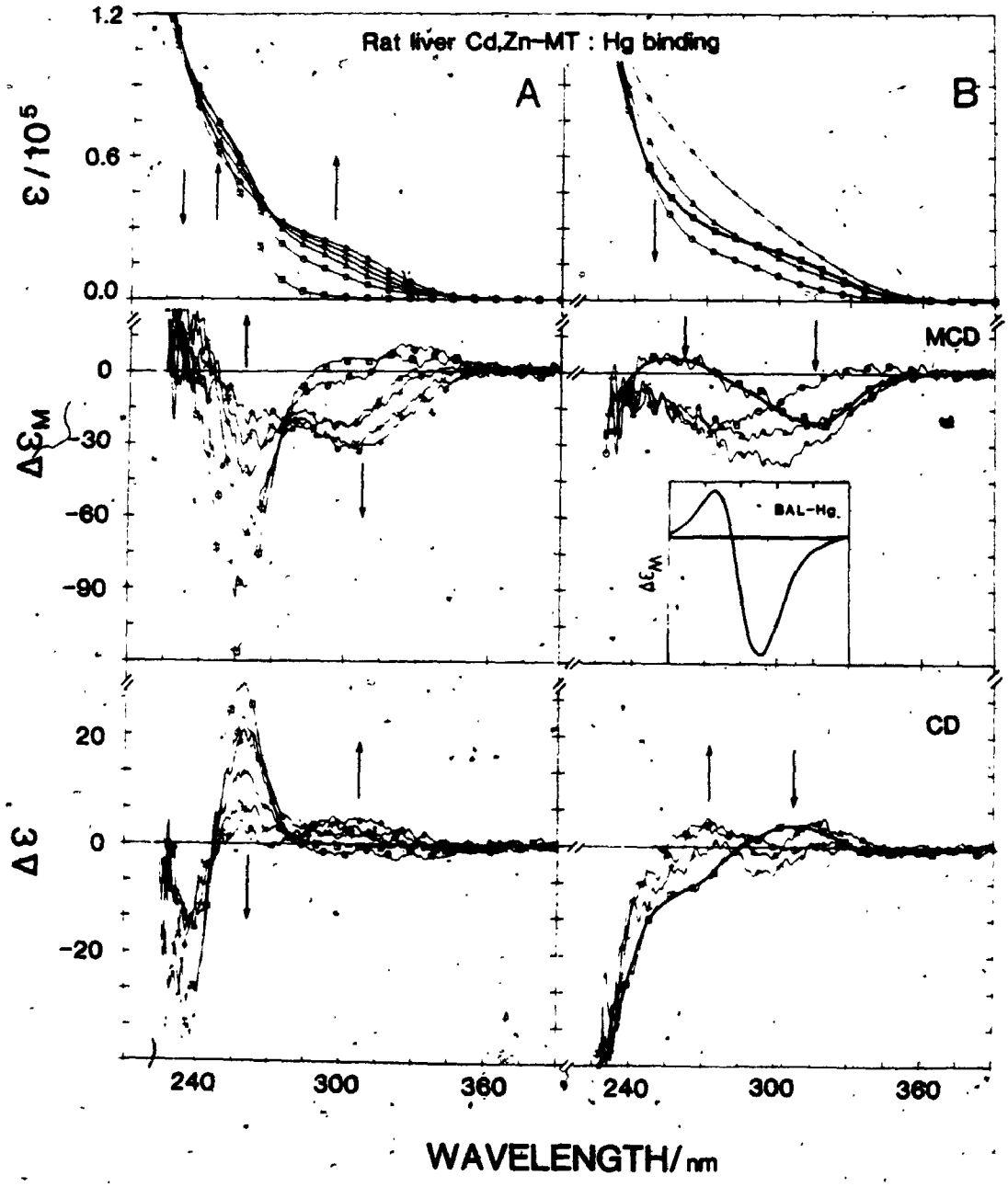
Rat liver Cd,Zn-MT : Hg binding
A
B
1.2
0.6
0.0
ε/10⁵
MCD
0
-30
-60
-90
ΔεM
BAL-Hg
ΔεM
CD
20
0
-20
Δε
240
300
360
240
300
360
WAVELENGTH/nm

when the amount of Hg^{2+} added equals the amount of Zn^{2+} present. The CD spectrum shows a decrease in the overall intensity of the derivative-shaped signal with the formation of a weak positive band around 295 nm. In the second stage in the Hg^{2+} loading experiment the absorption spectrum is now characterized by isosbestic changes in the 250 nm shoulder and the 290 nm band with an isosbestic point at 266 nm (lines 3-6). Isosbestic changes were also observed in the MCD spectra. The CD signal collapses completely when 5.3 mole equivalents of Hg^{2+} have been added (solid line in FIG. 22B). The MCD spectrum exhibits a broad derivative-shaped signal at this stage. The MCD signal due to a tetrahedral Hg-BAL complex is shown for comparison (insert).

FIG. 23 shows plots of the relative intensity changes of the absorption and MCD bands at several wavelengths against mole equivalents of Hg^{2+} added. FIG. 23A shows the changes in the absorption intensity at 255 nm, 266 nm (isosbestic point) and 290 nm. A gradual increase in absorbance at the three wavelengths is observed up to the point when the number of moles of Hg^{2+} added are sufficient to displace all the Zn^{2+} present. Further addition of Hg^{2+} beyond this concentration results in a decrease in the absorption at 255 nm with a corresponding increase in the absorbance at 300 nm. More importantly, the decrease in the $A_{255\ nm}$ is directly proportional to the increase in $A_{300\ nm}$. The MCD band intensity at 258 nm is observed to decrease in a linear fashion.

5.3.2. Hg^{2+} Dialysis Experiment

The following experiment was used to determine the maximum number of moles of Hg^{2+} that can be bound to MT. FIG. 24 shows a plot of the mole equivalents of metal ions that remain bound to MT when a series

FIG. 23 A plot of the changes in the absorption and MCD spectra at several wavelengths versus the mole equivalents of Hg^{2+} added. The protein solution contained 3.9 mol eq Cd^{2+} and 1.9 mol eq Zn^{2+}. The line joining the data point does not have any theoretical significance.

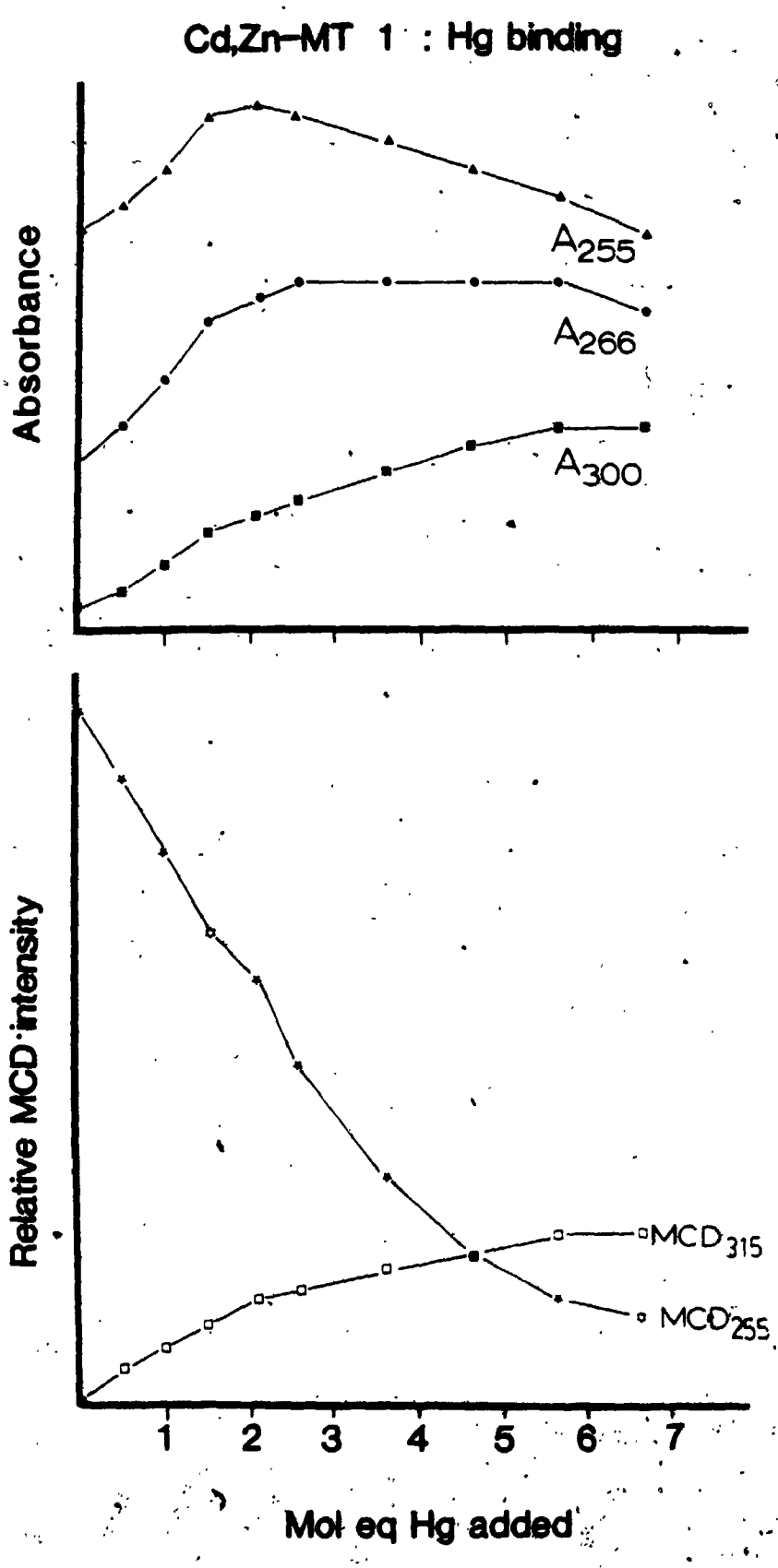
Cd,Zn-MT 1 : Hg binding
Absorbance
A255
A266
A300
Relative MCD intensity
MCD315
MCD255
1
2
3
4
5
6
7
Mol eq Hg added

FIG. 24 Rat liver Cd,Zn-MT 1: Hg binding and dialysis experiments. The native protein contained 3.4 mol eq Cd^{2+} and 1.8 mol eq Zn^{2+}. A series of Cd,Zn-MT solutions containing different amounts of Hg^{2+} were dialysed in triply distilled water, at pH 8, for 8.5 hours. The plot shows the mole equivalents of Cd^{2+}, Zn^{2+} and Hg^{2+} that remained bound to the protein after dialysis versus the mole equivalents of Hg^{2+} added. Each data point for Hg^{2+} represents the average of 4 separate determinations of the solution with the standard deviation as illustrated. The data points on the Cd^{2+} and Zn^{2+} plots represent a mean of 2 determinations with a SD of less than 3 %. The absorption spectra of several solutions before and after dialysis are also shown.

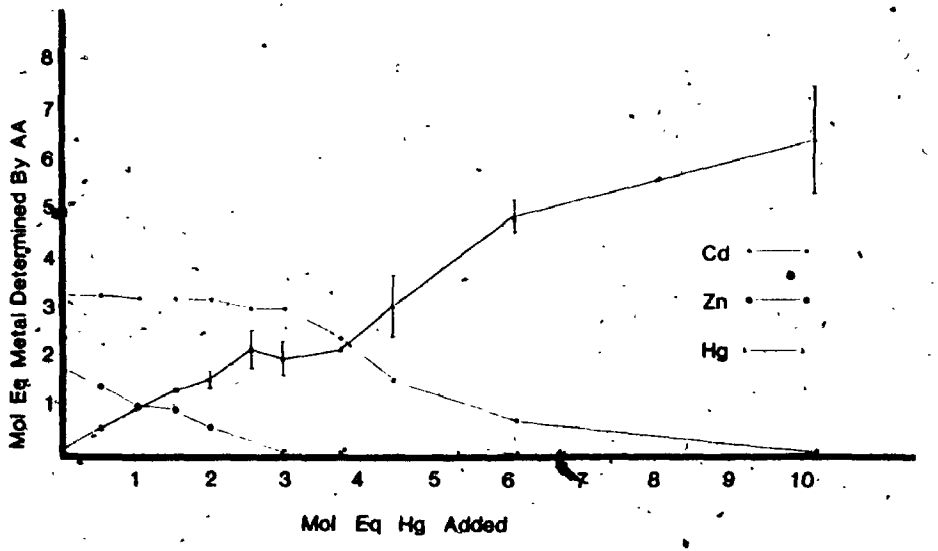
Mol Eq Metal Determined By AA
Mol Eq Hg Added
Cd
Zn
Hg

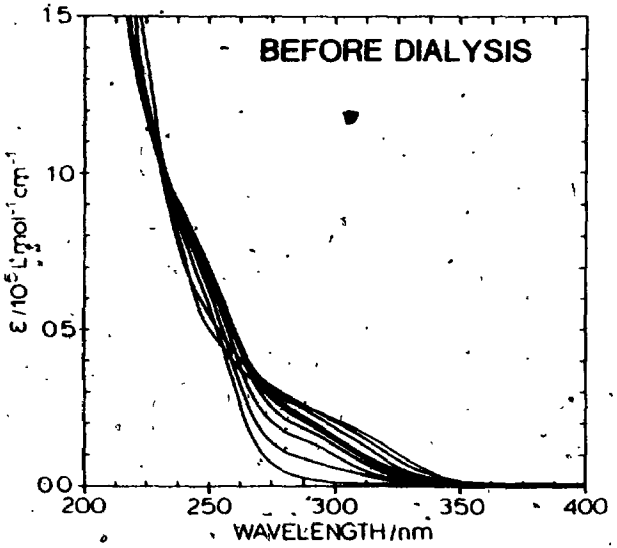
BEFORE DIALYSIS
ε /10⁵ L mol⁻¹ cm⁻¹
WAVELENGTH/nm

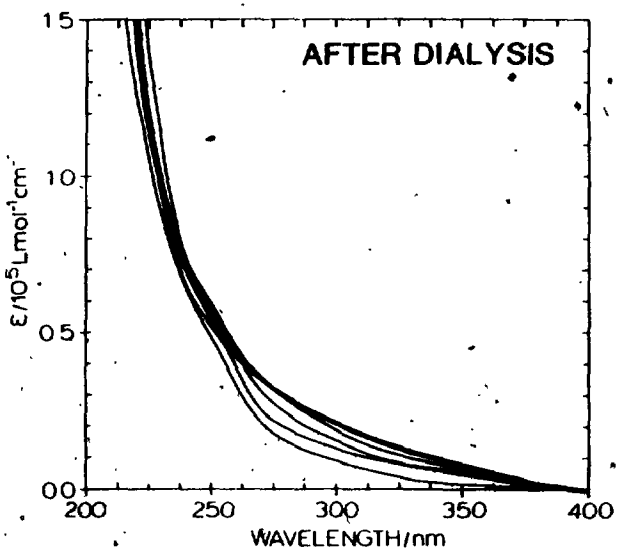
AFTER DIALYSIS
ε /10⁵ L mol⁻¹ cm⁻¹
WAVELENGTH/nm

of solutions of Cd,Zn-MT containing different amounts of Hg^{2+} added were dialysed. This dialysis experiment demonstrates the sequential displacement of Zn^{2+} followed by Cd^{2+} when Hg^{2+} is added. The mole equivalents of Cd^{2+} that remains bound to the MT after dialysis is found to stay constant during the early additions of Hg^{2+}. When the majority of the Zn^{2+} has been displaced from the protein, the Cd^{2+} concentration starts to decrease in a linear fashion. The absorption spectra recorded for each solution before and after dialysis show a small decrease in intensity in the 300 nm region. The maxiumum number of Hg^{2+} ions that could be bound after dialysis was about 1.3 times the sum of the Cd^{2+} and Zn^{2+} ions present in the native protein.

5.3.3. Hg^{2+} binding to apo-MT

An apo-MT solution prepared by dialysis at pH 1 was used to study the reconstitution reaction with Hg^{2+}. All solutions were deaerated before use and the reaction was carried out in a nitrogen atmosphere to prevent air oxidation. FIG. 25 shows the absorption, CD and MCD spectra of the apo-MT solution at pH 1. Neither spectra exhibit much spectral change when 11.0 mole equivalents of Hg^{2+} were added to the apo-MT solution at this pH. The pH of the solution was then raised to 7.3 using a 2 M Tris solution. The broad, negative band now observed in the MCD spectrum resembles that obtained earlier when in excess of 7 mole equivalents of Hg^{2+} were added.

5.3.4. ^{199}Hg nmr

The ^{199}Hg nmr spectrum was recorded for a sample of ^{199}Hg-MT prepared by the *in vitro* displacement of the Cd^{2+} and Zn^{2+} from a solution of horse kidney Cd,Zn-MT. This sample did not give any ^{199}Hg signals in the region expected for mercury thiolates.

FIG. 25 The binding of Hg^{2+} to apo-MT prepared by dialysis, at pH 1 for 24 hours. The absorption, CD and MCD spectra of the native Cd,Zn-MT 1 before dialysis (□ □ □); apo-MT at pH 1 (△ △ △). 11 mol eq Hg^{2+} were added to the solution at pH 1. The pH of the solution was then raised to 7.3 using a 2 M Tris solution (○ ○ ○ ○). The units for ε and $\Delta\varepsilon$ are L mol^{-1} cm^{-1}. The units for $\Delta\varepsilon_M$ are L mol^{-1} cm^{-1} T^{-1}.

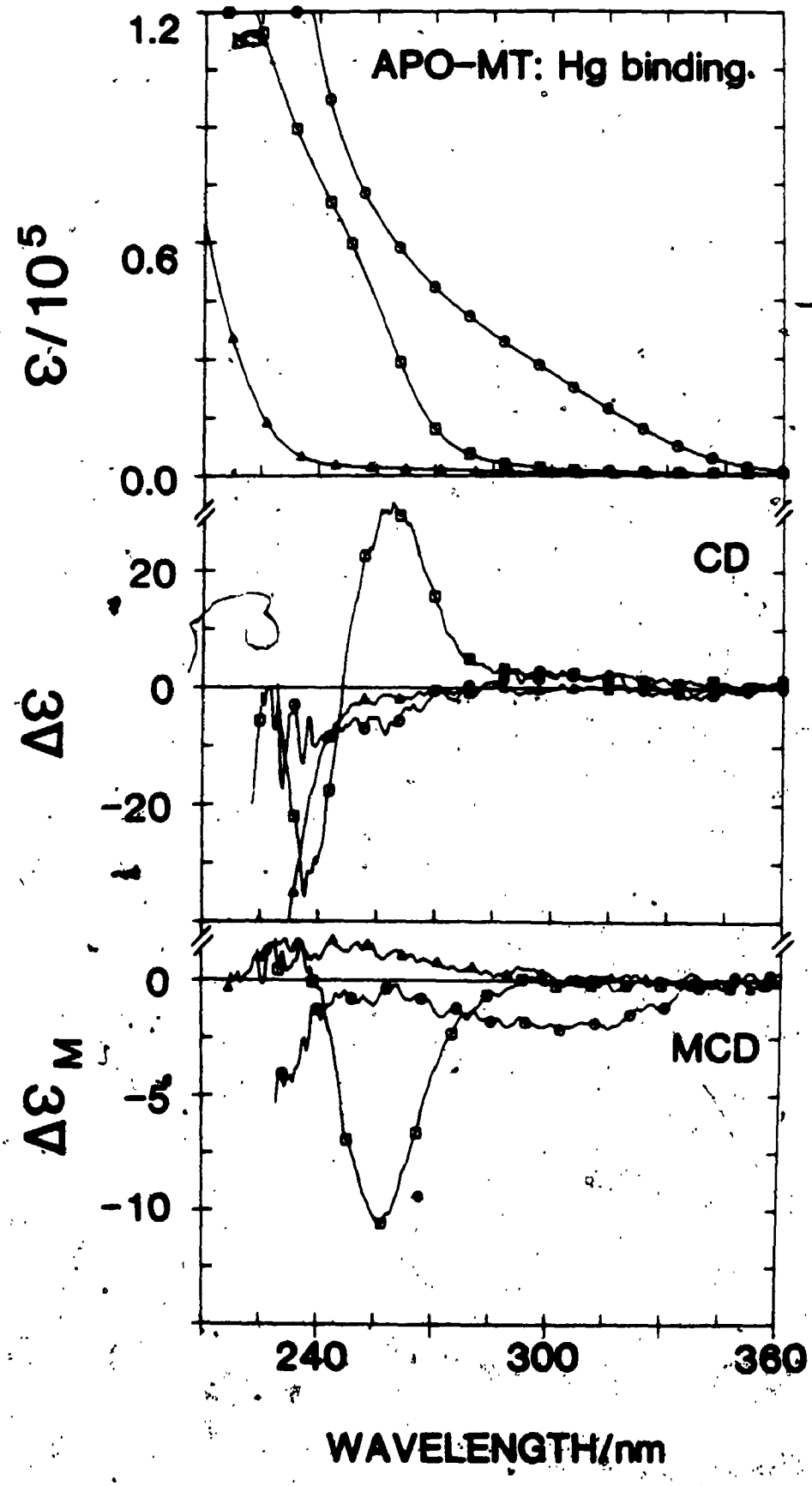
APO–MT: Hg binding.
1.2
0.6
0.0
ε/10⁵
CD
20
0
−20
Δε
MCD
0
−5
−10
Δε M
240
300
360
WAVELENGTH/nm

5.3.5. Co^{2+} binding

The addition of 27 mole equivalents of Co^{2+} to a Cd,Zn-MT solution at pH 7 did not result in the displacement of either Cd^{2+} or Zn^{2+} from MT since no changes in either the absorption or CD spectra are observed. The acidification of the solution containing added Co^{2+} followed by reneutralization of the solution to pH 7 did not give rise to significant changes in the spectra.

The passage of a solution of acidified protein through a column pretreated with Co^{2+} solution again did not result in the formation of Co-MT. However, metal analysis showed that all the Zn^{2+} ions were removed from the MT. The absorption spectrum obtained for the protein solution after equilibrium dialysis of a Cd,Zn-MT sample in a 0.98 M $CoSO_4$ solution, shows three new absorption shoulders at 285 nm, 320 nm and 640 nm.

FIG. 26 shows the absorption and MCD spectra recorded for a sample of reconstituted Co-MT. The Co^{2+} solution was added to the apo-MT sample under nitrogen and at pH 1. When the pH of this solution was raised to 7.0 by the addition of μL aliquots of a 2 M Tris solution, the protein solution immediately turns a deep green colour with a small amount of precipitates being slowly formed.

5.4. DISCUSSIONS

The discovery that Hg^{2+} is associated with the metallothionein fraction isolated from Hg^{2+} injected rats (21,184-188) has aroused special interest as it implies that metallothionein may be involved in a detoxification mechanism for Hg^{2+}. A recent report on the characterization of mercury-containing proteins isolated from rat kidneys has confirmed that they belong to the metallothionein class of

FIG. 26 The absorption and MCD spectra for Co-MT. The apo-MT was prepared by dialysis at pH 1. An μL aliquot of $CoSO_4$ solution was added to the apo-MT and the pH of the solution was raised to 7 using a 2 M Tris solution. The spectra in the UV region were measured using a 0.2 cm quartz cell and a 1 cm cell was used for spectra recorded in the visible region. The units for the absorption and MCD spectra are absorbance units.

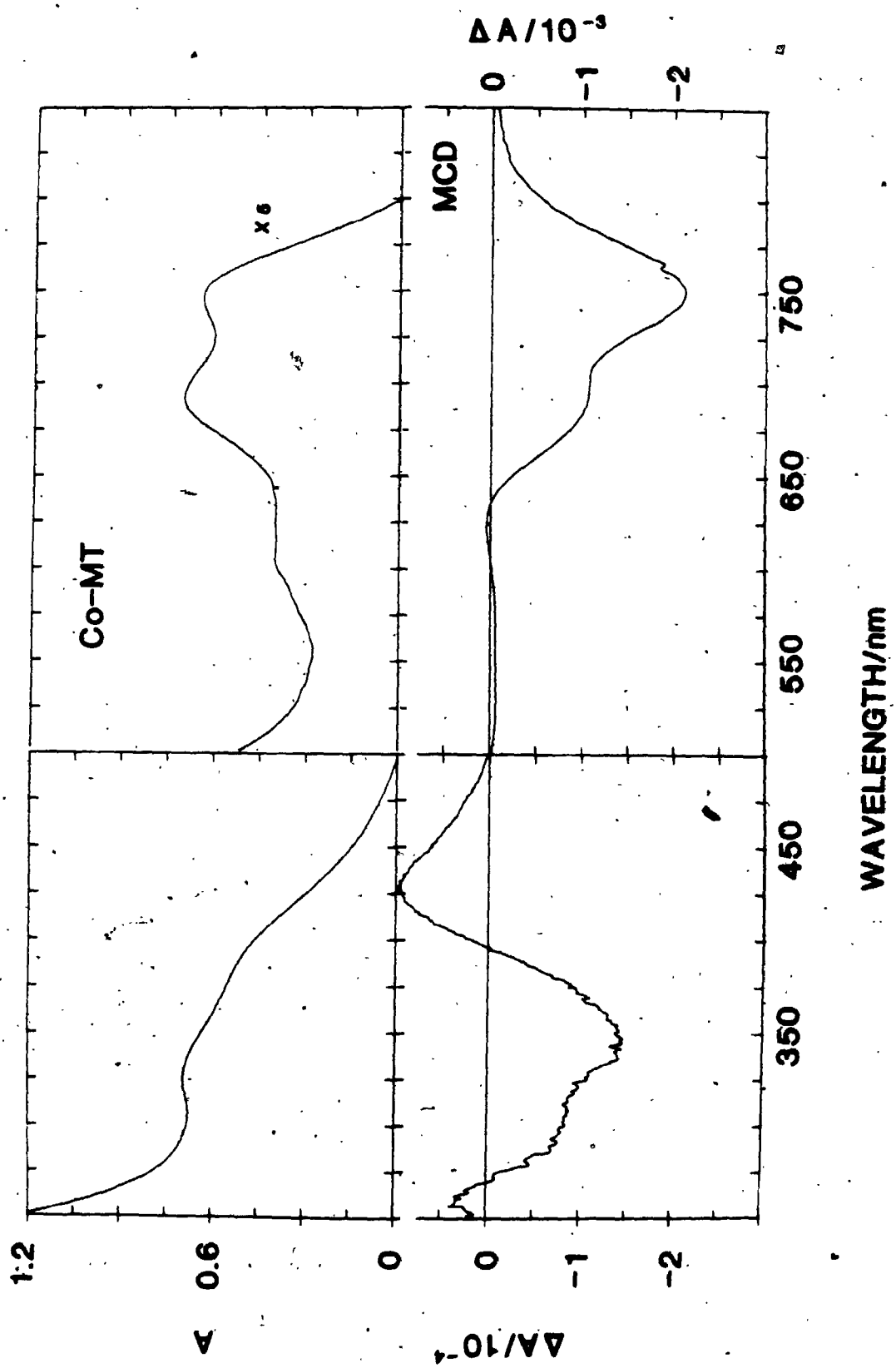
ΔA/10⁻³
0
-1
-2
MCD
Co-MT
x6
750
650
550
450
350
WAVELENGTH/nm
1·2
0·6
0
A
ΔA/10⁻⁴

proteins (31). However, there is no detailed spectroscopic study of the Hg^{2+} binding sites in Hg-containing MT synthesized in vivo. Hence it is not known whether these proteins contain the alpha and beta cluster structures similar to that observed in Cd,Zn-MT. An early X-ray photoelectron study of a reconstituted Hg-MT has provided information on the mode of binding of Hg^{2+} in Cd,Zn-MT. It was reported that the binding of Hg^{2+} involved the cysteine thiolate groups (189). Only recently that native Hg,Cu-MTs, isolated from rat kidneys, have been characterized. It was found that these MTs contained three isoforms, each with a different Cu^{+} to Hg^{2+} mole ratio in the range from 1.2 to 2.4 (74). A subsequent study have shown that the three isoforms exhibit different light emission characteristics (74,192). As the Hg^{2+}/Cu^{+} ratio increases, the emission due to the Cu^{+} is quenched which suggests that the Hg^{2+} is bound in close vincinity to the the Cu^{+} ions. These results provide evidence that the Cu^{+} and Hg^{2+} ions are not randomly distributed in the MT and that there is a difference in the binding affinity of the metal ions for the two cluster sites.

The results shown here clearly demonstrate that the changes in the absorption and MCD spectra of MT occurred in 2 steps upon addition of Hg^{2+}. In the model compound study of BAL with Hg^{2+} described earlier in chapter 4, a well-resolved absorption band centred at 284 nm with a band width of about 20 nm is observed. This provides supporting evidence that the broad absorption shoulder observed in the titration arises from a S->Hg charge transfer transition. A similar absorption profile has been reported for a Hg^{2+} titration with bismuth-induced Zn-MT (192) as well as for a Hg-MT prepared from reconstituted apo-MT

(23,47). The characteristic increase in the intensity and resolution of the 250 nm shoulder signifies that the Zn^{2+} is removed from the binding sites. The species formed at this stage of the titration may be regarded as Cd,Hg-MT with 3 moles of Hg^{2+} bound to the beta cluster. Unlike the Cu^{+} binding to Cd,Zn-MT (which will be discussed later in Chapter 6) in which 2 moles of Cu^{+} displace one mole of Zn^{2+}, giving a beta cluster that contains 6 moles of Cu^{+}, the Hg^{2+} does not behave in a similar manner.

The second stage of the titration is flagged by the isosbestic changes in the 250 nm absorption shoulder and the Hg-related absorption at 290 nm. The two stages in the Hg^{2+} binding experiment appear to distinguish between the binding of Hg^{2+} to the 3-metal cluster (previously suggested to contain primarily Zn^{2+}) followed by the displacement of Cd^{2+} from the 4-metal cluster. The isosbestic points observed in the MCD spectra indicate that only one species is being formed in the reaction and, therefore, this suggests that the Cd^{2+} ions in the cluster are displaced in a cooperative manner. The changes in the absorption spectrum, together with results from AAS measurements essentially support the 1:1, sequential displacement of first Zn^{2+} and then followed by Cd^{2+}. The results from the dialysis experiments strongly support the conclusion that Zn^{2+} is displaced from the protein before the Cd^{2+}.

Both the ^{113}Cd nmr data (98) and a comparison of the MCD spectra obtained for Cd-MT and those of the model compounds of Cd^{2+}, suggest that the Cd^{2+} ions in MT binding sites involve a tetrahedral arrangement of cysteine sulfurs. The MCD spectra of the Cd^{2+} model compound prepared in this study resemble that of Cd-MT very closely in

both their band positions and band widths which suggests that the microsymmetry of the metal binding sites of the model compounds and that of Cd-MT is identical. MCD spectra of BAL with both Cd^{2+} and Hg^{2+} have shown a near symmetrical, derivative-shaped envelope (a Faraday A term) for sulfur to metal charge transfer transitions when the symmetry is close to tetrahedral. Similar MCD spectra have been reported for a series of tetrahalo complexes of Hg^{2+} where the derivative-shaped MCD band has been attributed to a Faraday A term (177). The MCD spectrum obtained in this work when the amount of Hg^{2+} added is equivalent to the total Cd^{2+} and Zn^{2+} initially present in the protein shows a broad derivative-shaped signal which crosses the zero line at about 275 nm. The MCD maxima obtained in this titration study correspond closely to those observed previously, in both their band widths and band positions. However, a comparison with the MCD spectrum obtained for a BAL-Hg^{2+} model compound shows that there is a significant difference in the band widths observed. The discrepancy in the band widths implies that there is a considerable difference between the symmetry of the binding sites in the Hg-MT and that of the model compound. Based on the relatively low signal intensity observed in the MCD spectrum of the Hg-MT prepared by Hg^{2+} titration when compared to the MCD band due to Cd^{2+}, and the significant difference in the band widths when compared to those of the model compound, we conclude that the derivative-shaped MCD envelope observed in this study does not represent an MCD A term but two B terms of opposite signs. Hence, the Hg^{2+} binding sites in MT do not appear to involve a tetrahedral symmetry.

The changes observed in the MCD spectrum when in excess of 7 mole

equivalents of Hg^{2+} were added suggest that the geometry of the Hg^{2+} binding sites is different. This can be rationalized by the tendency of Hg^{2+} to form 2- coordinate species (157,158).

In contrast to Cd^{2+} titrations with Cd,Zn-MT where the displacement of Zn^{2+} by Cd^{2+} only induces relatively minor spectral changes in the CD spectrum, the addition of Hg^{2+}, results in a dramatic decrease in the CD intensity due to Cd,Zn-MT. This suggests that the initial binding of Hg^{2+} induces a change in the protein conformation which probably results from the large difference in the ionic radii between the Cd^{2+}/Zn^{2+} and Hg^{2+}. The markedly different chemical shift of the $2p_{1/2,3/2}$ levels of sulfur observed in the x-ray photoelectron spectrum of Hg-reconstituted MT (189) also supports this conclusion.

The addition of Hg^{2+} to bismuth induced Zn-MT has resulted in the formation of a complex set of CD signals as well as a derivative-shaped MCD spectrum (192). It is difficult to rationalize the dramatically different CD spectrum obtained for this titration as compared to that observed with the Zn-MT unless the Cd^{2+} present exerts a structural influence on the binding of the Hg^{2+}.

Results from the dialysis experiments further support the sequential nature of the metal replacement reactions. The isomorphous displacement of the metal ions in MT is clearly demonstrated in the plot of the different metal concentrations in solutions versus the mole equivalents of Hg^{2+} added.

The binding of Hg^{2+} to apo-MT has also been demonstrated in this work. The MCD spectrum obtained for the solution containing 11 mole equivalents of added Hg^{2+} corresponds closely to those observed in the Hg^{2+} titration when more than 7 mole equivalents of Hg^{2+} have been

added. This suggests that in the presence of excess Hg^{2+}, 2-coordinated Hg^{2+} predominates in the metal binding sites in metallothionein. Therefore, the mode of Hg^{2+} binding in MT changes with the Hg^{2+} content.

An attempt to study the binding of Hg^{2+} to horse MT using ^{199}Hg nmr was not successful. No ^{199}Hg nmr signals were observed in the region expected for mercury thiolates (194) probably due to the lability of the Hg^{2+} in the binding sites.

The in vitro titration study with Co^{2+} indicates that Co^{2+} has a much lower affinity for the binding sites containing Cd^{2+} and Zn^{2+}, such that even in the presence of a large excess of Co^{2+}, the displacement of either the Cd^{2+} or Zn^{2+} does not take place. The reaction is not time dependent since no change in either the absorption or CD spectrum was observed after 24 hours. The pH experiment was used to test the relative binding constants of Cd^{2+} and Co^{2+} to apo-MT. Even though the concentration of the Co^{2+} in solution was much higher than that of Cd^{2+}, the CD spectrum obtained after the pH cycle exhibited only a very slight change in the CD spectrum due to the native protein. This suggests that the affinty of Co^{2+} for the metal binding sites in MT is very low.

The absorption spectrum obtained for the solution after equilibrium dialysis with Co^{2+} displayed a number of new absorption shoulders which suggests that some reconstitution has occurred. This has probably resulted from the loss of Zn^{2+} from the beta clusters.

The method used for the reconstitution of the apo-MT with Co^{2+} follows very closely that reported for rabbit Co-MT (106). The absorption, and MCD spectra observed for the Co-MT prepared in this

work show spectral characteristics remarkably similar to those observed previously. The close resemblence between both the absorption and MCD spectra of the rat Co-MT and the rabbit Co-MT suggests that both proteins bind Co^{2+} in a similar manner.

In conclusion, Hg^{2+} has been shown to bind to MT readily. The displacement of Zn^{2+} and Cd^{2+} by Hg^{2+} follows a sequential pattern in which the Zn^{2+} was displaced first. The distinct species formed in the reactions between Cd,Zn-MT and Hg^{2+} can be monitored by the changes in the absorption spectrum with the initial formation of Cd,Hg-MT followed by the formation of Hg-MT when sufficient Hg^{2+} has been added to displace Cd^{2+} and Zn^{2+} in a 1:1 fashion. The similarities between the MCD spectra of Hg-MT prepared in this work and that prepared from other MT species suggest that the geometry of the Hg^{2+} binding sites are the same. The derivative-shaped MCD spectrum formed resembles closely that observed for Hg-reconsituted apo-MT from rabbit liver (47), however, the large difference between the MCD band widths observed for BAL-Hg model compound and that for Hg-MT prepared in this work argues against the early conclusion drawn by other workers. We suggest that MCD signal observed does not represent a MCD A term but rather 2 opposite signed B terms. Therefore, the geometry around the bound Hg^{2+} is not tetrahedral. Furthermore, the stereochemistry around the Hg^{2+} as indicated by the MCD spectrum is changed when in excess of 7 mole equivalents of Hg^{2+} are added to the Cd,Zn-MT. This change can be rationalized by the formation of 2-coordinated Hg^{2+} species. Furthermore, a species with similar MCD spectral characteristic is obtained when 11 mole equivalents of Hg^{2+} are added to apo-MT which

suggests that tetrahedral coordination is not favoured under these conditions.

TABLE X

Positions of MCD band maxima observed for Hg-MT prepared in vitro

Source of native MT	Band positions (nm) and band widths (nm)		Reference
rabbit apo-MT	315(-)	~50	47
	265(+) sh		
	240(+)		
	227(+)		
	223(-) sh		
Rat Zn-MT	310(-)	~44	192
	266(+)		
Horse Cd,Zn-MT	308(-)	~43	193
	240(+)		
	265(+) sh		
Rat Cd,Zn-MT	318(-)	~55	this work
	263(+)		

sh: shoulder

CHAPTER 6: Cu binding to MT

6.1 INTRODUCTION

In addition to Hg-containing metallothioneins, emphasis has recently been placed on Cu-containing MTs. Early attempts to isolate a Cu-containing protein from tissues were met with extreme difficulties due to the ease of polymerization and the susceptibility of Cu^+ to autooxidation (195). Consequently, several Cu-binding proteins isolated were found to contain a variable percentage of cysteine residues and a variable copper content. Early work by Porter et al. (196,197) described a protein with a high content of half-cystine which was comparable to MT (198), while Winge et al. isolated another Cu-binding protein with only 14% of cysteine. The latter protein was named copper chelatin (199). The discrepancy in the cysteine contents was subsequently explained by Bremner (200) and Irons & Smith (201) as a result of the method of preparation used rather than the presence of different forms of Cu-MT.

Since then, Cu-containing MTs have been found to be widely distributed in many tissues (220) and have been isolated from adults and fetal livers of humans and animals (75,76,202-207), as well as chicken intestines (208) and microorganisms, such as yeast (12) and the fungus Neurospora crassa, (13). Despite the extensive biochemical studies undertaken so far, little spectroscopic data have been reported for these native Cu-containing proteins. The spectroscopic studies of the metal binding properties of Cu-MT have only recently been reported. Cu-MT from yeast and Neurospora crassa have been the most actively studied (12,82,182,183,209-212). In addition, Cd,Cu-MT isolated from rat kidneys (74,219) and Cu,Zn-MT from pig and calf

livers (73,213) have also been investigated. Both the yeast and Neurospora crassa protein are classified as metallothionein mainly because of their high cysteine contents and their ability to bind Cu^+. However both proteins have a much lower molecular weight and may be considered as a fragment of the mammalian protein. In particular, the amino acid sequence of Neurospora crassa has been shown to exhibit extensive homology with the first seven cysteine residues of the beta domain in mammalian proteins. Both proteins exhibit a similar absorption spectrum in the 250 nm region, but the significantly different CD spectra observed suggest a difference in the arrangenment of the amino acid residues around the bound Cu^+. Both Cd^{2+} and Co^{2+} binding to neuropora crassa has been reported and the results indicate similar binding features to those observed for Cd-MT and Co-MT, respectively (183).

The isolation and spectroscopic studies of Cu,Zn-MT Cu,Cd-MT from mammalian sources are more interesting. The fact that these mixed-metal Cu-containing MTs can be isolated from Cu^+ or Cd^{2+} injected animals suggests that a metal exchange mechanism exist in <u>in vivo</u>. While the Cu-MTs isolated from microorganisms have been characterized recently, no spectroscopic characterization of Cu-MT obtained from mammalian sources has been reported. In order to analyze the spectral characteristics associated with the mixed-metal MTs, a better understanding of the Cu^+ binding to MT is, therefore, a prerequisite.

A Cu^+ titration study using chicken Cd,Zn-MT, monitored by absorption spectroscopy has been reported by Rupp & Weser (195). The results indicated a loss of the S -> Cd charge transfer absorption as Cu^+ displaced the Cd^{2+} from the protein. No information on the changes

in the stereochemistry of the binding sites could be obtained from these absorption data. In a later report, Rupp et al. (214) demonstrated that changes in the CD spectrum did occur during the Cu^+ titration. The spectral changes observed were very complex; however, no attempts were made by these authors to rationalize the new signals observed in the CD spectrum or identify the species formed during the titration. In addition, the protein sample used in their study contained 8.2 moles of Cd^{2+}/12000 g of protein. The relatively different metal contents in the native protein (in contrast to the 7 mole-equivalents of metal ions normally expected), together with the 15 mole equivalents of Cu^+ (thought to be bound to the protein in the presence of an excess of Cu^+) demonstrate the need to reinvestigate the stoichiometry of Cu^+ binding in Cd,Zn-MT. Winge et al. have recently reported a Cu-MT isolated from rat liver which contains 9-11 mole equivalents of Cu^+ ions (107,215). More importantly, Cu^+ is known to replace Cd^{2+} and Zn^{2+}, hence it represents an additional probe for the study of metal ion affinities of the two metal clusters in metallothionein. Furthermore, the results obtained from this titration study may be used as a basis for the interpretation of spectroscopic data observed in mixed-metal Cu-containing MTs synthesized *in vivo*. A recent report describes the optical study of a Cd,Cu-MT prepared *in vivo* (219) and it demonstrates the potential of CD and MCD techniques in monitoring the changes in the metal-binding sites on protonation of the cysteine sulfurs.

In this chapter, detailed studies of *in vitro* Cu^+ binding to Cd,Zn-MTs from rat liver and guinea pig using absorption, CD and MCD spectroscopies are presented. The effect of Cu^+ binding on the CD and

MCD spectra of a sample of alpha fragment prepared from rat liver is also described. A Cu^+ salt was used in the titration study because previous reports have shown that the copper bound in MT is in the +1 oxidation state (75,82,215,210).

6.2. EXPERIMENTAL

Both isoforms 1 and 2 of rat liver Cd,Zn-MT, guinea pig Cd,Zn-MT 2 and a sample of an alpha fragment prepared from the rat liver protein were used in the Cu^+ titration experiments. All protein samples were prepared as reported previously (125-127).

6.2.1. Cu^+ titration experiments

(i) Rat liver Cd,Zn-MT 1 and 2

The freeze dried protein sample was dissolved in a CH_3CN/H_2O (1:3 vol/vol) solution. The $Cu(CH_3CN)_4ClO_4$ salt was prepared according to Hemmerich & Sigwart (147) and dissolved in a CH_3CN/H_2O mixture. All solutions were prepared in a glove bag and deaerated with nitrogen and/or argon before use. Two Cu^+ solutions were prepared with a concentration of 8.8×10^{-3} M and 2.2×10^{-2} M, respectively. The less concentrated solution was used for the initial addition of Cu^+ and the more concentrated one was used in the latter part of the experiment to prevent excessive dilution of the protein sample. Aliquots of Cu^+ were added to a 3 mL volume of the protein and a separate 3 mL volume was used for each spectrum. All absorption spectra were recorded immediately following addition of Cu^+ ions, while the CD and MCD spectra were recorded within 10 mins after each addition.

(ii) Rat liver alpha fragment

The protein sample and Cu^+ solutions were prepared as described earlier with the Cd,Zn-MT 1. This sample contained 4.8 mole

equivalents of Cd^{2+}. The protein concentration was determined using the DTNB method (see Chapter 2) and assuming 11 sulfurs in the alpha fragment (98,125). The volume of the sample used was 2.5 mL and the Cu^{+} was added directly into the 1 cm cuvette. All solution preparations were carried out under nitrogen with deaerated H_2O or CH_3CN/H_2O mixtures.

(iii) Guinea pig Cd,Zn-MT 2

The titration experiment was carried out in a similar manner as described previously for the alpha fragment sample. The protein sample used contained 4 moles of Cd^{2+} and 2 moles of Zn^{2+} per mole of protein. The protein concentration was determined from the reaction with DTNB.

6.2.2. Dialysis and pH experiments

μL aliquots of a Cu^{+} solution were added to four 2.5 mL volume of the protein solution. The absorption and CD spectra of these solutions were recorded. These solutions were then dialysed in deaerated triply distilled water, with two changes of solutions. The total time of dialysis was 10 hours and dialysis tubing with a molecular weight cutoff of 3500 was used. The metal content in the solutions after dialysis were measured using atomic absorption spectrophotometry (AAS).

6.2.3. Spectra

As described in Chapter 2.

6.3. RESULTS

6.3.1. Cu^{+} loading experiment

6.3.1.1. Rat liver metallothionein

(i) Rat liver Cd,Zn-MT 1

FIG. 27 shows the results obtained from a titration experiment for a sample of rat liver Cd,Zn-MT 1 with Cu^+. This protein solution contained 4.5 moles of Cd^{2+} and 2.1 moles of Zn^{2+} per mole of protein. The absorption changes occur in three stages, in a similar manner to that observed for Cd^{2+} binding to metallothionein. Due to the complexity of the spectral changes observed, the spectra have been replotted in 3 stages (FIG. 27 A-C). The initial addition of up to 2.0 mole equivalents of Cu^+ (which is very close to the mol eq of Zn^{2+} initially bound in MT) results in an increase in the absorption shoulder in the 250 nm region and absorbance in the 280 nm region (line 1-8). The increase in absorption and resolution of the 250 nm shoulder has previously been suggested (in Chapter 3) as a red-shift of the S->Cd charge transfer transition, and is present regardless of the metal ions used to displace Zn^{2+}. The second stage of the Cu^+ binding (lines 8-11) is characterized by a decrease in $A_{250\ nm}$ and an increase in the absorption in the 280 nm region with isosbestic points near 240 nm and 260 nm, respectively. These absorption changes demonstrate the displacement of Cd^{2+} by Cu^+. The S->Cd charge transfer band is replaced by a broad absorption band at about 300 nm. The final stage represents the point where more than 10.1 mole equivalents of Cu^+ have been added (lines 14-16) and the absorption spectrum shows an overall increase in absorbance.

The changes in the CD spectrum are much more complex. Initial changes in the CD spectrum involve mainly the 225 nm and 238 nm bands, while the 258 nm band remains unchanged. The MCD spectrum exhibits a red shift of the negative lobe due to the removal of the Zn-related band at a higher energy. At the same time, a new positive band

develops at about 292 nm in the CD spectrum which is accompanied by a broad, negative MCD signal. When the concentration of Cu^{+} in the protein solution is double that of the Zn^{2+} concentration initially present, more dramatic changes are observed in the CD and MCD spectra. The original derivative-shaped CD signal due to the Cd^{2+} binding sites diminishes in intensity, while the positive CD band at 292 nm gains significantly in intensity. When up to 8.4 mole equivalents of Cu^{+} have been added, a new CD signal appears which consists of two positive and one negative bands: 292 nm(+), 268 nm(-) and 242 nm(+). While the intensity of the 292 nm band does not change significantly when a further 1.7 mole equivalents of Cu^{+} (a total of 10.1 mole equivalents) were added, the two CD bands at 245 nm and 268 nm continues to increase in intensity and reaches a maximum when 10.1 moles of Cu^{+} had been added. Further addition of Cu^{+} beyond the 10.1 moles results in the disappearance of the newly formed CD signal and the formation of a new set of CD bands. The final four traces were obtained with a Cu:protein mole ratios of 12.9, 19, 25, 28.9, respectively . The final CD spectrum observed has three broad bands: 260 nm(+), 285 nm(-) and 340 nm(+). This CD spectrum resembles closely that obtained by Rupp & Weser (195,214) during an in vitro Cu^{+} titration of chicken Cd,Zn-MT.

The changes in the MCD spectrum are characterised by a decrease in the negative lobe due to the Cd-chromophore (with the isosbestic point at 248 nm), and the increase of a weak broad negative band at around 300 nm. The final MCD spectrum obtained when more than 12.9 mole equivalents of Cu^{+} are added exhibits two broad negative bands at around 300 nm and 250 nm.

FIG. 27 The effect of adding Cu^{+} on the absorption, CD and MCD spectra of a sample of rat liver Cd,Zn-MT 1. The native solution contained 4.5 mol eq Cd^{2+} and 2.1 mol eq Zn^{2+}. The total mol eq of Cu^{+} in each solution was A: (1) 0 (native), (2) 0.78, (3) 1.1, (4) 1.5, (5) 2.0, B: (6) 2.4, (7) 3.1, (8) 3.8, (9) 6.1, (10) 6.4, (11) 7.1, (12) 8.4, (13) 10.1, C: (14) 12.9, (15) 19.0, (16) 25.0, (17) 29.0. The units for ε and $\Delta\varepsilon$ are L mol^{-1} cm^{-1}. The units for $\Delta\varepsilon_M$ are L mol^{-1} cm^{-1} T^{-1}.

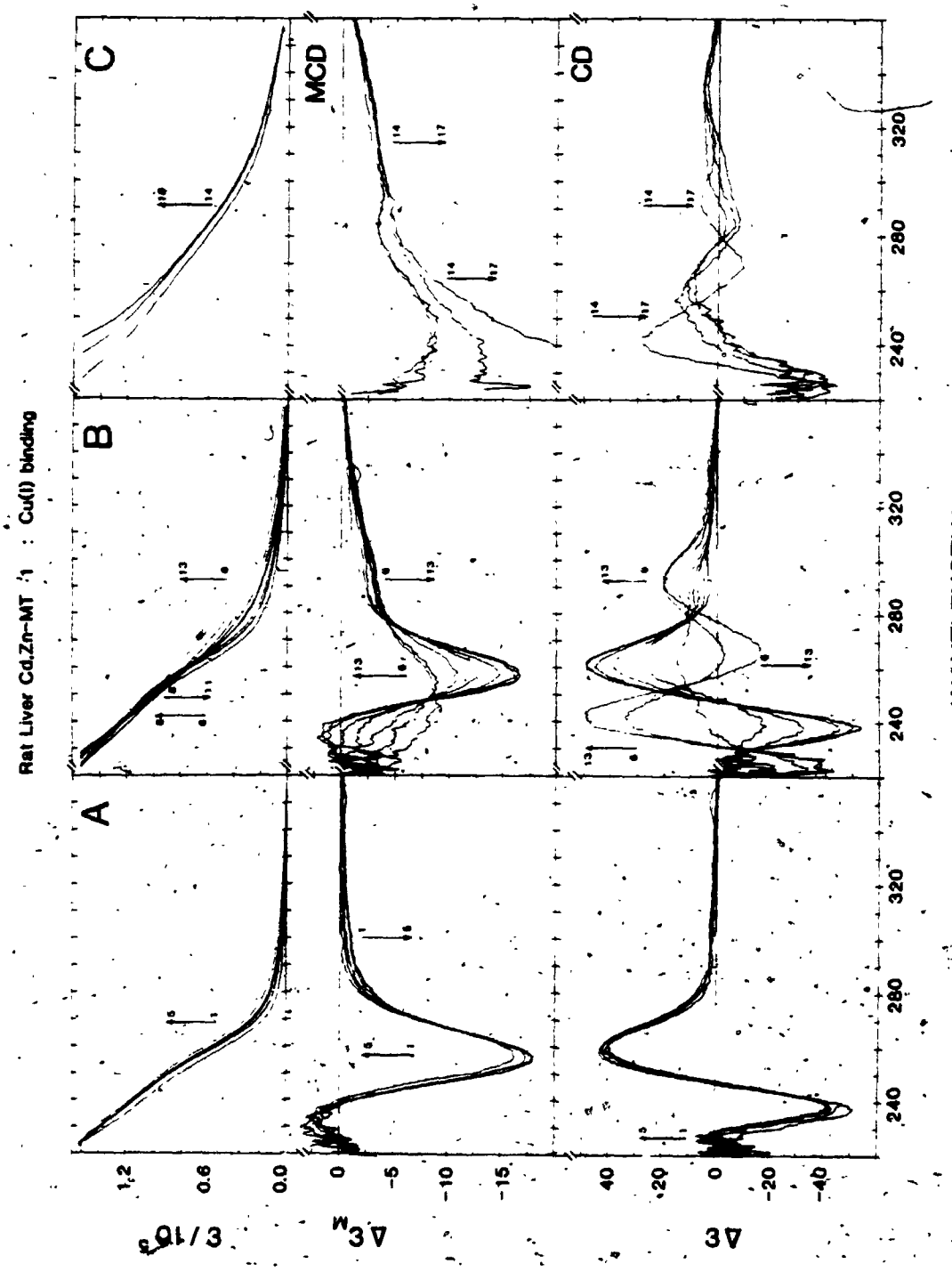
Rat Liver Cd,Zn-MT : Cu(I) binding
A
B
C
MCD
CD
ε / 10³
Δε_M
Δε
WAVELENGTH/nm

FIG. 28 A plot of the changes in the CD band intensities versus mole equivalents of Cu^{+} added to the rat Cd,Zn-MT 1. The three wavelengths plotted correspond to the maximum peak positions of the new CD signal observed during the Cu^{+} titration.

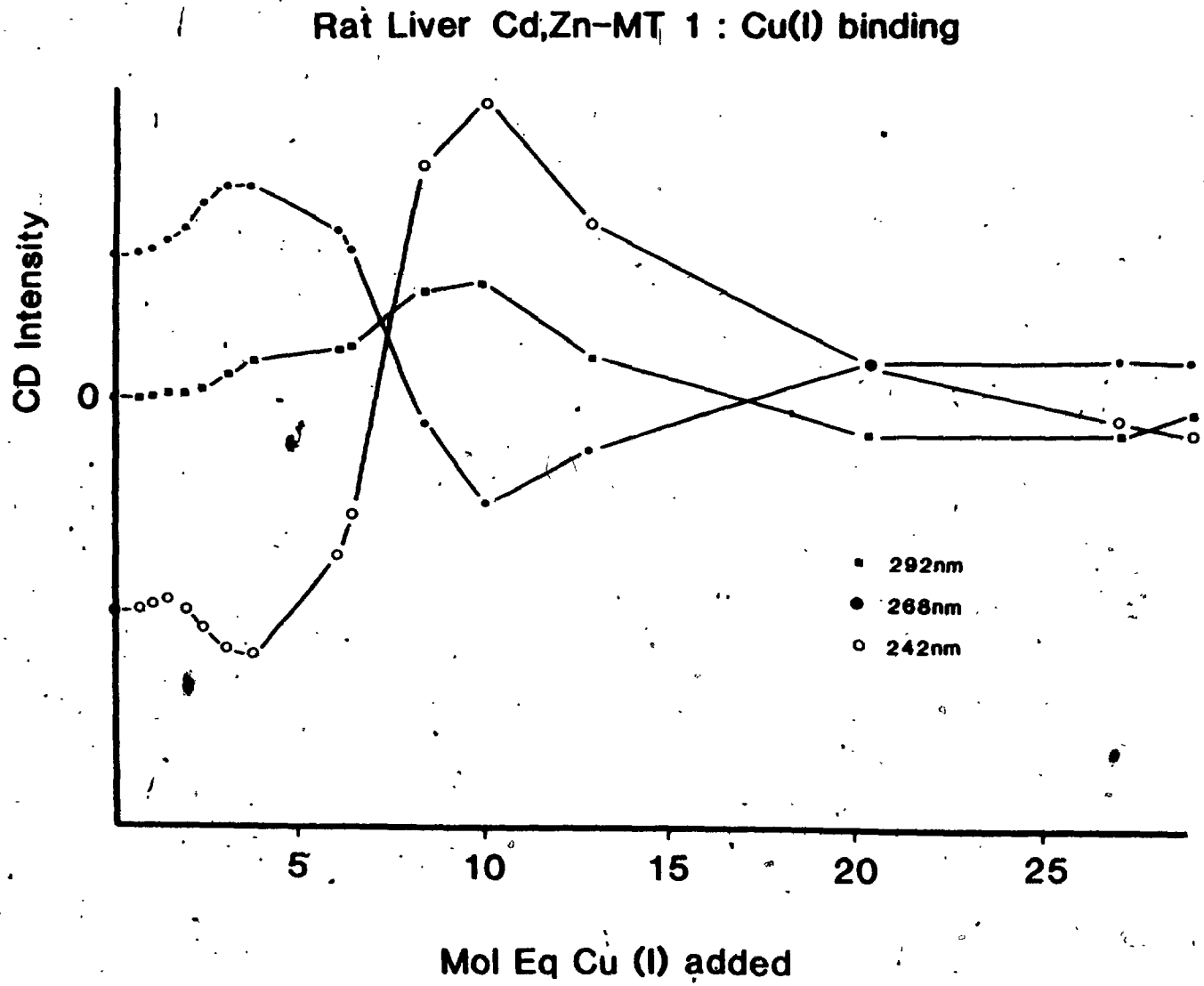
Rat Liver Cd,Zn-MT 1 : Cu(I) binding
CD Intensity
0
292nm
268nm
242nm
5
10
15
20
25
Mol Eq Cu (I) added

FIG. 28 shows a plot of the intensity changes in the CD spectrum at several wavelengths versus the mole equivalents of Cu^+ added. The three wavelengths plotted correspond to the peak positions of the new CD signal observed during the Cu^+ titration (FIG. 27, line 13). It is clear that the new derivative CD signal reached its maximum intensity when about 10 mole equivalents of Cu^+ had been added. When the Cu^+ content is more than double that of the Zn^{2+} ions present in the protein sample, the changes in the CD intensity at 292 nm become significant. A similar set of titration data was also obtained for both the rat liver Cd,Zn-MT 2 and guinea pig Cd,Zn-MT 2.

(ii) Rat liver Cd,Zn-MT 2

FIG. 29 shows the effect of the addition of aliquots of Cu^+ to a Cd,Zn-MT-2 solution. This protein sample contained 3.9 mole equivalents of Cd^{2+} and 2.5 mole equivalents of Zn^{2+}. The initial addition of up to 5.1 mole equivalents of Cu^+ results in an increase in the 250 nm absorption shoulder as well as a gradual decrease of the CD spectrum due to the native protein. A small increase in the 292 nm CD band is also observed. The last trace in FIG. 29A represents the point where the mole equivalents of Cu^+ added was twice that of the Zn^{2+} bound initially. The effect of further additions of Cu^+ on the absorption and CD spectra is illustrated in FIG. 29B. Both the absorption and CD spectra show isosbestic changes. The 225 nm CD band of the native protein collapses completely when 6.1 mole equivalents of Cu^+ had been added. Further addition beyond 6.1 mole equivalents show a gradual disappearance of the remaining 258 nm CD band and with a corresponding increase in the 292 nm band intensity. The final CD spectrum obtained in this second stage (line 10) is characterized by 3

FIG. 29 The effect of adding Cu^{+} on the absorption and CD spectra of rat liver Cd,Zn-MT 2. The metal concentrations of this solution are: Cd^{2+}= 5.9×10^{-8} moles; Zn^{2+}= 3.8×10^{-8} moles. Moles of Cu^{+} ($\times 10^{-8}$ moles) added were A: (1) 0 (native), (2) 1.4 (1.0), (3) 2.8 (2.0), (4) 4.2 (3.1), (5) 5.6 (4.1), (6) 7.0 (5.1), B: (7) 8.4 (6.1), (8) 9.8 (7.2), (9) 11.2 (8.2), (10) 12.7 (9.3), C: (11) 14.2 (10.4), (12) 15.4 (11.5), (13) 16.8 (12.3), (14) 18.2 (13.3) (- - - - -), (15) 21.0 (15.3). The values in brackets are mole equivalents of Cu^{+} added. The units for ε and $\Delta\varepsilon$ are L mol^{-1} cm^{-1}.

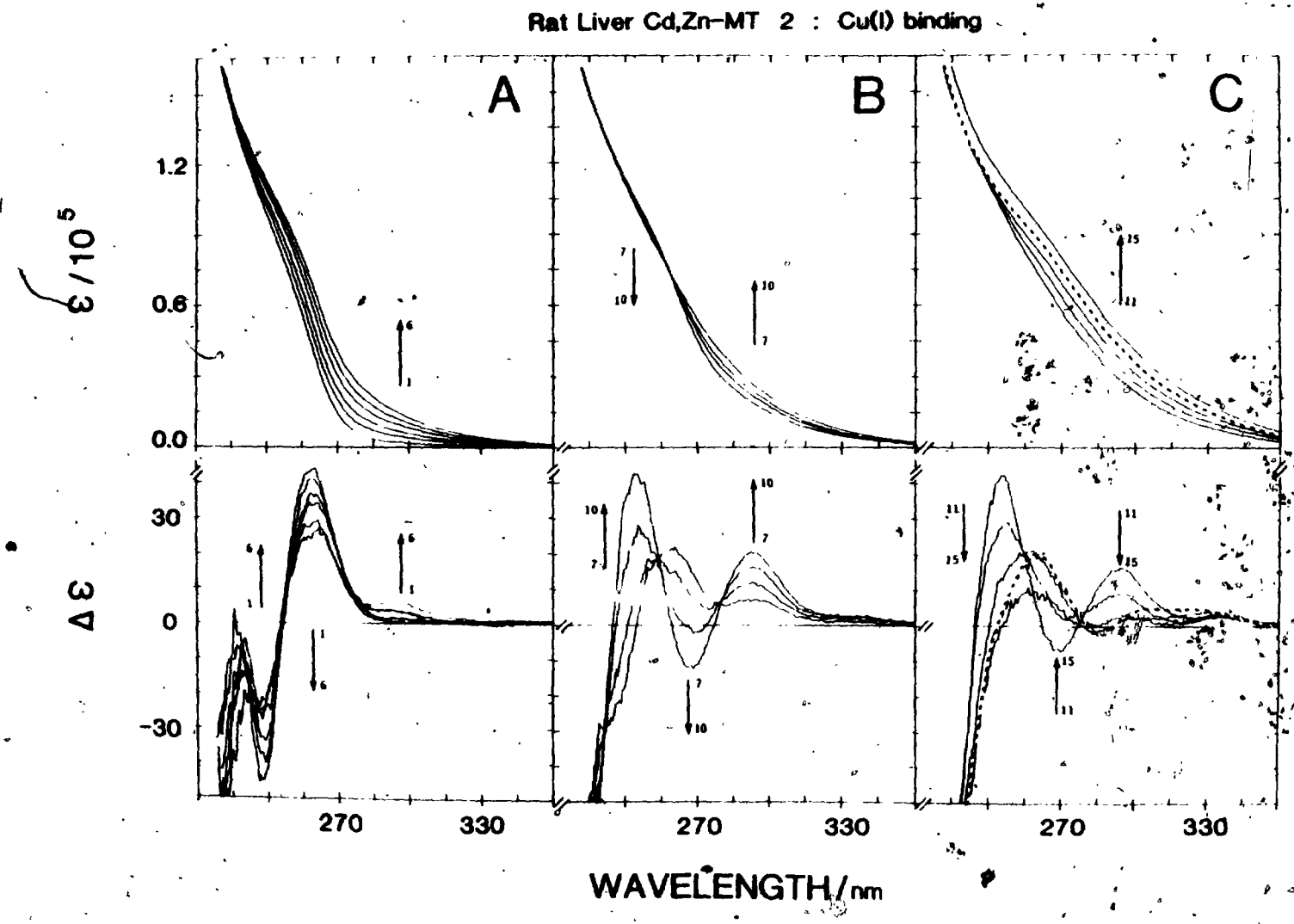
Rat Liver Cd,Zn-MT 2 : Cu(I) binding
A
B
C
1.2
0.6
0.0
ε/10^5
30
0
-30
Δε
270
330
WAVELENGTH/nm

bands (292 nm (+), 268 nm (-) and 242 nm (+)) and is very similar to the transient spectrum obtained during a titration of Cd,Zn-MT 1 with Cu^+ (FIG. 27). FIG. 29C shows the last stage in the Cu^+ binding to MT and the subsequent formation of Cu-MT. The CD spectrum illustrated by the dashed line represents a MT solution containing about 13 mole equivalents of Cu^+. Further increase in the Cu^+ concentration in the sample results in an overall increase in the absorption spectrum and a drop in the CD band intensity.

FIG. 30 shows a plot of the changes in the CD intensity at several wavelengths. Both the 258 nm and 238 nm band due to the native protein were observed to lose intensity as Cu^+ ions were added to the solution. Similar to the case with Cd,Zn-MT 1, the new CD signal with bands at 242 nm(+), 268 nm(-) and 292 nm(+) was found to reach its maximum intensity when the Cu^+ added was about 9.3 mole equivalents.

6.3.1.2 Guinea pig Cd,Zn-MT 2

FIG. 31 shows the absorption and CD spectra recorded during a titration of guinea pig MT 2 with Cu^+. This protein sample contained 4.1 moles of Cd^{2+}, 1.7 moles of Zn^{2+} and 0.4 moles of Cu^+. Initial addition of up to 3.9 mole equivalents of Cu^+ results in the gradual decrease in the CD signal intensity (lines 1-4). As further Cu^+ is added (up to 5.6 mole equivalents), the 225 nm positive band of the native CD spectrum collapses completely. A new band at 292 nm increases in intensity, while the 258 nm CD band shows a large drop in intensity. The 292 nm band reaches a maximum when 6.1 mole equivalents of Cu^+ had been added and remains at this intensity even after another 1.4 moles of Cu^+ had been added (to a total of 7.5 mole equivalents of Cu^+). At the same time a new positive band at 242 nm also develops and

FIG. 30 A plot of the changes in the CD band indtensities versus mole equivalents of Cu^+ added to rat liver Cd,Zn-MT 2. The CD bands at 258 nm and 238 nm are due to the native protein. The CD intensity at 242 nm, 268 nm and 292 nm is plotted against the mol eq Cu^+ added.

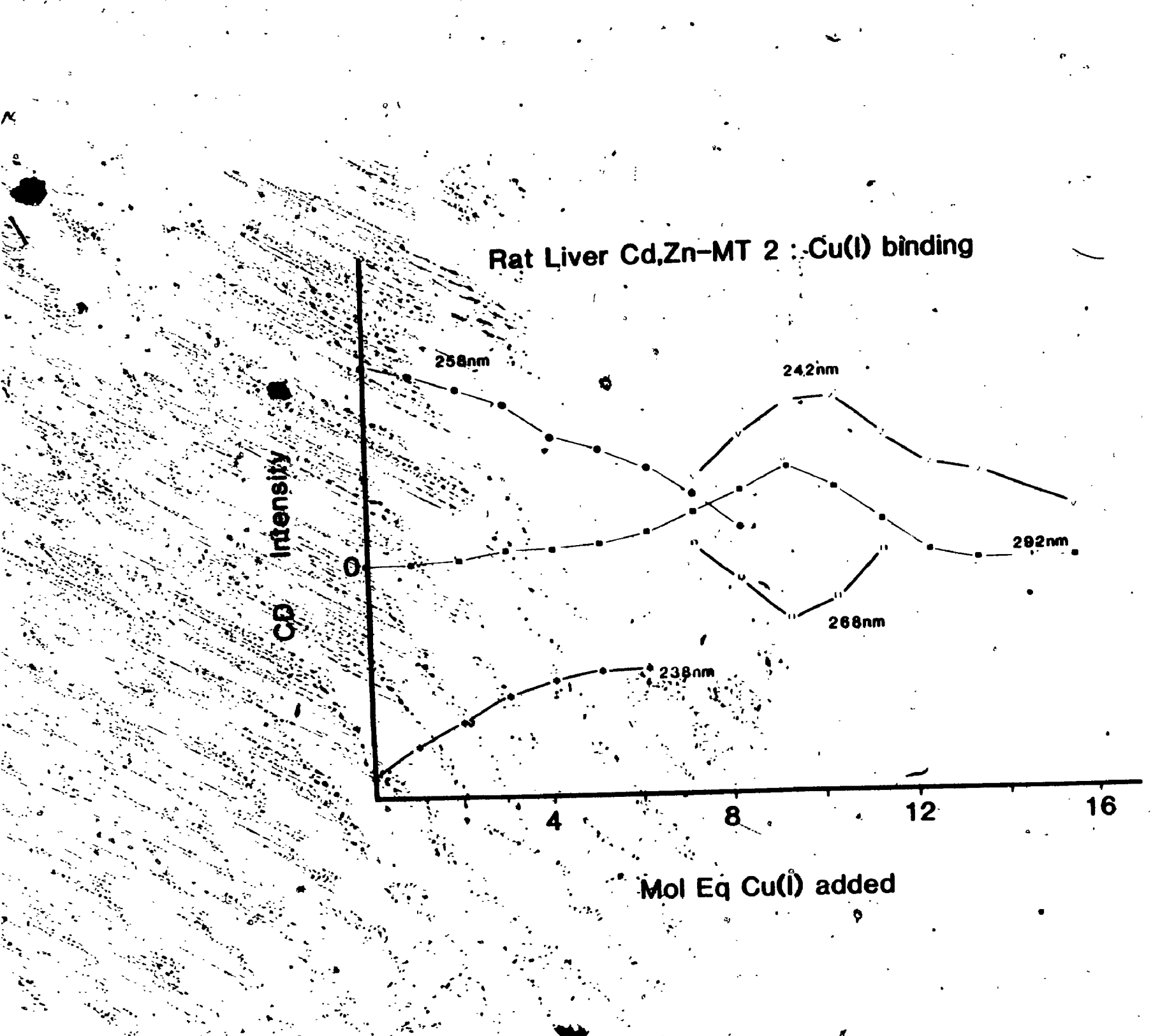
Rat Liver Cd,Zn-MT 2 : Cu(I) binding
258nm
242nm
292nm
268nm
238nm
CD Intensity
0
4
8
12
16
Mol Eq Cu(I) added

FIG. 31 The effect of adding Cu^+ on the absorption and CD spectra of guinea pig Cd,Zn-MT 2. The metal content of this solution was: Cd^{2+}= $7.3x10^{-8}$ moles; Zn^{2+}= $3.1x\ 10^{-8}$ moles; A_{250} = 0.39 before the addition of Cu^+ (dashed line in FIG. 31A represents the spectrum of the native protein). Moles of Cu^+ ($x10^{-8}$ moles) added were A: (1) 0 (native), (2) 1.8 (1.0), (3) 3.6 (2.0), (4) 7.1 (3.9), (5) 10.1 (5.6), (6) 11.0 (6.1), B: (7) 13.5 (7.5), (8) 15.5 (8.6), (9) 17.3 (9.6), (10) 19.1 (10.6), (11) 25.1 (13.9). The values in brackets are mole equivalens of Cu^+ added. In FIG. 31B, the final spectrum containing 13.9 mole equivalents of Cu^+ added (dashed line). The units for ε and $\Delta\varepsilon$ are $L\ mol^{-1}\ cm^{-1}$.

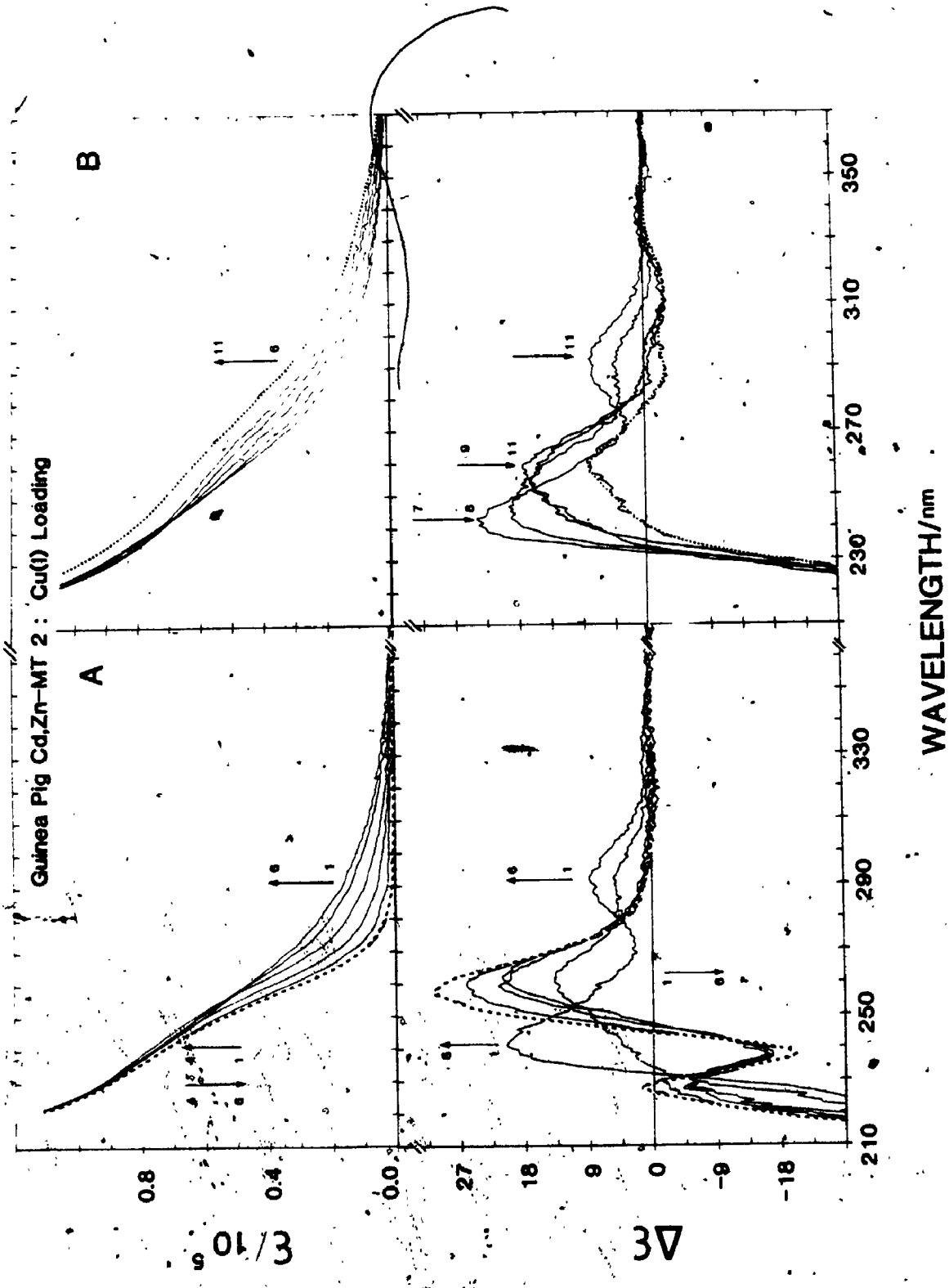
Guinea Pig Cd,Zn-MT 2 : Cu(I) Loading
A
B
ε/10⁵
Δε
WAVELENGTH/nm
0.8
0.4
0.0
27
18
9
0
-9
-18
210
230
250
270
290
310
330
350

FIG. 32 (A) A plot of the changes in the CD intensity versus the mole equivalents of Cu^{+} added to the guinea pig MT solution. Δ CD intensity at 242 nm and 292 nm is plotted in FIG. 32B.

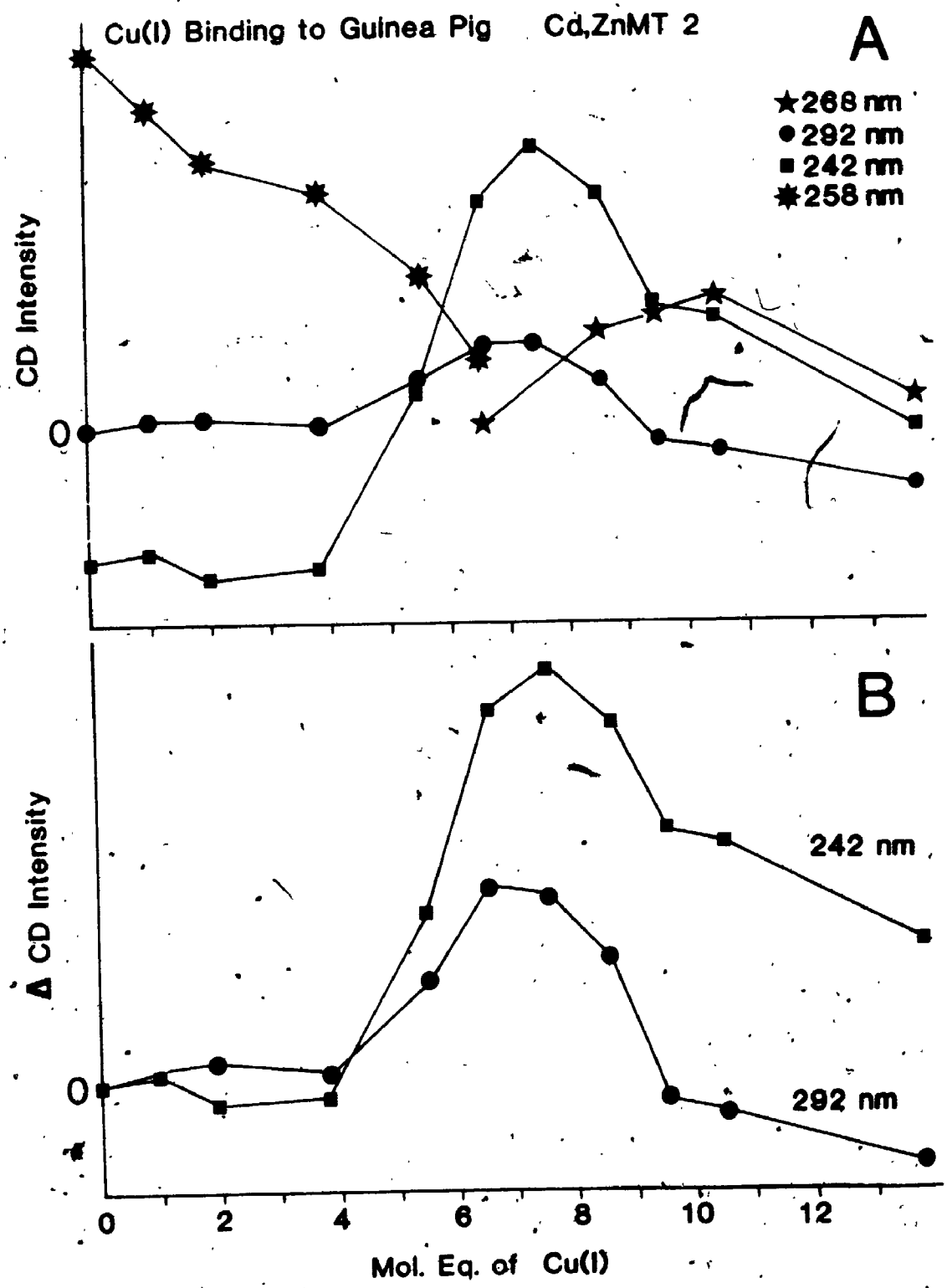
Cu(I) Binding to Guinea Pig Cd,ZnMT 2
A
★268 nm
●292 nm
■242 nm
✱258 nm
CD Intensity
0
B
Δ CD Intensity
242 nm
292 nm
0
0
2
4
6
8
10
12
Mol. Eq. of Cu(I)

reaches a maximum intensity at 7.5 mole equivalents of Cu^+. Further addition of Cu^+ results in a shift of the 242 nm band to longer wavelength, as well as a decrease in the 292 nm band intensity. The changes in the absorption spectrum follow a similar pattern as in the Cd^{2+} loading experiment: where the first aliquots of Cu^+ result in a red-shift of the 250 nm absorption, generating a better resolved shoulder (lines 1-4). The next aliquots added result in isosbestic changes in the 250 nm absorption as the Cu^+ concentration is increased to 6.1 mole equivalents (lines 4-6). The isosbestic points are lost when a total of 7.5 mole equivalents of Cu^+ has been added. Any further additions now result in a general increase in intensity of all bands in the absorption spectrum. The changes in the CD spectrum as Cu^+ is added are clearly evident when the CD intensity at several wavelengths are plotted against the mole equivalents of Cu^+ added, in FIG. 32. The CD intensity at 292 nm and 242 nm did not show sigificant changes until the amount of Cu^+ added was more than 4 mole equivalents. The CD intensity at 268 nm was also plotted to illustrate the growth of the CD band due to Cu^+ binding in the saturated Cu-MT.

6.3.1.3. Cu^+ binding to alpha fragment

The Cu^+ titration studies of a sample of alpha fragment are particularly important because the effect of the Cu^+ addition on the CD and MCD spectra of the isolated 4-metal cluster can be investigated. Moreover, any differences in the Cu^+ binding properties of MT in the absence of the 3-metal cluster can be elucidated.

FIG. 33A shows the absorption, CD and MCD data for a titration of a sample of alpha fragment with Cu^+. This sample contained about 4.8 mole equivalents of Cd^{2+} where the protein concentration was

determined using the DTNB reaction. No Zn^{2+} or Cu^{+} was present in the native protein. The insert in FIG. 33A shows the changes in absorbance at 250 nm and 285 nm as the titration proceeds. The set of data has been replotted in FIGS. 33B-D, in order to illustrate more clearly the sequence of changes that occur in the CD and MCD spectra during the different stages in the displacement of Cd^{2+} by Cu^{+}. Similar to the Cu^{+} titration studies with Cd,Zn-MTs, the Cu^{+} binding reactions in the alpha fragment proceeds in several steps. However, the initial red-shift and increase in intensity of the 250 nm absorption shoulder, a common spectral feature in other metal replacement studies with Cd,Zn-MT, is not observed in the absorption spectrum. This further supports the suggestion that the apparent red-shift and increase in the 250 nm absorption during the early stage of the metal replacement reaction in Cd,Zn-MT is related to the displacement of Zn^{2+} from the protein. In FIG. 33B, the absorption spectrum shows the isosbestic decrease of the S->Cd charge transfer band and a corresponding increase in the absorption in the 285 nm region when up to 3.6 mole equivalents of Cu^{+} are added. This represents about 76 % of the Cd^{2+} initially present. Two sharp isosbestic points at 230 nm and 260 nm are observed.

In the CD spectrum, the derivative envelope due to the Cd-chromophore is shown to decrease with the mole equivalents of Cu^{+} added while a broad band at 292 nm is seen to grow in intensity. When the amount of Cu^{+} added has reached 2.7 mole equivalent which represents about 56% of the Cd^{2+} bound initially to the alpha fragment, the native CD spectrum collapses completely. On the other hand, the MCD spectrum shows the loss of the tetrahedral Cd^{2+} isosbestically and is replaced by a distorted negative signal. Though

both the absorption and MCD spectra exhibit isosbestic behaviour, the absence of isosbestic points in the CD spectra suggests that the displacement of Cd^{2+} during this stage involves more than one reaction. FIG. 33C shows the effect of adding Cu^{+} beyond 3.6 mole equivalents. The CD spectrum shows the isosbestic formation of the characteristic derivative-shaped bands (242 nm (+), 268 nm (-) and 292 nm (+)), which are similar to that observed earlier in Cu^{+} titration studies using rat and guinea pig MTs. The sharp isosbestic points indicate that a single species is now formed which is characterized by the CD spectrum. The MCD spectrum (line 7) shown in FIG. 33C demonstrates a blue-shift of the band maximum to 250 nm. Addition of Cu^{+} beyond 6.3 mole equivalents quenches the CD spectrum (FIG. 33D). The CD spectrum for the final solution containing 16.7 mole equivalents of added Cu^{+} is essentially featureless and the corresponding MCD band shows a significant change in band shape and intensity. FIG. 34 shows a plot of the changes in the CD spectrum at several wavelengths. The absorbance at 250 nm decreases to a minimun when a the amounts of Cd^{2+} and Cu^{2+} are equivalent, while the absorption at 280 nm increases in a linear fashion. A decrease in the 225 nm and 238 nm bands with respect to the mole equivalents of Cu^{+} added to the protein solution is observed. The new CD signal attains its maximum intensity when the Cu^{+}:Cd^{2+} mole ratio is close to 1.1.

6.3.2 Cu^{+} binding and dialysis experiments

6.3.2.1. Alpha fragment

The sharp CD signal observed during the Cu^{+} titration experiment is intriguing because the well defined signal must represent a specific structural arrangement around the bound metal ions. Results from the

FIG. 33 (A) The effect of adding Cu^{+} on the absorption, CD and MCD spectra of rat liver alpha fragment. This solution contained 4.8 mole equivalents of Cd^{2+}. The mole equivalents of Cu^{+} added were: (1) 0 (native), (2) 0.9, (3) 1.8, (4) 2.7, (5) 3.6, (6) 4.5, (7) 5.4, (8) 6.3, (9) 8.7, (10) 11.1, (11) 16.7. The spectra were replotted in three stages (B,C and D). The units for ε and $\Delta\varepsilon$ are L mol^{-1} cm^{-1}. The units for $\Delta\varepsilon_M$ are L mol^{-1} cm^{-1} T^{-1}.

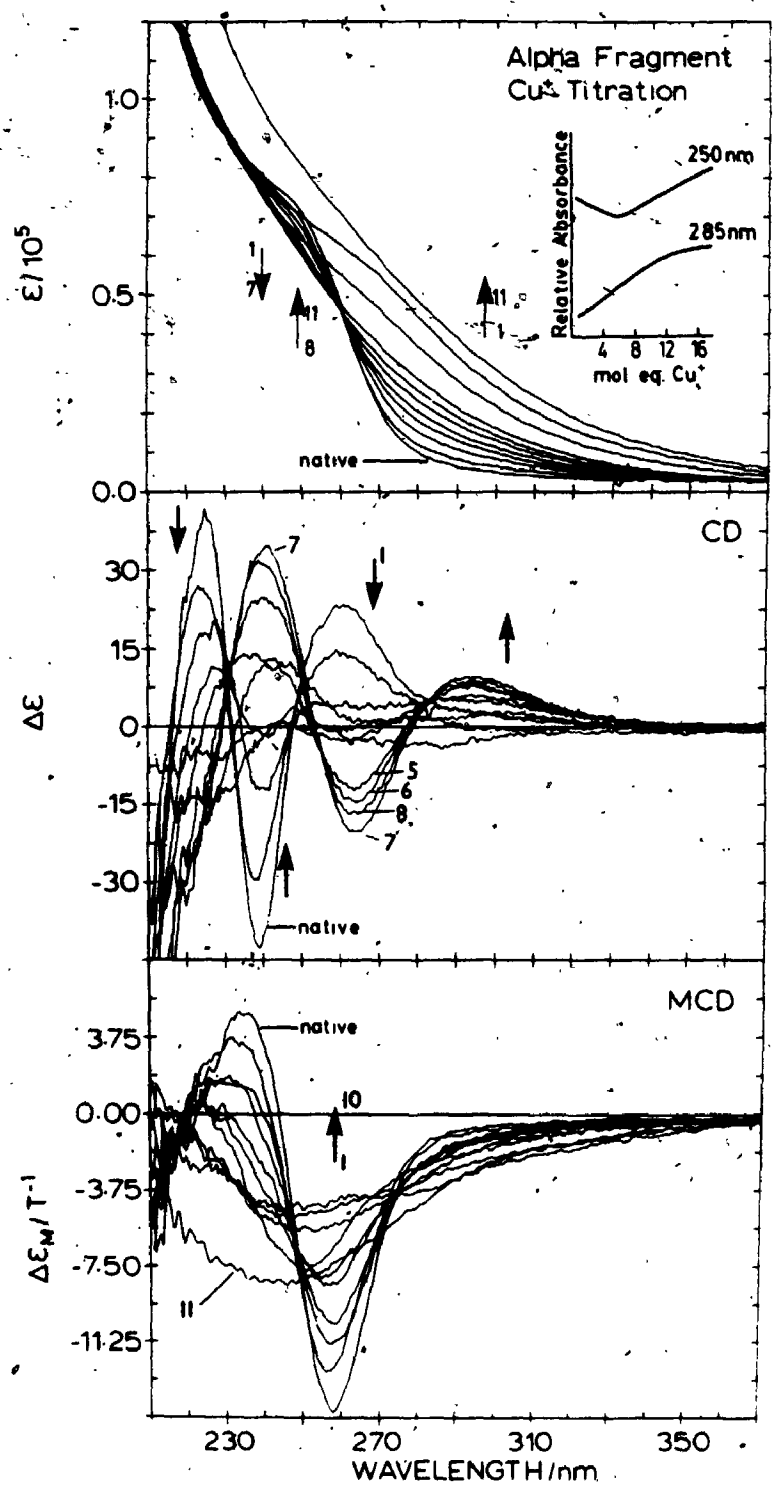
Alpha Fragment
Cu+ Titration
250nm
285nm
Relative Absorbance
4 8 12 16
mol eq. Cu+
ε/10^5
1.0
0.5
0.0
native
CD
Δε
30
15
0
-15
-30
native
MCD
native
3.75
0.00
-3.75
-7.50
-11.25
ΔεM/T-1
230
270
310
350
WAVELENGTH/nm

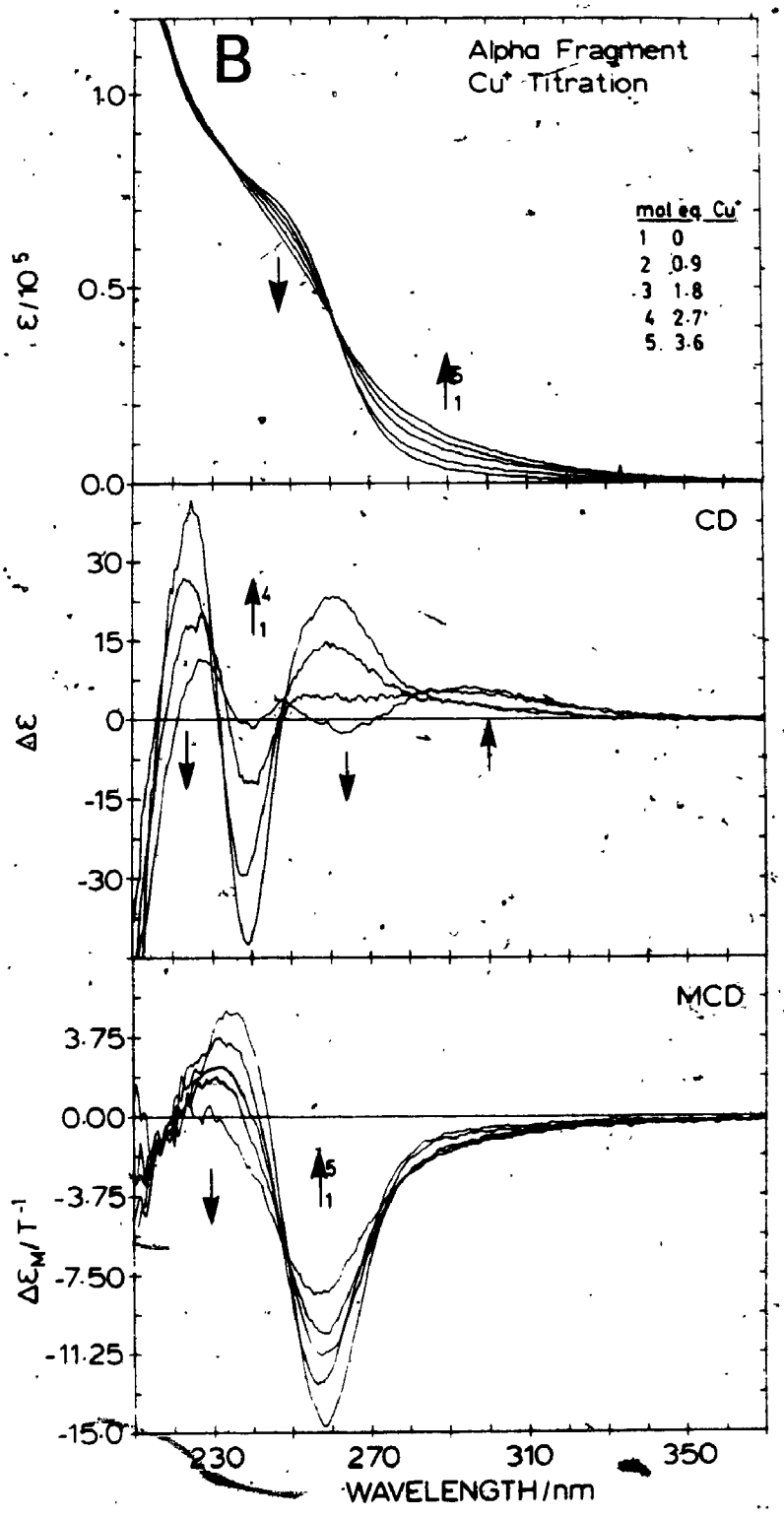
B
Alpha Fragment
Cu⁺ Titration
mol eq Cu⁺
1 0
2 0.9
3 1.8
4 2.7
5 3.6
ε/10⁵
1.0
0.5
0.0
CD
Δε
30
15
0
-15
-30
MCD
$\Delta\varepsilon_M/T^{-1}$
3.75
0.00
-3.75
-7.50
-11.25
-15.0
230
270
310
350
WAVELENGTH/nm

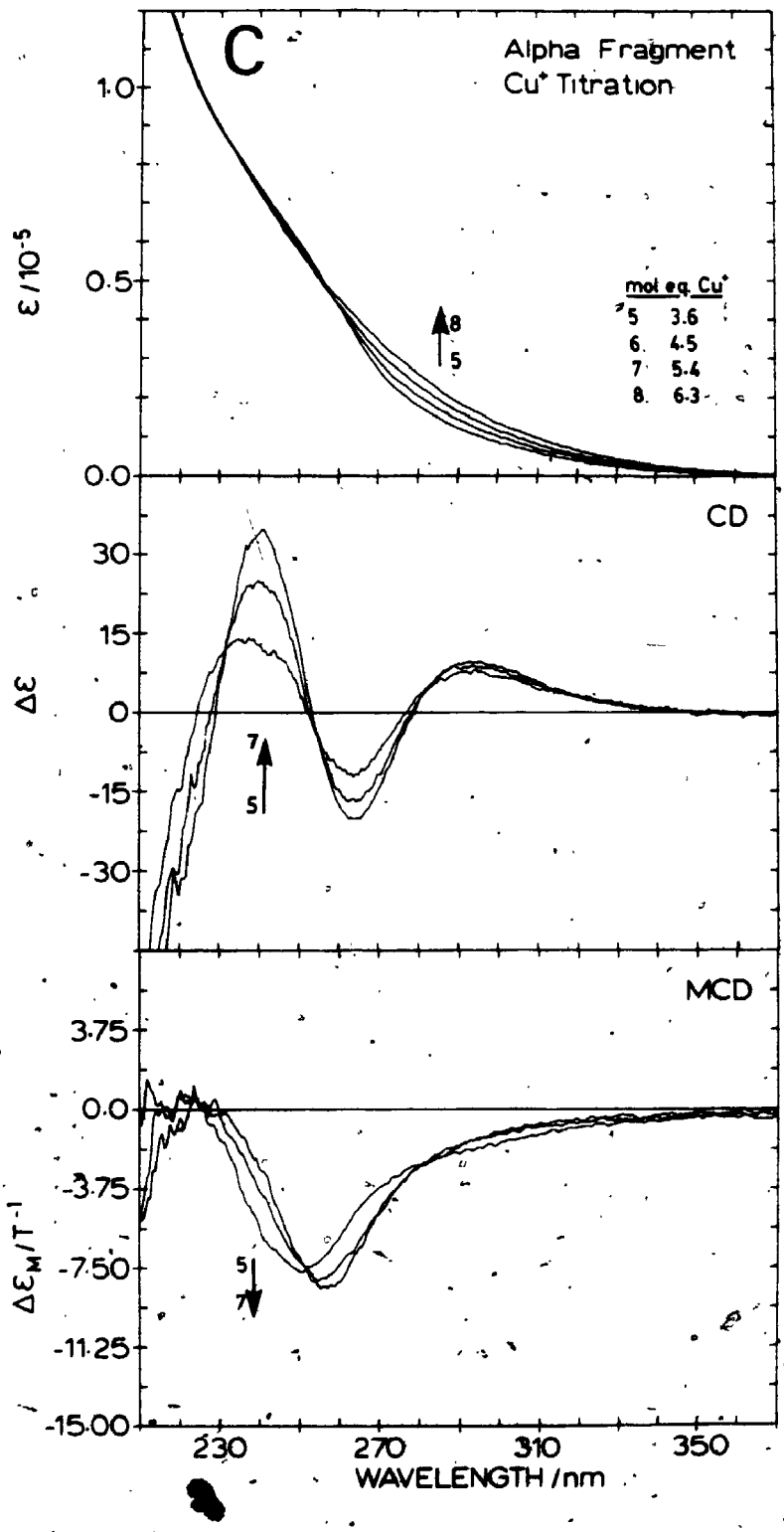
C
Alpha Fragment
Cu⁺ Titration
mol eq. Cu⁺
5 3.6
6 4.5
7 5.4
8 6.3
ε /10⁻⁵
1.0
0.5
0.0
8
5
CD
Δε
30
15
0
-15
-30
7
5
MCD
ΔεM/T⁻¹
3.75
0.0
-3.75
-7.50
-11.25
-15.00
5
7
230
270
310
350
WAVELENGTH /nm

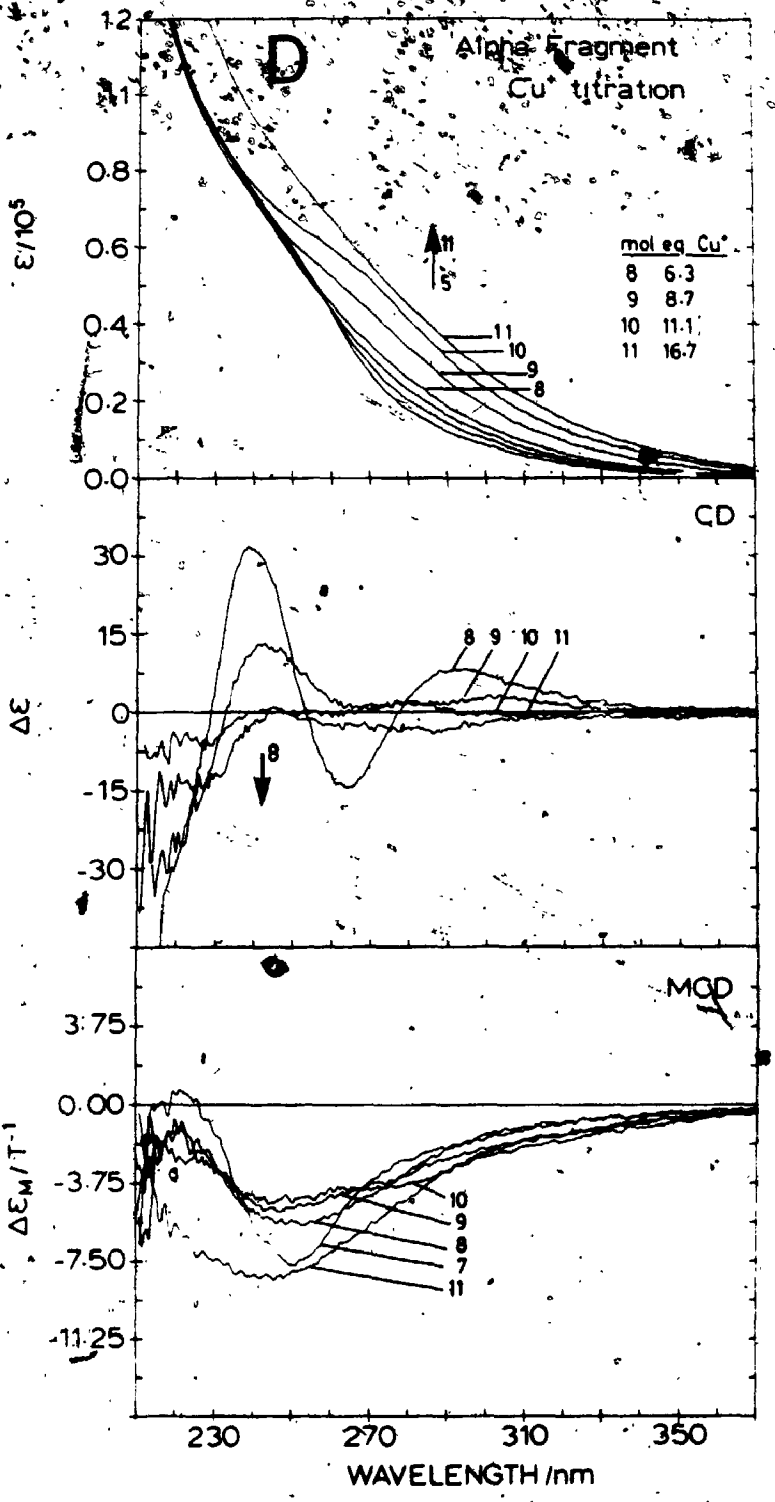
D
Alpha fragment
Cu⁺ titration
ε/10⁵
mol eq. Cu⁺
8 6·3
9 8·7
10 11·1
11 16·7
CD
Δε
MCD
ΔεM/T⁻¹
WAVELENGTH /nm

FIG. 34 A plot of the changes in the (A) absorbance and (B) CD bands intensity versus mole equivalents of Cu^{+} added to the alpha fragment solution.

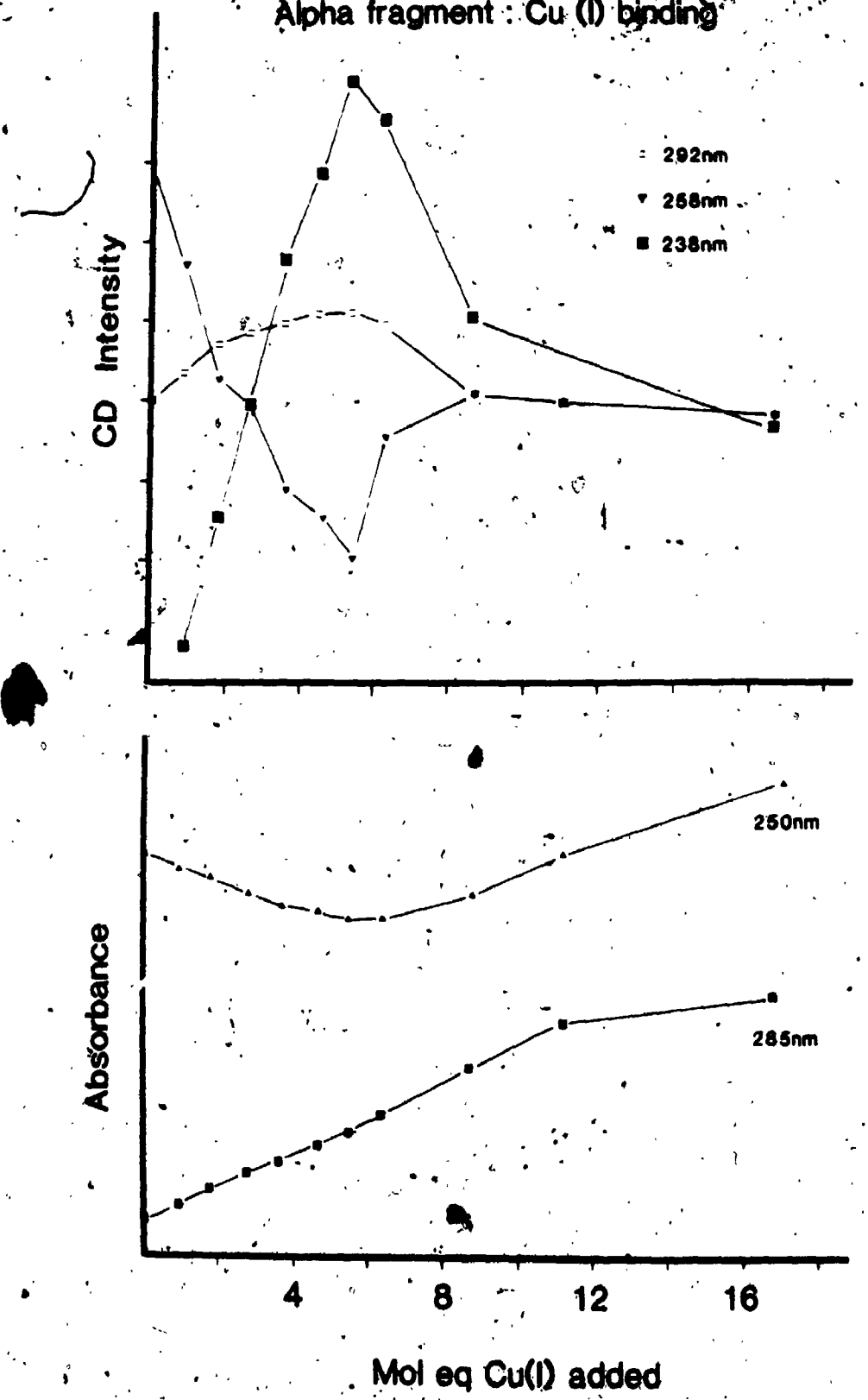
Alpha fragment : Cu (I) binding
292nm
258nm
238nm
CD Intensity
250nm
285nm
Absorbance
4
8
12
16
Mol eq Cu(I) added

Cu-BAL model compound study and the CD spectrum reported for Neurospora crassa (182,183) show that Cu-S related transitions are present in this wavelength region. Therefore, it is attractive to assign this new CD signal as resulting from the binding of Cu^+ to MT. In order to confirm this assignment, a series of Cu^+ binding and dialysis experiments were carried out to determine the amount of metal ions bound in MT during the different stages of the Cu^+ titration. Moreover, the relationship between the content of metal ions and the changes in the CD spectrum was studied. The alpha fragment sample presents a simple system whereby the binding of Cu^+ to the 4-metal cluster can be studied. FIG 35 shows the absorption and CD spectra of a solution of alpha fragment containing 37 nmol Cd^{2+} and 43 nmol Cu^+. The metal content of the solution (Solution 1) before and after dialysis are shown in TABLE XI. The CD spectrum is characterized by the unique derivative-shaped signal. After dialysis, both the Cd^{2+} and Cu^+ concentrations in solution decrease with 21 nmol Cd^{2+} and 26 nmol Cu^+ still bound to the protein. The CD spectrum still exhibits the same signal but with a decrease in the overall intensity. In the dialysis experiment with the another sample of alpha fragment solution (solution 2 in TABLE XI), the protein solution contained 11 nmol Cd^{2+} and 17 nmol Cu^+. After dialysis, the Cd^{2+} was completely displaced and the Cu^+ that remained bound to the alpha fragment is very close to the Cd^{2+} content present initially.

The pH stability of the species in solution that give rise to the CD spectrum has also been investigated. FIG. 36 shows the effect of pH on the absorption and CD spectra. The initial spectrum represents a solution of alpha fragment that contained 5.5 mole equivalents of Cu^+

added at pH 6.9. The pH of the solution was then lowered to 3.3 by adding μL aliquots of a concentrated HCl solution. At pH 3.3, the CD spectrum collapses. In the absorption spectrum there is no change in the 300 nm absorption but there is a significant decrease in the absorbance in the 250 nm region. The solution was then exposed to air for a short period of time and air was bubbled into the solution for up to 90 seconds during each exposure. No significant change in the CD spectrum is observed after each exposure. When the pH of the solution was raised to 8.4, the derivative CD signal reappears, but with a lower intensity.

6.3.2.2. Rat liver Cd,Zn-MT 2

A similar set of Cu^+ binding and dialysis experiments was carried out with rat liver Cd,Zn-MT 2 to study the Cu^+ binding properties in the presence of the 3-metal cluster. FIG. 37A shows the absorption and CD spectra of a Cd,Zn-MT 2 solution where the mole equivalents of Cu^+ added were the same as the amount of Zn^{2+} present in the native protein. The absorption spectrum shows a red-shift and an increase in the absorption in the 300 nm region. The CD spectrum exhibits a small increase in the positive band intensity at 290 nm and a corresponding decrease in the CD signal due to the native protein. After dialysis, AAS analysis shows the complete loss of Zn^{2+} and a small decrease in the Cd^{2+} content. The absorption at 250 nm decreases significantly but no change is observed in the 300 nm region. The derivative CD bands decrease further in intensity while the 290 nm CD band remains constant. TABLE XII shows the metal contents for each of the solutions (in FIGS. 37 and 38) before and after dialysis.

FIG. 37B shows the absorption and CD spectra of a solution

FIG. 35 The effect of adding Cu^{+} to a sample of alpha fragment followed by dialysis. The absorption and CD spectra of the native protein (□ □ □,) which contained 4.8 mol eq Cd^{2+}. 5.5 mol eq Cu^{+} were added at pH 6.9 (○ ○ ○). The same solution after dialysis at 4° C, for 6 hours under a nitrogen atmosphere (△ △ △). The units for ε and $\Delta\varepsilon$ are L mol^{-1} cm^{-1}.

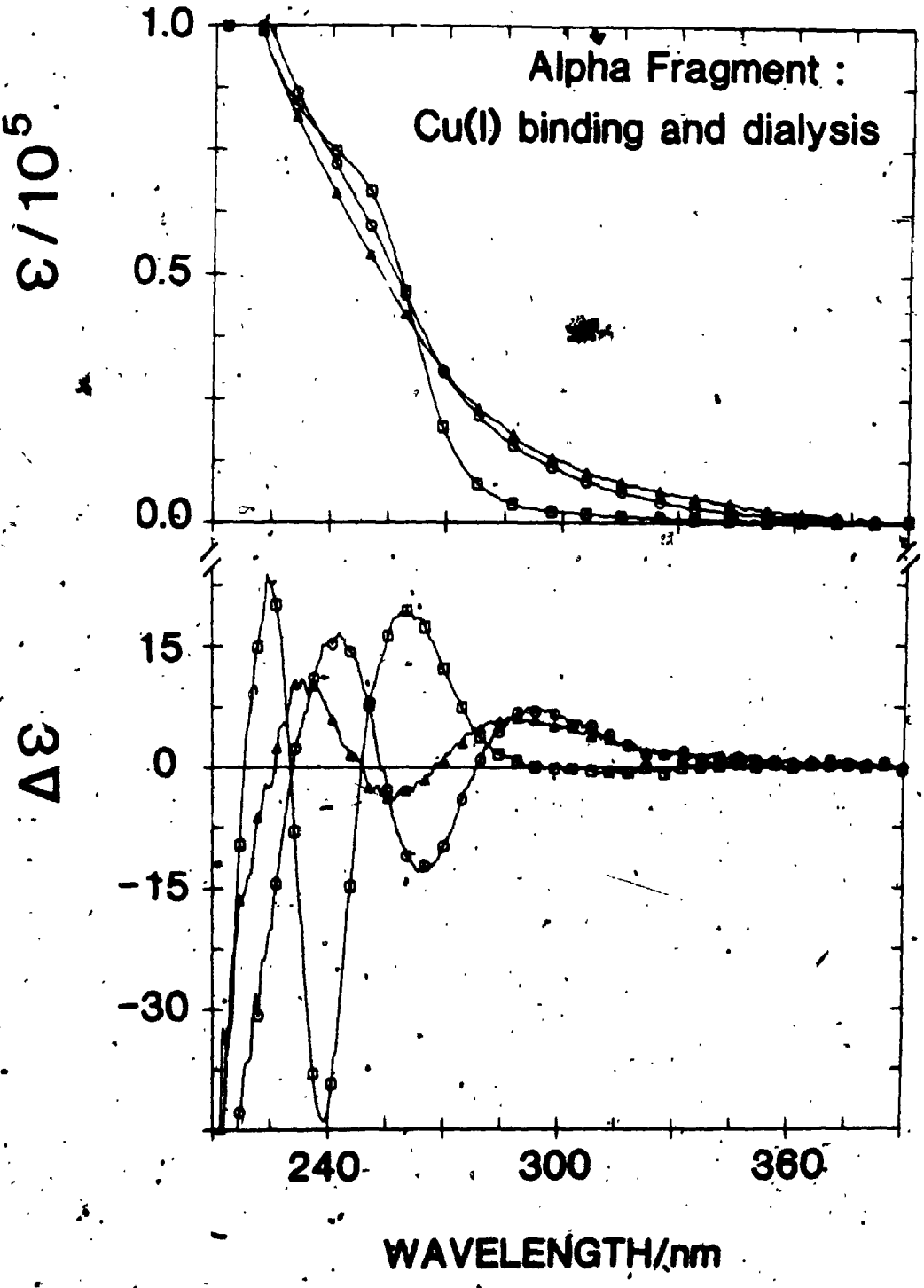
Alpha Fragment :
Cu(I) binding and dialysis
1.0
0.5
0.0
ε/10^5
15
0
-15
-30
Δε
240
300
360
WAVELENGTH/nm

FIG. 36 The effect of pH on a solution of alpha fragment which contained 5.5 mol eq Cu^+ added. The absorption, CD spectra of the native solution (————) and after Cu^+ addition (- - - - - -). The pH of the solution was lowered to 3.3 by using uL aliquots of a concentrated HCl solution and then exposed to air repeatedly for about 1 min each time. The spectra were recorded after each exposure. The pH of the solution was then raised to 8.4 (—·—·—). The units for ε and $\Delta\varepsilon$ are L mol^{-1} cm^{-1}.

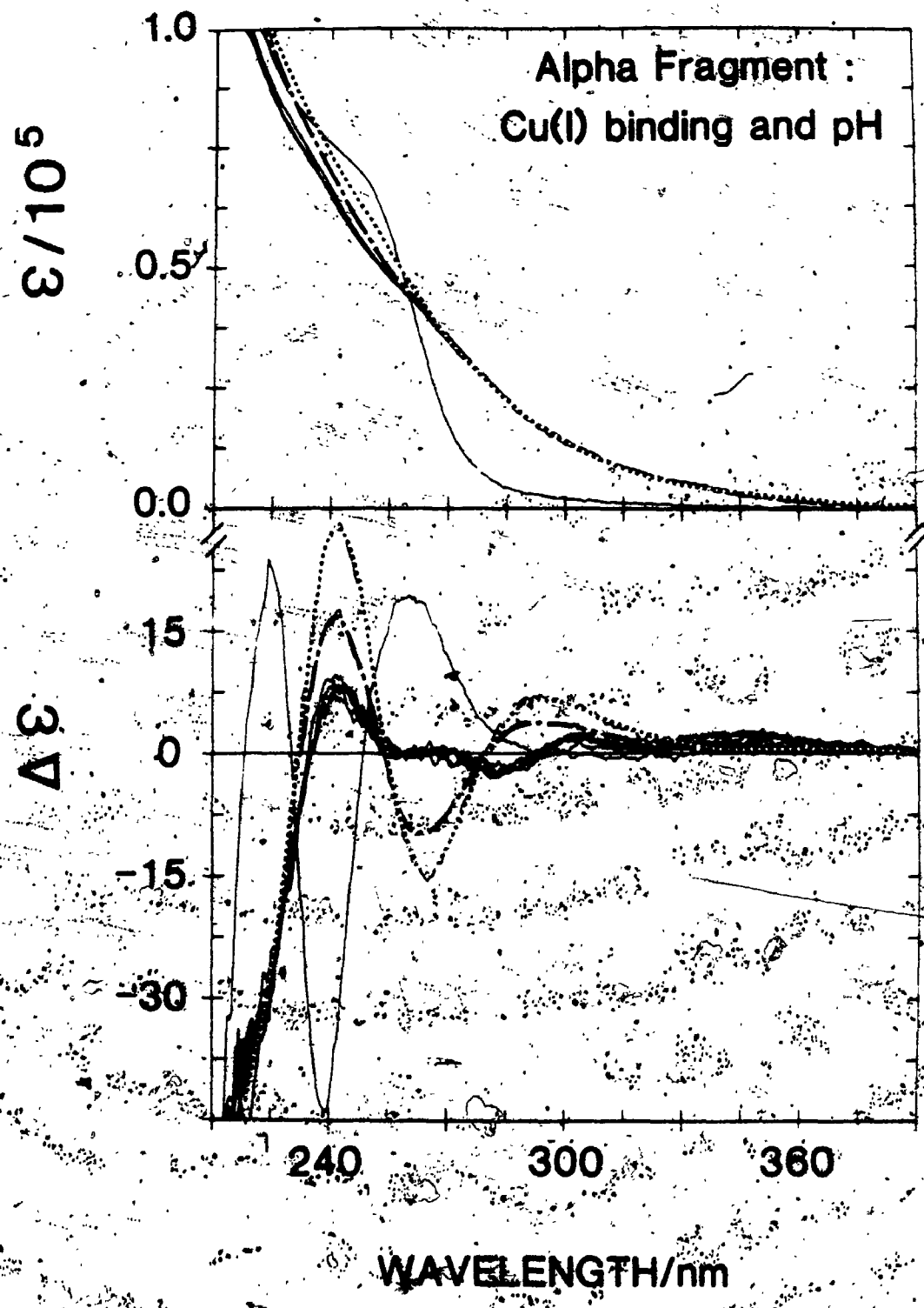
Alpha Fragment :
Cu(I) binding and pH
ε/10⁵
1.0
0.5
0.0
Δε
15
0
-15
-30
240
300
360
WAVELENGTH/nm

FIG. 37. The effect of adding Cu^+ to a rat Cd,Zn-MT 2 solution followed by dialysis. The absorption and CD spectra of the native solution (□ □ □). The solution after (A) 2.8 mol eq and (B) 7.1 mol eq Cu^+ were added (○ ○ ○). The solution after dialysis in water for 10 hours (△ △ △) contained (A) 2.5 mol eq (B) 7.0 mol eq Cu^+. All Cu^+ additions and dialysis were carried out under a nitrogen atmosphere. The units for ε and $\Delta\varepsilon$ are L mol^{-1} cm^{-1}.

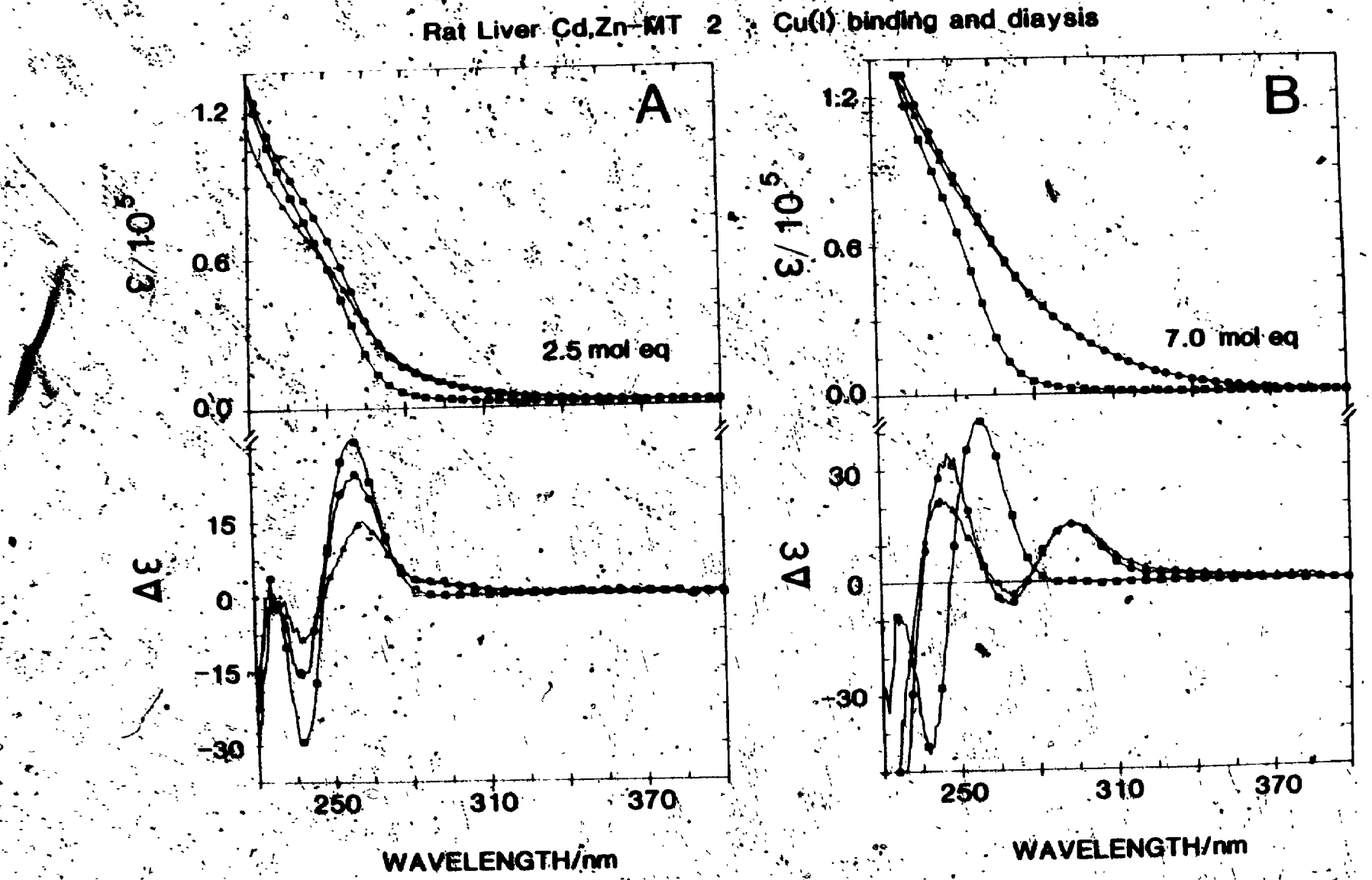
Rat Liver Cd,Zn-MT 2 : Cu(I) binding and diaysis
A
B
2.5 mol eq
7.0 mol eq
ε/10^5
Δε
1.2
0.6
0.0
15
0
-15
-30
30
-30
250
310
370
WAVELENGTH/nm

containing 7.2 mole equivalents of Cu^+ added. The absorption spectrum resembles that observed in FIG. 37A but is at a higher intensity. The CD spectrum shows the characteristic new signal observed in the Cu^+ titration experiments described earlier. Little change is observed in the overall absorption spectrum when this solution has dialysed. However, the CD spectrum shows some loss of intensity in the 240 nm band while the rest of the spectrum remains the same. This solution is found to contain only 57 % of the original Cd^{2+}, while Zn^{2+} is completely absent. Furthermore, 7 mole of Cu^+ are bound to MT together with 2.2 moles of Cd^{2+} to give a Cd,Cu-MT species.

FIG. 38A shows the absorption and CD spectra of the solution where 9.2 mole equivalents of Cu^+ were added. Before dialysis, both the absorption and CD spectra are very similar to that observed in FIG. 37B. However, a significant change is observed in the CD spectrum after dialysis. The 292 nm band decreases in intensity and the new derivative shaped signal collapses to form a broad positive band at about 260 nm. After dialysis, only 8.2 mole equivalents of Cu^+ and 1 mole equivalent of Cd^{2+} still remained in the protein. FIG. 38B shows the absorption and CD spectra for a solution containing 13.3 mole equivalents of Cu^+. After dialysis, all the Cd^{2+} and Zn^{2+} in the native MT have been displaced by the 11.2 mole equivalents of Cu^+ that are bound to the protein. The absorption spectrum before and after dialysis shows minor changes in the 250 nm region. The CD spectrum exhibits the positive 260 nm band and weak negative bands at longer wavelengths.

The results from the dialysis experiments with both the alpha fragment and Cd,Zn-MT 2 solutions indicate that the characteristic CD

spectrum observed during the Cu^+ titration experiments is related to the presence of both Cd^{2+} and Cu^+ in the MT. Since Cu^+ bound in MT has previously been shown to be highly stable at low pH and its CD spectrum was found to remain unchanged until the pH of the solution was lowered to 0.5 (82), the pH stability of the species in solution which contributed to the unique CD spectrum was investigated. FIG. 39 shows the effect of pH on the absorption and CD spectra of a Cd,Zn-MT 2 solution which contained 8.8 mole equivalents of Cu^+ added as $Cu(CH_3CN)_4.ClO_4$. The concentrations of Cd^{2+} and Zn^{2+} present initially were 3.9 mole equivalents and 2.7 mole equivalents, respectively. The initial CD spectrum is characterized by the derivative-shaped signal observed in the Cu^+ titrations described earlier. When the pH was lowered from 7.0 to 3.6, a decrease in the CD intensity of all three bands is observed, with a slight red shift of the 243 nm band centre. The 243 nm band shifts further to about 260 nm when the pH of the solution has reached 2.8 and remains constant at pH 1.8, while the 292 nm band loses its intensity completely at pH 1.8. The absorption changes follow an isosbestic pattern with a substantial decrease in the absorption of the 250 nm region. At pH 1.5, the 292 nm signal is replaced by a weak, broad negative band at about 300 nm, while the 260 nm band is decreased slightly. Furthermore, the changes in the CD spectrum are related by a common isosbestic point at about 280 nm during the pH titration down to pH 1.5. The final spectrum was recorded at pH 0.8 which shows a large decrease in the intensity of the 260 nm band in the CD as well as an overall drop in the intensity of the absorption spectrum.

FIG. 38 The effect of adding Cu^+ to a rat Cd,Zn-MT 2 solution, followed by dialysis in water, at 4° C for 10 hours. The absorption and CD spectra of the native protein solution (□ □ □). The solution after (A) 8.3 and (B) 12.3 mol eq Cu^+ were added (○ ○ ○). The same solution after dialysis (△ △ △) contained (A) 8.2 mol eq, (B) 11.2 mol eq Cu^+. All Cu^+ additions and dialysis were carried out under a nitrogen atmosphere. The units for ε and $\Delta\varepsilon$ are L mol^{-1} cm^{-1}.

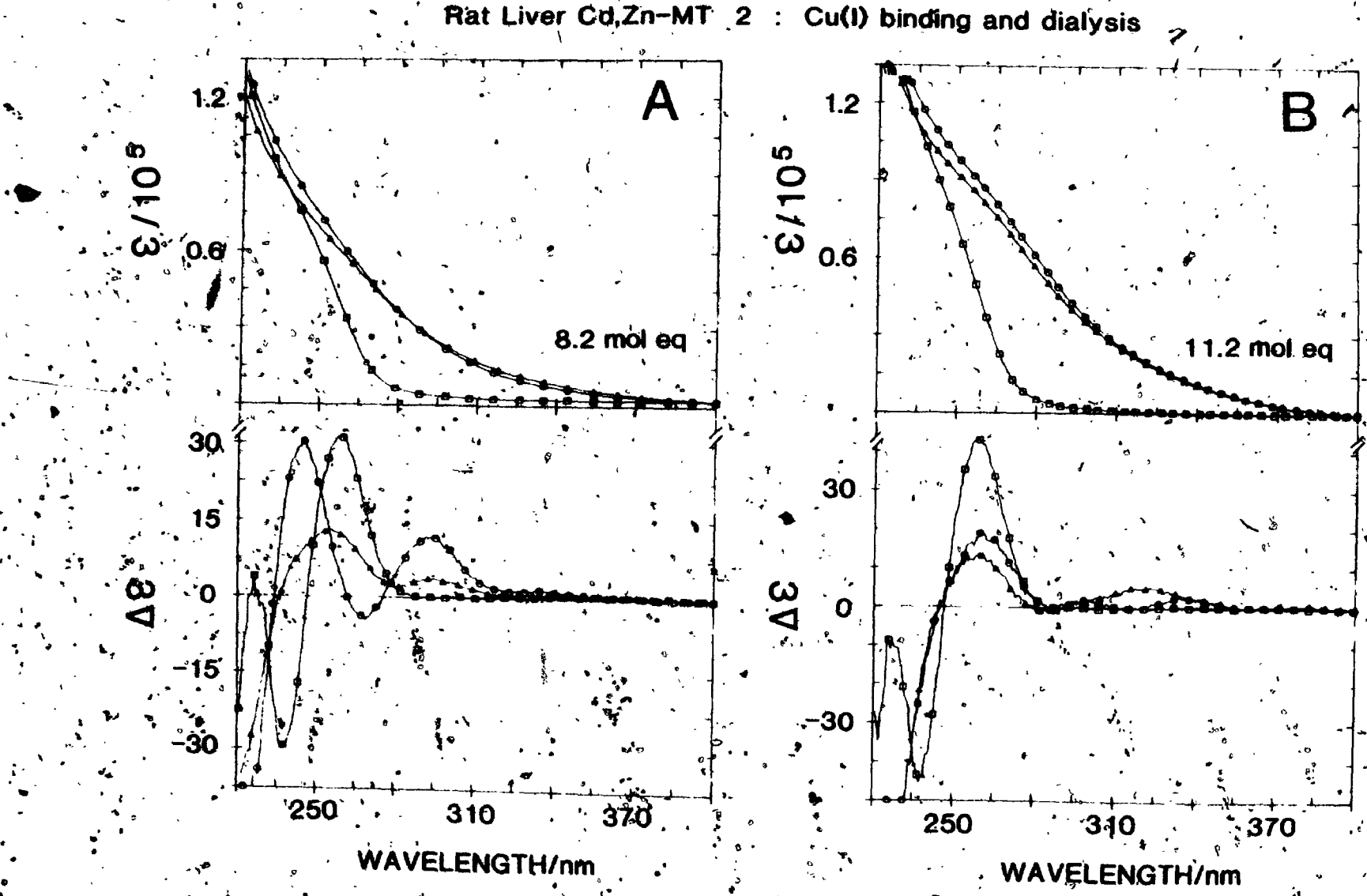
Rat Liver Cd,Zn-MT 2 : Cu(I) binding and dialysis
A
B
8.2 mol eq
11.2 mol eq
ε/10⁵
Δε
1.2
0.6
30
15
0
-15
-30
250
310
370
WAVELENGTH/nm

OF / DE

3

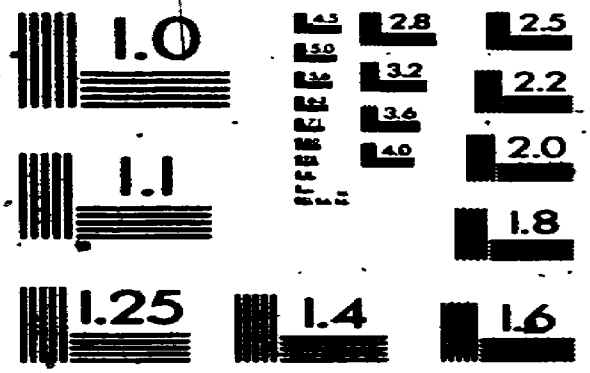

FIG. 39 The effect of pH on the absorption and CD spectra of a rat Cd,Zn-MT 2 solution containing 8.8 mol eq Cu^{+} added. The pH of the solution was lowered by addition of μL aliquots of a concentration HCl solution. The units for ε and $\Delta\varepsilon$ are L mol^{-1} cm^{-1}.

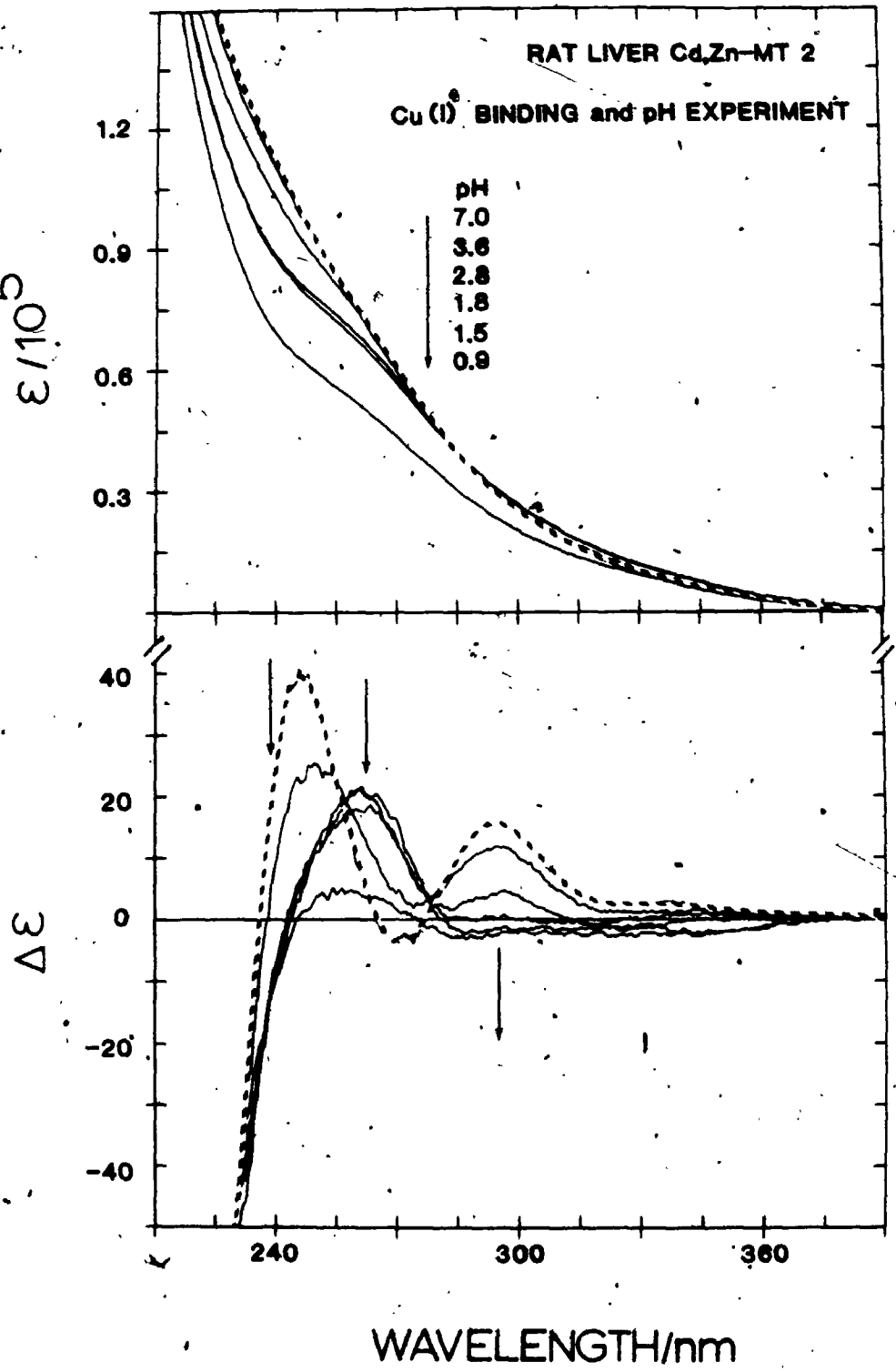
RAT LIVER Cd,Zn–MT 2
Cu (I) BINDING and pH EXPERIMENT
pH
7.0
3.6
2.8
1.8
1.5
0.9
ε/10^5
1.2
0.9
0.6
0.3
Δε
40
20
0
-20
-40
240
300
360
WAVELENGTH/nm

TABLE XI

The effect of dialysis on the number of mole equivalents of Cd^{2+} and Cu^{+} bound to alpha fragment

	Cd^{2+} ($\times 10^{-8}$ moles)	Cu^{+}	Cu^{+}/Cd^{2+} mole ratio
Alpha fragment Solution 1			
Before dialysis	3.7	4.3	1.1
After dialysis	2.1	2.6	1.2
Alpha fragment Solution 2			
Before dialysis	1.1	1.7	1.6
After dialysis	.07	1.1	16

TABLE XII

The effect of dialysis on the number of moles equivalents of metal bound to Cd,Zn-MT

	Cd^{2+}		Zn^{2+}		Cu^{+}	
	mole	mol.eq.	mole	mol.eq.	mole	mol.eq.
A. Cd,Zn-MT 2 native	6.2×10^{-8}	3.9	3.9×10^{-8}	2.5	0	0
$+4.4\times10^{-8}$ mol. Cu^{+}, after dialysis	5.0×10^{-8}	3.1	0	0	3.9×10^{-8}	2.5
B. Native	6.1×10^{-8}	3.9	4.1×10^{-8}	2.6	0	0
$+11.1\times10^{-8}$ mol. Cu^{+}, after dialysis	3.54×10^{-8}	2.2	0	0	11.0×10^{-8}	7.0
C. Native	6.2×10^{-8}	3.9	3.9×10^{-8}	2.5	0	0
$+13.2\times10^{-8}$ mol. Cu^{+}, after dialysis	1.8×10^{-8}	1.1	0	0	13.0×10^{-8}	8.2
D. Native	6.1×10^{-8}	3.9	4.1×10^{-8}	2.6	0	0
$+19.2\times10^{-8}$ mol. Cu^{+}, after dialysis	0	0	0	0	17.5×10^{-8}	11.2
E. Native	6.1×10^{-8}	3.9	4.1×10^{-8}	2.6	0	0
$+30.5\times10^{-8}$ mol. Cu^{+}, after dialysis	0	0	0	0	23.2×10^{-8}	15.3

6.4. DISCUSSION

Cu^+ binding to chicken Cd,Zn-MT was first demonstrated *in vitro* by Rupp and Weser (195,214) using absorption and CD spectroscopies. However, their study only served to report the spectrum obtained for a Cu^+ saturated MT, while the complex spectral changes that occurred in the CD spectrum during the metal replacement reaction were left unexplained. Since the Cd,Zn-MTs of mammalian origin have now been established to contain two metal binding clusters, and results from our studies with Cd^{2+} and Hg^{2+} have indicated that distinct spectroscopic changes took place during the different stages of metal replacement reaction. Therefore, a thorough spectroscopic re-investigation of the Cu^+ binding properties of Cd,Zn-MT becomes important, in order to determine the relative affinity of Cu^+ for the two cluster sites as well as the stoichiometry in the Cu^+ binding site.

The results from metal binding studies described in previous chapters have shown that isomorphous replacement of Zn^{2+} by Cd^{2+} and Hg^{2+} occurred in rat liver MT. Though the alpha cluster appears to be resistant to the binding of Cd^{2+} in excess of 4 mole equivalents, the beta cluster, on the other hand, can bind 3 extra moles of Cd^{2+} thus giving rise to a $[Cd_6S_9]^{3+}$ unit. Since Cu^+ is known to form a series of cluster compounds in which one of the structures observed involves a $[Cu_6S_9]^{3-}$ unit, it is important to probe the structure of clusters being formed in the Cd,Zn-MT upon Cu^+ replacement. In addition to absorption and CD spectra, the MCD data provide additional information on the stereochemical properties of the Cu^+ binding sites in these Cu-substituted MTs.

From the results shown in FIGS. 27, 29 and 30, it is clear that all three species of metallothionein (rat liver Cd,Zn-MT 1 and 2 and guinea pig Cd,Zn-MT 2) bind Cu^+ in a similar manner. The characteristic spectral changes in the absorption , CD and MCD spectra were observed for all three titrations which suggests that the sequence of Cu^+ binding is unique for Cd,Zn-MTs. The effects of Cu^+ binding to Cd,Zn-MT can be classified into three stages: (i) the displacement of Zn^{2+}; (ii) the formation of the unique mixed Cd,Cu-MT species which is characterized by a well defined CD spectrum and (iii) the formation of Cu-MT.

The changes in the CD spectra indicate that the binding of Cu^+ to the beta cluster does not contribute to significant CD intensity, since the overall CD spectrum remains very similar to that of the native protein until the displacement of the Cd^{2+} ions from the alpha cluster has occurred. A similar CD spectrum has previously been observed for a Cd,Cu-MT isolated from rat kidneys (219) which contained a Cd^{2+}:Cu^{2+} mole ratio of 2.5:1.6. The close resemblance of the CD spectrum due to the native Cd,Cu-MT and that of the native Cd,Zn-MT suggests that the Cd^{2+} in the Cd,Cu-MT is bound to the alpha cluster while the Cu^+ ions are associated with the beta sites. A ^{113}Cd nmr study of a Cu,Cd-MT prepared by the *in vitro* displacement of Zn^{2+} by Cd^{2+} in the native Cu,Zn-MT from calf liver has also revealed that the Cu^+ ions are bound predominantly in the beta cluster (73). Thus these results summarily suggest that Cu^+ has a higher affinity for the beta domain during *in vivo* binding and are preferentially bound in the beta cluster in the native protein.

The sequence of spectral changes observed here with the alpha

fragment closely follow those described earlier for Cu^+ titrations with Cd,Zn-MTs from rat and guinea pig. The main spectral difference between the Cu^+ binding to Cd,Zn-MT and the alpha fragment is reflected in the early stage of the titration. The absence of the red-shift and resolution of the 250 nm absorption shoulder during the early additions of Cu^+ to the alpha fragment solution provides strong evidence that this particular spectral change observed previously in both the Cd^{2+} and Hg^{2+} replacement studies with Cd,Zn-MT is related to the displacement of Zn^{2+} from the protein.

The same characteristic, derivative-shaped CD signal (292 nm(+), 268 nm (-) and 242 nm (+)) is also present during the titration of the alpha fragment solution with Cu^+. The complete collapse of the native CD spectrum due to Cd^{2+} binding to the alpha cluster when the Cu^+ concentration is 2.7 mole equivalents suggests the loss of tetrahedral Cd^{2+} and the single species formed in the reaction exhibits the new CD spectrum. The concentration of this species increases with further additions of Cu^+ and reaches its maximum intensity when the Cu^+/Cd^{2+} mole ratio is close to 1 (FIG. 33D, line 7). The loss of tetrahedrally bound Cd^{2+} from the cluster is flagged by the decrease in the MCD envelope. More significantly, a distinct blue-shift of the MCD band centre to 250 nm is apparent.

In a Cu^+ titration study using bismuth induced Zn-MT (192), the unique, new, derivative-shaped CD spectrum obtained during Cu^+ titration with Cd,Zn-MTs and alpha fragment was not observed. The spectral changes during the addition of Cu^+ is much simpler. They resemble the characteristic sequence of changes observed during the last stages of Cu^+ binding to Cd,Zn-MT, when the new, derivative-

shaped CD spectrum starts to lose intensity and the 240 nm band gradually shifts to longer wavelengths with subsequent formation of the CD spectrum due to Cu-MT. This observation is significant since it suggests that, in addition to Cu^{+}, Cd^{2+} is also an integral component of the species that gives rise to the new CD spectrum. The spectral evidence obtained so far suggests that the species formed during the Cu^{+} titration contains both Cd^{2+} and Cu^{+} ions bound to the alpha fragment.

The dialysis experiments described in FIG. 35, 37 and 38 represent a series of experiments used to study the stoichiometry of Cu^{+} binding in MT and the relationship of the stoichiometry to the CD spectra observed. The metal contents of each of the solutions containing added Cu^{+} were measured both before and after dialysis. The results are summarized in TABLE XI and XII. The dialysis experiments carried out with the alpha fragment demonstrate the Cu^{+} binding properties of the alpha cluster. The number of moles of Cu^{+} bound to the alpha cluster after dialysis is very close to the Cd^{2+} content initially present, which suggests that at least 4 Cu^{+} ions can be bound to the alpha fragment. Further experiments were not carried out to to determine the number of moles Cu^{+} that could be bound when Cu^{+} is present in large excess because there was not enough protein sample. However, dialysis experiments with Cd,Zn-MT have shown that more than 4 moles of Cu^{+} may be bound to the alpha cluster. The MCD spectrum of the saturated Cu-MT exhibits 2 broad negative B terms. Therefore, the binding of Cu^{+} in the alpha cluster does not appear to involve the tetrahedral symmetry as suggested for the yeast Cu-MT (211,212,217). The propensity of Cu^{+} to form polynuclear clusters with various Cu^{+}/S mole

ratios have been amply documented in the literature. Furthermore, the coordination number of Cu^+ varies from 2 to 4. Therefore, it is not unreasonable to expect that the Cu^+ bound in the alpha fragment may involve a coordination geometry other than tetrahedral. It is relevant to note that results of a recent preliminary XAFS study of pig liver Cu-MT suggest that the Cu^+ ions are bound with a trigonal geometry, a geometry which is commonly observed in structurally characterized Cu^+ cluster compounds. On the other hand, the fact that the alpha fragment solution containing equivalent number of moles of Cd^{2+} and added Cu^+ retains the same characteristic CD spectrum even after exhaustive dialysis provides strong evidence that the Cu^+ ions are bound to MT. It also suggests that the species in solution that contributes to the CD spectrum contains both Cd^{2+} and Cu^+ ions. The dialysed solution (TABLE XI, solution 1) indicates the presence of approximately 2 mole equivalents of Cd^{2+} and Cu^+ respectively, thus implying that a Cd_2Cu_2-alpha fragment species is formed. The sharp isosbestic points observed during the titration indicate that a single species is generated, which may be represented by the following equation.

$$Cd_4 + 2\ Cu^+ \longrightarrow Cd_2Cu_2 + 2\ Cd^{2+}$$

A two-fold excess of Cu^+ is required to achieve the maximum CD signal intensity. As the Cd_4 protein persists in the presence of 4 moles of Cu^+ added, this implies that the reaction attains an equilibrium and that the alpha cluster has a higher affinity for Cd^{2+} than Cu^+.

The interpretation of the Cu^+ binding to Cd,Zn-MT which contains both the alpha and beta clusters, though much more complex, is considerably simplified when considering the results obtained from the

alpha fragment experiments. Results from the Cu^+ binding and dialysis experiments with Cd,Zn-MT 2 show the number of moles of Cu^+ that are bound in the alpha and beta domains during the various stages of the displacement reaction (TABLE XII). The fact that the CD spectrum of the solution containing an amount of Cu^+ which is the same as the native Zn^{2+} content, still retains the derivative-shaped signal similar to the native protein, with only a small increase in the positive CD band at 292 nm, suggests that the Cd^{2+} ions that remain bound to MT are still maintained in the original binding sites and that Cu^+ displaces Zn^{2+} from the beta cluster. This is confirmed by the fact that there is no Zn^{2+} left after dialysis, while the Cd^{2+} content remains relatively constant.

Similar to results obtained for the Cd^{2+} titration studies described in Chapter 3 in which the beta cluster is found to bind a total of six mole equivalents of Cd^{2+}, the data from the second Cu^+ binding and dialysis experiment (FIG. 37B) also indicate that more than 3 mole equivalents of Cu^+ can be bound to the beta cluster. Metal analysis of the solution after dialysis shows that the species in solution contains 7.2 mole equivalents of Cu^+ and 2.2 mole equivalents of Cd^{2+}. Based on the assumption that the new CD spectrum arises from a Cd_2Cu_2 species formed in the alpha cluster, one can postulate that the remaining 5.2 moles of Cu^+ (which represents twice the amount of Zn^{2+} bound in the native protein) are associated with the beta cluster. This implies that it takes 2 moles of Cu^+ to displace one mole of Zn^{2+}. The fact that the CD spectrum changes so dramatically after dialysis (FIG. 38A) suggests that there is a change in the arrangement of the amino acid residues around the bound Cd^{2+}. The 5.2 mole

equivalents of Cu^+ associated with the beta cluster suggests that a $[Cu_6S_9]$ species is formed. Cluster structures containing Cu:S ratio of 2:3 are common and have been shown to contain trigonally-coordinated Cu^+ ions (165,167,171).

The addition of 8.2 mole equivalents of Cu^+ (compared to the 6.5 mole equivalents of Cd^{2+} and Zn^{2+} in the native protein) also results in the derivative-shaped new CD spectrum. However, the change in the CD spectrum observed after dialysis suggests that a rearrangement of the binding of the Cd^{2+} and Cu^+ in MT has occurred. The CD spectrum may represent a mixture of the two species, namely Cu-MT and Cd_2Cu_8-MT. The results from these experiments strongly suggest that the stoichiometry of Cu^+ binding in the alpha and beta cluster sites are different. While the alpha fragment appears to bind at least 4 Cu^+ ions, a total of 6 Cu^+ can be bound in the beta cluster. Results from the last two sets of dialysis experiments with Cd,Zn-MT 2 (TABLE XII, Solutions D and E) also show that MT can bind more than 10 mole equivalents of Cu^+.

An important conclusion which can be drawn from Cu^+ titration studies is related to the different metal affinity of the 2 metal cluster units in MT. Unlike the Hg^{2+}, where isomorphous replacement of Zn^{2+} in the beta cluster is followed by the replacement of Cd^{2+}, an extra 3 moles of Cu^+ are bound to the beta cluster before interaction with the alpha domain takes place. The fact that an excess of Cu^+ is required to displace Cd^{2+} with the formation of a stable intermediate species also suggests that binding constant of Cd^{2+} to the alpha cluster is higher than that of the Cu^+. Based on the similarity between the CD spectra of the Neurospora crassa and the native

Hg,Cu-MT, and the higher affinity of Cu^+ for the beta cluster unit, it can be postulated that the Cu^+ ions present in Hg,Cu-MT are probably bound in the beta sites. Overall, the following order of binding can be proposed for the alpha cluster (in vitro):

Hg > Cd > Cu > Zn

while for the beta cluster (in vitro):

Cu, Hg > Cd > Zn

Amino acid sequence studies have revealed the close similarity between the Neurospora crassa and the first seven cysteine residues of the N-terminus of mammialian MTs, which constitute the beta domain. It is important to note that the Neurospora crassa binds 6 moles of Cu^+ which is consistent with the findings here in the Cu^+ titration that 6 moles of Cu^+ can be bound in the beta cluster. Therefore the Neurospora crassa appears to be a good model for the study of the Cu^+ binding in the beta fragment. In addition, Neurospora crassa has been reported to bind 3 moles of Cd^{2+} (183) with spectral features similar to that of equine Cd-MT which implies a tetrahedral symmetry. A possible structure of the beta cluster containing 6 Cu^+ ions can be postulated in which 5 Cu^+ ions possess trigonal geometry and the sixth Cu^+ is close to linear. Many Cu^+ cluster compounds have previously been shown by X-ray crystallography to contain a mixture of coordination geometries within the same cluster unit (167-170).

The pH experiment probes the stability of the species formed in the Cu^+ titration experiment that gives rise to the unique CD spectrum. The changes in the CD spectrum (FIG. 39) suggest that the Cd^{2+} is released from the protein and the further binding of Cu^+ in MT results in the formation of the saturated Cu-MT. These results further support

the conclusion that the species in solution that exhibits the new derivative CD signal contains both Cd^{2+} and Cu^{+}.

In conclusion, the binding of Cu^{+} to MT can be represented by the following schemes.

(1) Cd_4Zn_3-MT + 6 Cu^{+} -----> Cd_4Cu_6-MT + 3 Zn^{2+}

(2) Cd_4Cu_6-MT + 2 Cu^{+} $\xrightarrow{H^{+}}$ Cd_2Cu_8-MT + 2 Cd^{2+}

(3) Cd_2Cu_8-MT + 2 Cu^{+} $\xrightarrow{H^{+}}$ Cu_{10}-MT + 2 Cd^{2+}

The replacement of Zn^{2+} in the beta cluster results in a species containing 6 mole equivalents of Cu^{+}, i.e. $[Cu_6S_9]^{3-}$. The MCD spectrum does not exhibit the derivative-shaped envelope expected for tetrahedrally coordinated binding site. In view of the tendency of Cu^{+} to form polynuclear species, it is quite possible that a $[Cu_6S_9]^{3-}$ cluster unit is formed which contains trigonally-coodinated Cu^{+}. The intermediate species formed which exhibits well resolved CD bands and a broad MCD signal is difficult to rationalize based on the spectral data obtained. However, the loss of the derivative MCD envelope due to S->Cd charge transfer transfer suggests that the Cd^{2+} is no longer bound in the original cluster with tetrahedral symmetry.

IONS

orption, CD and MCD spectroscopies have been used
metal binding properties of Cd,Zn-metallothioneins
sources: rat liver, guinea pig liver and crab
se techniques represent three different approaches
l binding site propetties of MT. Absorption
least informative. The CD spectrum provides
on the stereochemical arrangement of the amino
nd metal ions, while information on the symmetry
sites may be obtained from the MCD spectrum.
ere show that the three species of MTs exhibit very
tures in both the absorption and MCD spectra. The
D envelope observed for native Cd,Zn-MT is very
ined for a tetrahedrally-coordinated Cd-BAL model
ts that the Cd^{2+} binding sites in MT involve a
. This is consistent with the conclusions derived
(97-99), as well as results from XAFS studies
nce of 4 sulfur atoms in the first coordination
bound in sheep MT (103).
pecies of Cd,Zn-MT contain metal ions bound in a
e significantly different CD spectrum observed for
a different stereochemical arrangement of the
ound the bound metal ions. This is consistent with
Cd nmr data which proposed that two 3-metal
in the crab MT (136), while a 4- and a 3-metal
ted in other Cd,Zn-MTs (98). Hence this also
ulness of the CD technique in the characterization

of metallothioneins.

To date the identification of the majority of the MT-like proteins has been based mainly on their gel filtration properties, their high cysteine and metal content. In this work, we have demonstrated the use of optical techniques to provide additional criteria for the identification and characterization of new MTs. ^{113}Cd nmr has been shown to differentiate between the different metal ions in the two cluster units, however, in view of the high concentrations of protein and the considerable length of time required for the collection of data, the nmr technique is less favorable than optical methods for the routine characterization of metal binding in MTs. Moreover, at the present time, the application of nmr in the study of metallothioneins is limited to ^{113}Cd. Another metal ion probe (^{199}Hg), which has been investigated in this work, fails to give useful information because of the inherent lability of Hg^{2+} ions in the metal binding sites.

This thesis has also described the spectroscopic changes in the absorption, CD and MCD spectra in metal replacement studies of metallothioneins, in order to characterize the binding properties of Cd^{2+}, Zn^{2+}, Cu^{+}, Hg^{2+} and Co^{2+} to MT. Specific spectral changes associated with the different stages of the release and binding of Zn^{2+} and Cd^{2+} in the native MT have been shown in this work. The data obtained show that the alpha cluster has a higher affinity for Cd^{2+} than those in the beta cluster, i.e. Cd^{2+} binds preferentially to the alpha cluster. In the presence of excess Cd^{2+}, the MT can accommodate up to 6 mole equivalents of Cd^{2+} in the beta unit probabaly through binding to the terminal cysteine sulfurs present, while the alpha cluster remains unchanged. This is an important feature because it

suggests a mechanism by which MT can accommodate more Cd^{2+} during high Cd^{2+} exposure with the possible redistribution of the excess Cd^{2+} to newly synthesized MT at a later time. That the beta cluster can bind 3 extra moles of metal ions which have a lower binding constant than those of the first seven Cd^{2+} bound allows speculation that the binding and release of metal ions from this cluster may play an important role in the metabolism of metal ions in vivo.

Cd^{2+} displaces Zn^{2+} readily. Therefore, the presence of naturally-occurring Zn-MT in mammalian organs suggests that Zn-MT may act as a precursor for Cd,Zn-MT. The replacement of Zn^{2+} by Cd^{2+} in vivo may occur during acute exposure to Cd^{2+}. However, the Cd^{2+} binding properties of the apo-MT also suggests that Cd-MT may be synthesized in a similar manner in vivo. It is important to note that the reducing condition required for such reactions is present in the cell. In the presence of a large excess of Zn^{2+} ions, metal exchange also occurs without degradation of the cluster structure. This suggests that the Zn^{2+} ions are also bound in tetrahedral sites similar to that of the Cd^{2+} ions.

The Cd^{2+} in MT has a higher binding constant than that of Zn^{2+} and the proton-induced degradation of the cluster structure appear to proceed in a cooperative manner.

The ease of metal substitution in MT supports the suggestion that in the presence of excess metal ions, metal exchange can occur at physiological pH which results in the formation of mixed-metal MT or homogenous MT containing metal ions other than Cd^{2+} and Zn^{2+}. Hg^{2+} has been shown to displace Zn^{2+} and Cd^{2+} sequentially in a 1:1 fashion. The MCD spectrum obtained upon complete replacement of Cd^{2+}

and Zn^{2+} consists of both positive and negative lobes which resemble a MCD A term. However, the MCD A term observed for the BAL-Hg model compound exhibits a much higher intensity as well as a smaller band width. This suggests that the MCD spectrum observed here for Hg-MT probably consists of 2 B terms of opposite signs. Hence, we conclude that the Hg^{2+} ions bound in MT do not involve a tetraheral symmetry, in contrast to the conclusion of other workers (23).

Cu^{+} displaces Cd^{2+} and Zn^{2+} readily. The replacement of Zn^{2+} in the beta cluster is followed by the binding of up to 6 mol eq of Cu^{+}, thus forming a $[Cu_6S_9]^{3-}$ species. It is interesting to note that neurospora crassa, which has a amino acid sequence similar to the first seven cysteine residues of the beta domain of Cd,Zn-MT, also binds 6 moles of Cu^{+}. Though tetrahedrally coordinated Cu^{+} ions have been postulated for yeast Cu-MT, the MCD data obtained in this work do not suggest such a structure. The Cu^{+} ions bound in MT most likely involve a 3-coordinate structure which is commonly observed for Cu^{+} polynuclear species with Cu_2S_3 units (165,167,171). However, a cluster structure which contains both trigonally and linearly-coordinated Cu^{+} could not be eliminated. Native Cu-MT has been shown to bind an average of 10 moles of Cu^{+} (207). The results from the Cu^{+} titration experiment indicate that 6 Cu^{+} bind to the beta cluster, while 4 Cu^{+} are bound to the alpha cluster, suggesting that the native Cu-MT also contains two metal binding domains but with a cluster strucure different from that in Cd,Zn-MT. The binding of Cu^{+} in the alpha fragment proceeds via two steps in which a stable intermediate is formed. The unique intermediate formed in the alpha fragment consists of a $[Cd_2Cu_2]$ species. However, the structure of the this species can not be

postulated based on the information available at this time.

Co^{2+} has a much weaker binding constant than both the Cd^{2+} and Zn^{2+} bound in MT and metal replacement does not occur even in the presence of a large excess of Co^{2+}. The Co-MT prepared in this work exhibits similar spectral characteristics to that observed for Co-MT obtained from rabbit liver MT suggesting that the rat and rabbit MTs bind Co^{2+} in a similar manner. The MCD spectral properties of Co-MT indicate tetrahedrally-coordinated Co^{2+}.

As part of this study, new information has been obtained regarding the mode of binding of several metal ions to MT, under a variety of different conditions. More significantly, metal ion specificity of the two metal clusters in MT has been demonstrated. The two clusters have a different affinity for different metal ions. The following order of metal binding for the two clusters has been concluded from this work (in vitro):

For the alpha cluster: Hg > Cd > Cu > Zn,

while for the beta cluster: Cu, Hg > Cd > Zn.

PROSPECTS FOR THE FUTURE

MTs containing metal ions other than Cd^{2+} and Zn^{2+} have become increasingly important and much work has to be carried out in order to characterize these proteins. One of the more interesting MTs is Au-MT. Gold complexes have long been used in the treatment of rheumatoid arithritis. However, little is known about the mechanism and chronic toxicity of these drugs. Recent studies have suggested that Au binds to a low molecular weight protein in the cytosol (34,35,221-223) and MT has been proposed as the protein involved. It is important to establish the role of MT in the metabolism of these gold drugs.

Therefore optical characterization of the *in vitro* reconstituted Au-MT as well as the *in vivo* synthesized Au-containing protein should be carried out to probe the identity of this species.

REFEENCES

1. N. Hagano, Accident Med. 11, 1390-1397(1968).
2. L. Friberg, M. Piscator, G.F. Nordberg, T. Kjellstrom, in Cadmium in the Environment, 2nd Ed., Chemical Rubber Co., Cleveland, 1974.
3. T. Rahola, R.K. Aaran, J.K. Miettinen, in Health Physics Problems of International Contamination, E. Bujdosa ed., Akademiai Kiado, Budapest, pp213-218, 1973.
4. M. Margoshes and B.L. Vallee, J. Am. Chem. Soc., 79, 4813-4814(1957).
5. J.H.R. Kagi and B.L. Vallee, J. Biol. Chem., 235, 3460-3465(1960).
6. T. Nagano, Y. Watanabe, K. Hida, Y. Suketa, S. Okada, Proc. 7th Symp. Environm. Pollut. & Toxicol., Kobe S-81(1981).
7. W.E. Rauser and N.R. Curvetto, Nature, 287, 563-564(1980).
8. H. Kito, Y. Ose, V. Mizuhira, T. Sato, T. Isihikawa, T. Tazawa, Comp. Biochem. Physiol., 73C, 121-127(1982).
9. F. Neol-Lambot, C.H. Gerday, A. Disteche, Comp. Biochem. Physiol., 61C, 177-187(1978).
10. J. Overnell, T.L. Coombs, Biochem. J., 183, 277-283(1979).
11. H. Kito, T. Tazawa, Y. Ose, T. Sato, T. Ishikawa, Comp. Biochem. Physiol., 73C, 129-134(1982).
12. R. Prinz and U. Weser, Hoppe-Seyler's Z. Physiol. Chem., 356, 767-776(1975).
13. K. Lerch, Nature, 284, 368-370(1980).
14. G. Resi jadi, Mar. Environ. Res., 4, 167-179(1980-81).
15. R.W. Olafson, R.G. Sim and K.G. Boto, Comp. Biochem. physiol. 62B, 407-416(1979).
16. R.W. Olafson, A. Kearns and R.G. Sim, Comp. Biochem. Physiol. 62B,

417-424(1979).

17. R.W. Chen and P.D. Whanger, Biochem. Med., 24, 71-81(1980).

18. Y. Kojima, C. Berger and J.H.R. Kagi in Metallothionein (J.H.R. Kagi and M. Nordberg, eds.) Experientia Supp. 34, pp 153-163.

19. K. Arizono, T. Ito and M. Yamaguchi, J. Pharm. Dyn., 6, S-19(1983).

20. P.D. Whanger and J.T. Deagen, Biol. Trace Elem. Res., 4, 199-210(1982).

21. D.R. Winge, R. Premakumar and K.V. Rajagopalan, Arch. Biochem. Biophys. 170, 242-252(1975).

22. R.W. Chen, P.D. Whanger and P.H. Weswig, Biochem. Med. 12, 95-105(1975).

23. W. Bernard, M. Good, M. Vasak and J.H.R. Kagi, Inorg. Chim. Acta, 79, 154-155(1983).

24. J.A. Szymanska and M.J. Stillman, private communication.

25. K.S. Squibb and R.J. Cousin, Environ. Physiol. Biochem. 4, 23-30(1974).

26. M. Webb and M. Daniel, Chem. Biol. Interact. 10, 269-276(1975).

27. K.S. Squibb, R.J. Cousins and S.L. Feldman, Biochem. J. 164, 223-228(1977).

28. I. Bremner and B.W. Young, Biochem. J. 155, 631-638(1976).

29. I. Bremner and N.J. Davies, Biochem. Soc. Trans. 2, 425-427(1974).

30. I. Bremner and N.T. Davies, Biochem. J. 149, 733-738(1975).

31. A.J. Zelazowski and J.K. Piotrowski, Biochem. Biophys. Acta, 625, 89-99(1980).

32. M.G. Cherian and R.A. Goyer, Trace Sub. Environ. Health, 11, 193-200(1977).

33. J.A. Szymanska, E.M. Mogilnicka and B.W. Kaszper, Biochem. Pharm.

26, 257-258(1976).

34. R.P. Sharma and E.G. McQueen, Biochem. Pharm. 29, 2017-2021(1980).

35. E.M. Mogilnicka and J.K. Piotrowski, Biochem. Pharm. 28, 2625-2631(1979).

36. D.R. Winge, R. Premakumar and K.V. Rajapopalan, Arch. Biochem. Biophys. 188, 466-475(1978).

37. S.H. Oh, J.T. Deagen, P.D. Whanger and P.H. Weswig, Am. J. Physiol. 234, E282-285(1978).

38. K.N. Kotsonis and C.D. Klaassen, Toxicol. Appl. Pharm. 50, 347-354(1979).

39. P.Z. Sobocinski, W.J. Canterbury, Jr., C.A. Mapes and R.E. Dinterman, Am. J. Physiol. 234, E399-406(1978).

40. P.Z. Sobicinski, W.J. Canterbury, Jr., E.C. Hauer, F.A. Beall, Proc. Soc. Exp. Biol. Med. 160, 175-179(1979).

41. C.D. Klaassen, Toxicology, 20, 275-279(1981).

42. Z.A. Shaikh and O.T. Lucis, Arch. Environ. Health, 24, 419-425(1972).

43. D.R. Winge and K.V. Rajagopalan, Arch. Biochem. Biophys. 153,755-762(1972).

44. J.H.R. Kagi, S.R. Himmilhoch, P.D. Whanger, J.L. Bethune and B.L. Vallee, J. Biol. Chem., 249, 3537-3542(1974).

45. A.M. Fiskin, G. Peterson and F.O. Brady, Ultramicroscopy, 2, 389-395(1976).

46. D.R. Winge and K. Miklossy, Arch. Biochem. Biophys., 214, 80-88(1982).

47. M. Vasak and J.H.R. Kagi, Metal ions in Biological System,

H. Sigel, ed., pp213-273, Marcel Dekker Inc., New York, 1983.

48. R.H.O. Buhler and J.H.R. Kagi, FEBS Lett. 39, 229-234(1974).

49. Kissling and J.H.R. Kagi in Metallothionein (J.H.R. Kagi and M. Nordberg, eds.) Experientia Supp. 34, 1979, pp145-151.

50. G.F. Nordberg, Environ. Physiol. Biochem. 2, 7-36(1972).

51. M. Nordberg, G.F. Nordberg and M. Piscator, Environ. Physiol. Biochem. 5, 396-403(1975).

52. Metallothionein (J.H.R. Kagi and M. Nordberg, eds.) Experientia Supp. 34, 1979.

53. Y. Kojima, C, Berger, B.L. Vallee, J.H.R. Kagi, Proc. Natl. Acad. Sci. USA 73, 3413-3417(1976).

54. F.O. Brady, Trends. Biochem. Sci. 7, 143-145(1982).

55. M. Webb and K. Cain, Biochem. Pharm. 31, 137-142(1982).

56. Z.A. Shaikh, O.J. Lucis, Fed. Proc. 29, 298, Abs301 (1970).

57. A.P. Leber and T.S. Miya, Toxicol. Appl. Pharm. 37, 403-414(1976).

58. G.F. Nordberg, Environ. Physiol. Biochem., 1, 171-187(1971).

59. M.G. Cherian, Biochem. Pharm. 27, 1163-1166(1978).

60. G.F. Nordberg, M. Nordberg and R.A. Goyer, Arch. Pathol. 99, 192-197(1975).

61. M.G. Cherian and Z.A. Shaikh, Biochem. Biophys. Res. Commun. 65, 863-869(1975).

62. K. Tanaka, K. Sueda, S. Onosaka and K. Okahara, Toxicol. Appl. Pharm. 33, 258-266(1975).

63. M.G. Cherian, Bull. Environm. Contam. Toxicol., 30, 33-36(1983).

64. M.G. Cherian, J. Toxicol. Environ. Health, 2, 955-961(1977).

65. D.R. Johnson and E.C. Foulkes, Environ. Res. 21, 360-365(1980).

66. M. Nordberg, Environ. Res. 15, 381-404(1978).

67. H.D. Stowe, M. Wilson and R.A. Goyer, Arch. Pathol. 94, 389-405(1972).

68. M.G. Cherian, J. Nutr. 107, 965-972(1977).

69. I. Bremner, R.B. Williams and B.W. Young, Br. J. Nut. 38, 87-92(1977).

70. S.H. Oh, H. Nakane, J.T. Deagen, P.D. Whanger and G.H. Arscott, J. Nutr. 109, 1720-1729(1979).

71. A.O. Udom and F.O. Brady, Biochem. J. 187, 329-335(1980).

72. T. Li, A.J. Kraker, C.F. Shaw III and D.H. Petering, Proc. Natl. Acad. Sci. 77, 6334-6338(1980).

73. R.M. Briggs and I.M. Armitage, J. Biol. Chem. 257, 1259-1262(1982).

74. J.A. Szymanska, A.J. Zelazowski and M.J. Stillman, Biochem. Biophys. Res. Commun. 115, 167-173(1983).

75. H. Hartmann and U. Weser, Biochem. Biophys. Acta 491, 211-222(1977).

76. J.R. Riordan and V. Richards, J. Biol. Chem. 255, 5380-5383(1980).

77. K.A. Melis, D.C. Carter, C.D. Stout and D.R. Winge, J. Biol. Chem. 258, 6255-6257(1983).

78. R.H. Buhler, J.H.R. Kagi, in Metallothionein, J.H.R. Kagi, M. Nordberg, eds., Birkhauser, Basel, pp211-220, 1979.

79. J.H.R. Kagi and B.L. Vallee, J. Biol. Chem. 236, 2435-2442(1961).

80. M. Vasak, J.H.R. Kagi and H.A.O. Hill, Biochemistry, 20, 2852-2856(1981).

81. C.K. Jorgensen, Prog. Inorg. Chem. 12, 101-139(1970).

82. H. Rupp and U. Weser, Biochem. Biophys. Acta, 533, 209-226(1978).

83. A.Y.C. Law and M.J. Stillman, Biochem. Biophys. Res Commun. 102, 397-402(1981).

84. P. Pulido, J.H.R. Kagi and B.L.Vallee, Biochemistry, 5, 1768-1777(1966).

85. U. Weser, H. Rupp, F. Donay, F. Linnemann, W. Volter, W. Voetsch and G. Jung, Eur. J. Biochem. 39, 127-140(1973).

86. G. Sokolowski and U. Weser, Hoppe-Seyler's Z. Chem. 356, 1715-1726(1975).

87. A.Galdes, H.A.O. Hill, I. Bremner and B.W. Young, Biochem. Biophys. Res. Commun. 85, 217-225(1978).

88. H. Rupp; W. Volter and U. Weser, FEBS Lett. 40, 176-179(1974).39

89. A. Galdes, M. Vasak, H.A.O.Hill and J.H.R. Kagi, FEBS Lett. 92, 17-21(1978).

90. M. Vasak, A. Galdes, H.A.O. Hill, J.H.R. Kagi, I. Bremner and B.W. Young, Biochemistry 19,416-425(1980).

91. P.J. Sadler, A. Bakka and P.J. Beynon, FEBS Lett. 94, 315-318(1978).

92. R.A. Haberkorn, L. Que (Jr.), W.O. Gillum, R.H. Holm, C.S. Lui and R.C. Lord, Inorg. Chem. 15, 2408-2413(1976).

93. G.K. Carson, P.A.W. Dean and M.J. Stillman, Inorg. Chim. Acta, 56, 59-71(1981).

94. M.P. Dubois, W.C. Stevens, T.T.P. Cheung, S. Lacelle, B.C. Gerstein and D.M. Kurtz (Jr.) J. Am. Soc. Chem. 103, 4400-4405(1981).

95. K.T. Suzuki and T. Maitani, Specialia, 1449-1450(1978).

96. P.A.W. Dean, A.Y.C. Law, J.A. Szymanska, M.J. Stillman, Inorg. Chim. Acta, 78, 275-279(1983).

97. J.D. Otvos and I.M. Armitage, J.Am. Soc. Chem. 101, 7735-7736(1979).

98. J.D. Otvos and I.M. Armitage, Proc. Natl. Acad. Sci. USA, 77, 7094-7098(1980).

99. J.D. Otvos and I.M. Armitage, in Biochem. Structure Determination by NMR, J. Glickson, A.A. Bothner-By eds., Marcel Dekker, New York, pp65-95 (1981).

100. I.M. Armitage, J.D. Otvos, R.W. Briggs and Y. Boulanger, Fed. Proc. 41, 2974-2980(1982).

101. M. Vasak, R. Bauer, J. Am. Soc. Chem. 104, 3236-3238(1982).

102. J.K. Nicholson, P.J. Sadler, K. Cain, D.E. Holt M. Webb and G.E. Hawkes, Biochem. J. 211, 251-255(1983).

103. C.D. Garner, S.S. Hasain, I. Bremner and J. Bordas, J. Inorg. Biochem. 16, 253-256(1982).

104. I. Dance, J. Am. Chem. Soc. 102, 3445-3451(1980).

105. D. Swensen, N.C. Baenziger and D. Coucouvanis, J. Am. Chem. Soc. 100, 1932-1934(1978).

106. M. Vasak, J. Am. Chem. Soc., 102, 3953-3955(1980).

107. M. Vasak, J.H.R. Kagi, B. Holmquist and B.L. Vallee, Biochemistry, 20, 6659-6664(1981).

108. M. Vasak and J.H.R. Kagi, Proc. Natl. Acad. Sci USA, 78, 6709-6713(1981).

109. S.W. May and J-Y. Kuo, Biochemistry, 17, 3333-3338(1978).

110. S. Onosaka, K. Tanaka, M. Dio and K. Okahara, Eisei Kagaku, 24,128-33(1978).

111. R.W. Chen and H.E. Ganther, Environ. Physiol. Biochem. 5, 378-388 (1975).

112. J.K. Piotrowski, W. Balarowska and A. Sapota, Acta Biochem. Pol. 20, 207-215 (1973).

113. J.A. Zelazowski and J.K. Piotrowski, Acta Biochem. 24, 97-103 (1977).

114. F.N. Kotsonis and C.D. Klaassen, Tox. Appl. Pharm. 42, 583-588 (1977).

115. S. Onosaka and M. G. Cherian, Toxicol. Appl. Pharm. 63, 270-74 (1982).

116. S.R. Patierno, N.R. Pellis, R.M. Evans and M. Costa, Life Sci. 32, 1629-1636 (1983).

117. R.W. Olafson and R.G. Sims, Anal Biochem, 100, 343-351 (1979).

118. S. Klauser, J.H.R.Kagi and K.J. Wilson, Biochem. J. 209, 71-80(1983).

119. G.L. Ellman, Arch. Biochem. Biophys. 82, 70-77(1959).

120. C. Tohyama and Z.A. Shaikh, Fund. Appl. Toxicol. 1, 1-7 (1981).

121. C.C. Chang, R.J. VanderMallie and J.S. Garvey, Toxicol. Appl. Pharm. 55, 94-102(1980).

122. Y. Boulanger, I.M. Armitage, K. Miklossy and D.R. Winge, J. Biol. Chem. 258, 13717-13719(1982).

123. D.R. Winge, K. Miklossy, J. Biol. Chem. 257, 3471-76(1982).

124. K.B. Nielson and D.R. Winge, J. Biol. Chem. 258, 13063-13069(1983).

125. A.J.Zelazowski, J.A. Szymanska, A.Y.C. Law and M.J. Stillman, J. Biol. Chem., in press.

126. A.J. Zelazowski, J.A. Szymanska, Prep. Biochem. 10, 495-503(1980).

127. A.Y.C. Law, M.J. Stillman, E.M.K. Lui and M.G Cherian, submitted to Can. J. Biochem & Cell Biology.

128. A.Y.C. Law, M.G. Cherian and M.J. Stillman, Biochem. Biophys.

-61(1984).

J.Y. Yang, Anal. Chem. 10, 1195-1207(1977).

and R.V. Coleman, Biol. Chem. 247, 4718-4728(1972).

T.A. Kaden and B.L. Vallee, Biochemistry, 14, 1454-

d M.J. stillman, Biochem. Biophys. Res. Comm. 94,

Barth, C. Djerassi, H.J. Hartmmaa, P. Krauss, G.

Voelter and W. Voetsch, Biochem. Biophys. Acta, 278,

Ammer and R.W. Olafson, J. Biol. Chem. 257, 2420-

Ammer and R.W. Olafson, FEBS. Lett. 126, 165-

R.W. Olafson and J.M. Armitage, J. Biol. Chem. 257,

32).

ta and M.J. Stillman, private communication.

ta and M.J. Stillman, Biochem. Biophys. Res. Comm.

1982).

Jr., in Iron-Sulfur Protein, Vol. III, W.

, Acad. Press, New York, NY, 1977, Chapter 6.

Ann. Rev. Biochem., 43, 461 (1974). Fe-S review.

stry of Copper, J. Peisach, P. Aisen and W.E.

s., Acad. Press, New York, 1966.

on and V. DiStefans, in Drill's Pharmacology in

Palma, J.R. and Joseph R., eds., McGraw

n, Chapter 53, 1971.

142. M.G. Cherian, Nature, 287, 871-872(1980).

143. M.G. Cherian, J. Toxicol. Envrion. Health, 6, 393-401(1980).

144. M.G. Cherian, S. Onosaka, G. Carson and P.A.W. Dean, J. Toxicol. Environ. Health, 9, 389-99(1982).

145. A.J. Canty, ACS Symp. Ser. 82, 327-338(1978)

146. A.J. Carty, ACS Symp. Ser. 82, 339-358(1978).

147. P. Hemmerich and C. Sigwart, Experientia, 19, 488-489(1963).

148. K.S. Hagen and R.H. Holm, Inorg. Chem. 22, 3171-3174(1983).

149. I.G. Dance, M.L.Scudder and R. Secomb, Inorg. Chem. 22, 1794-97(1983).

150. H.B. Burgi, H. Gehrer, P. Strickler and F.K. Winkler, Helv. Chim. Acta 59, 2558-2565(1976).

151. P. Strickler, J. Chem. Soc. Chem. Comm. 655-656(1969)

152. J.C. Bayon, M.C. Brianso, J.L. Brianso and P. Gonzalez-Duarte, Inorg. Chem. 18,3478-3482(1979).

153. A. Choy, D. Craig, I.Dance and M.J. Scudder, J. Chem. Soc. Chem. Comm. 1246-1247(1982).

154. H. Burgi, Helv. Chim. Acta, 57, 513-519(1974).

155. J.C. Bayon, I. Casala, W. Gaete, P. Gonzalez-Duarte and J. Ros, Polyhedron, 1, 157-161(1982).

156. C. Chieh, Can. J. Chem. 56,564-566(1977).

157. N.J. Taylor and A.J. Carty, J. Am. Chem. Soc. 99, 6143-6145(1977).

158. A.J. Carty and N.J. Taylor, J. Chem. Soc. Chem. Comm. 214-216(1976).

159. Y. Okaya and C. Knobler, Acta Crystallogr. 17, 928-930(1964).

160. M.S. Weininger, G.W. Hunt and E.L. Amma, J. Chem. Soc. Chem. Comm. 1140-1141(1972).

161. R.L. Girling and E.L. Amma, Inorg. Chem. 10, 335-340(1971).

162. I.F. Taylor, Jr., M.S. Weininger and E.L. Amma, Inorg. Chem. 13, 2835-2842(1974).

163. W.A. Spofford III and E.L. Amma, Acta Crystallogr. Sect. B, 26,1474-1483(1970).

164. A.L. Crumbliss, L.J. Gestaut, R.C. Richard and A.T. McPhail, J. Chem. Soc. Chem. Comm. 545-546(1974).

165. D. Coucouvanis, C.N. Murphy and S.K. Konodia, Inorg. Chem. 19, 2993-2998(1980).

166. F.A. Cotton, B.A. Frenz, D.L. Hunter and Z.C. Mester, Inorg. Chim. Acta, 11, 111-117(1974).

167. E.H. Griffith, G.W. Hunt and E.L. Amma, J. Chem. Soc. Chem. Comm. 432-433(1976).

168. I.G. Dance, J. Chem. Soc. Chem. Comm. 103-104(1976).

169. I.G. Dance, Aust. J. Chem. 31, 2195-206(1978).

170. I.G. Dance, J. Chem. Soc. Chem. Comm. 68-69(1976).

171. I. G. Dance and J.C. Calabrese, Inorg. Chim. Acta, 19, L41-42(1976).

172. D. Coucouvanis, D. Swenson, N.C. Baenziger, R. Pedelty and M.L. Caffery, J. Am. Chem. Soc. 99, 8097-99(1977).

173. S.A. Koch, R. Fikar, M. Millar and T. O'Sullivan, Inorg. Chem. 23, 122-124(1984).

174. D.C. Bradley and N.R. Kunchur, J. Chem. Phys. 40, 2258-2261(1964).

175. C.D. Bradley and N.R. Kunchur, Can. J. Chem. 43, 2786-2792(1965).

176. N.R. Kunchur, Nature, 204, 468-469(1964).

177. J.D. Gunter, A.F. Schreiner and R.S. Evans, Inorg. Chem. 14, 1589-92(1975).

178. F.J. Hollander and D. Coucouvanis, J. Am. Chem. Soc. 99, 6268-6279(1977).

179. I.G. Dance, J. Am. Chem. Soc., 101, 6264-73(1979).

180. D. Coucouvanis, D. Swensen, N.C. Baenziger, C. Murphy, D.G. Holah, N. Sfarnas, A. Simopoulos and A. Kostikas, J. Am. Chem. Soc. 103, 3350-3362(1981).

181. E.R. Dockal, T.E. Jones, W.F. Sokol, R.J. Eugerer, D.B. Rorabacher and L.A. Ochrymowycz, J. Am. Chem Soc. 98, 4322-24(1976).

182. M. Beltramini and K. Lerch, Biochemistry, 22, 2043-2048(1983).

183. K. Lerch and M. Beltramini, Chem. Scripta, 21, 109-115(1983).

184. M. Jakaubowski, J. Piotrowski and B. Trojanowska, Toxicol. Appl. Pharm. 16, 743-753(1970).

185. J.M. Wisniewska, B. Trojamowska, J.K. Piotrowski and M. Jakubowski, Toxicol. Appl. Pharm. 16, 754-63(1970).

186. J.K. Piotrowski, B. Trojanowski, J.M. Wisniewski-Knypl and W. Bolanowska, Toxicol. Appl. Pharm. 27, 11-19(1974).

187. R.W. Ellis and S.F. Fang, Toxicol. Appl. Pharm. 20, 14-21(1971).

188. P.D. Whanger and J.T. Deagen, Environ. Res. 30, 372-380(1983).

189. G. Sokolowski, W. Pilz and U. Weser, FEBS Lett. 48, 222-225(1974).

190. J.E. Coleman, Prog. Bioorg. Chem. 1, 159-344(1971).

191. E.I. Solomon, J. Rawlings, D.R. McMillin, P.J. Stephens and H.B. Gray, J. Am. Chem. Soc. 98, 8046-8048(1976).

192. J.A. Szymanska and M.J. Stillman, unpublished.

193. J.A. Szymanska, A.Y.C. Law and M.J. Stillman, Inorg. Chim. Acta, 79, 123-124(1983).

194. G.K. Carson and P.A.W. Dean, Inorg. Chim. Acta 66, 157-161(1982).

195. H. Rupp and U. Weser, FEBS Lett. 44, 293-297(1974).

196. H. Porter, J. Johnston and E.M. Porter, Biochem. Biophys. Acta, 65,66-73(1962).

197. H. Porter, M. Sweeney and E.M. Porter, Arch. Biochem. Biophys. 104, 97-101(1964).

198. H. Porter in Biochem. of Copper (J. Peisach, P. Aisen, W.E. Blumberg, eds.) Acad. Press, New York, pp 159,1966.

199. D.R. Winge, R. Premakumar, R.D. Wiley and K.V. Rajagopalan, Arch. Biochem. Biophy. 170, 253-266(1975).

200. I. Bremner in metallothionein (J.H.R. Kagi & M. Nordberg,eds.) Birkhauser, Basel,1979, 273-280.

201. R.D. Irons and J.C. Smith, Chem-Biol. Int. 18, 83-89(1977).

202. L. Ryden and H.F. Deutsch, J. Biol Chem. 253, 519-524(1978).

203. K. Wong and C.D. Klaassen, J. Biol. Chem. 254, 12399-12403(1979).

204. I. Bremner and R.B. Marshall, Brit. J. Nutr. 32, 283-291(1974).

205. I. Bremner and R.B. Marshall, Brit. J. Nutr. 32, 293-300(1974).

206. I. Bremner and D.W. Young, Biochem. J. 157, 517-520(1976).

207. D.R. Winge, B.L. Geller and J. Garvey, Arch. Biochem. Biophys. 208, 160-166(1981).

208. B.C. Starcher, J. Nutr. 97, 321-326(1969).

209. U. Weser, H. Hartmann, A. Fretzdorff, G. Strobel, Biochem. Biophys. Acta, 493, 465-477(1977).

210. M. Beltramini and K. Lerch, FEBS Lett. 127, 201-203(1981).

211. J. Bordas, M.H.J. Koch, H. Hartmann and U. Weser, FEBS Lett. 140, 19-21(1982).

212. J. Bordas, M.H.J. Koch, H. Hartmann and U. Weser, Inorg. Chim.

Acta, 78, 113-120(1983).

213. I. Ross, B. Binstead, N.J. Blackburn, I. Bremner, G.P. Diakun, S.S. Hasnaim, P.F. Knowles, M. Vasak and C.D. Garner, Inorg. Chimica Acta, 79, 89-90(1983).

214. H. Rupp, W. Volter and U. Weser, Hoppe Seyler's Z. Physiol. Chem. 356, 755-756(1975).

215. B.L. Geller and D.R. Winge, Arch. Biochem. Biophys. 213, 109-117(1982).

216. I. Bremner and R.K. Mehra, Chimica Scripta, 21, 117-121(1981).

217. M. Linss, M.G. Weller and U. Weser, Inorg. Chim. Acta, 79, 105(1983).

218. K. Lerch and M. Beltramini, Inorg. Chim. Acta, 79, 7-8(1983).

219. M.J. Stillman and J.A. Szymanska, Biophys. Chem. 19, 163-169(1984).

220. K. Lerch, Metal Ions in Biol. Sys. 13, 299-318(1981).

221. E.M. Mogilnicha, M. Webb, Chem. Biol. Inter. 40, 247-256(1982).

222. E.M. Mogilnicka and M. Webb, J. Appl. Toxicol. 1, 42-50(1981).

223. C.F. Shaw, Inorg. Chem. Biol. Med. 40, 349-372(1979).

END

2603185

FIN